

**A study on water-heat patterns and regional climate of  
mountain-oasis-desert system in north Tianshan Mountains  
based on the WRF model**

**Studie van water-warmte patronen en regionaal klimaat van  
berg-oasis-woestijn systeem in de Noordelijke Tianshan  
bergketen op basis van het WRF model**

**Miao ZHANG**

**May, 2018**





Faculty of Sciences

Department of Geography

**A study on water-heat patterns and regional climate of  
mountain-oasis-desert system in north Tianshan Mountains  
based on the WRF model**

**Studie van water-warmte patronen en regionaal klimaat  
van berg-oasis-woestijn systeem in de Noordelijke Tianshan  
bergketen op basis van het WRF model**

Dissertation submitted in accordance with the requirements for the degree  
of doctor in sciences: Geography

**Miao Zhang**

(Double PhD of University of Chinese Academy of Sciences, China,  
and Ghent University, Belgium)

May, 2018



## **Members of the Examination Committee**

Prof. dr. CHEN Xi (co-chair)  
Xinjiang Branch. Chinese Academy of Sciences

Prof. dr. VAN EETVELDE, Veerle (co-chair)  
Department of Geography, Ghent University

Prof. dr. BAO Anming  
Xinjiang Institute of Ecology and Geography, Chinese Academy of Sciences

Prof. dr. BOURGEOIS, Jean  
Department of Archaeology, Ghent University

Prof. dr. DONG Yunshe  
Xinjiang Institute of Ecology and Geography, Chinese Academy of Sciences

Prof. dr. KURBAN Alishir  
Xinjiang Institute of Ecology and Geography, Chinese Academy of Sciences

Prof. dr. LIU Tie  
Xinjiang Institute of Ecology and Geography, Chinese Academy of Sciences

Prof. dr. TERMONIA, Piet  
Department of Physics and Astronomy, Ghent University

Prof. dr. ir. TAERWE, Luc  
Department of Structural Engineering, Ghent University

Prof. dr. VAN DE VOORDE, Tim  
Department of Geography, Ghent University

## **Promoters**

Prof. dr. DE MAEYER, Philippe  
Department of Geography, Ghent University

Prof. dr. LUO Geping  
Xinjiang Institute of Ecology and Geography, Chinese Academy of Sciences



---

# TABLE OF CONTENTS

<b>TABLE OF CONTENTS .....</b>	<b>I</b>
<b>LIST OF FIGURES .....</b>	<b>V</b>
<b>LIST OF TABLES .....</b>	<b>IX</b>
<b>ABBREVIATION LIST .....</b>	<b>XI</b>
<b>ACKNOWLEDGEMENTS .....</b>	<b>XIII</b>
<b>1. INTRODUCTION.....</b>	<b>1</b>
1.1 Overview .....	2
1.1.1. Research status and methods .....	3
1.1.2. Climate and land surface model development.....	5
1.1.3. Climate change and LUCC in the North Tianshan Mountains.....	7
1.1.4. Oasis effects.....	8
1.2 Study area .....	10
1.3 Methodology.....	11
1.3.1. WRF.....	11
1.3.2. Model configurations.....	14
1.3.3. Validation.....	16
1.4 Datasets.....	16
1.4.1. Forcing data .....	16
1.4.2. Station-based data .....	17
1.4.3. Land use (LU) types datasets.....	18
1.4.4. Land surface terrestrial datasets from MODIS .....	19
1.5 Rationale and synopsis .....	21
1.5.1. Research objectives and questions.....	21
1.5.2. Dissertation outline .....	26
1.5.3. Out of scope .....	28

---

**2 THE RESPONSES OF WRF TO VARIOUS ACTUAL TERRESTRIAL DATASETS .....31**

**ABSTRACT.....32**

2.1 Introduction ..... 32

2.2 Study area ..... 36

2.3 Data..... 36

2.3.1. Forcing data and in situ measurements ..... 36

2.3.2. Land use data ..... 37

2.3.3. Albedo product (MCD43A4)..... 37

2.3.4. LAI product (MYD15A2)..... 37

2.3.5. GVF data from the MODIS Vegetation Indices (MOD13A2) ..... 38

2.4 Methodology..... 38

2.4.1 Model configuration ..... 38

2.4.2 Experimental design ..... 38

2.5 Results ..... 39

2.5.1. Differences between the actual terrestrial datasets and the defaults..... 39

2.5.2. Impacts of the actual terrestrial datasets on the surface energy fluxes.. 42

2.5.3. Impacts of the actual terrestrial datasets on 2-m air temperature, humidity ..... 47

2.5.4. Impacts of the actual terrestrial datasets on the surface circulation..... 52

2.5.5. Response of WRF to various actual terrestrial datasets..... 54

2.6 Discussion..... 57

2.7 Conclusions ..... 58

**3 THE IMPACT OF DRIP IRRIGATION ON THE ATMOSPHERIC STRUCTURE AND THE LOCAL CLIMATE .....59**

**ABSTRACT.....60**

3.1 Introduction ..... 60

3.2 Study area and Data..... 64

3.2.1. Study area and its climate ..... 64

3.2.2. Forcing data and in situ measurements ..... 64

3.3 Methodology..... 64

3.3.1. Model description and configuration ..... 64

3.3.2. Irrigation in WRF-NOAH..... 65

3.3.3. Experiment design ..... 66

3.4 Results ..... 67

3.4.1 Validation..... 67

3.4.2 The effects of irrigation on the near-surface climate elements..... 69



3.4.3	The effects of irrigation on the atmospheric structure and dynamics (humidity, temperature and PBLH).....	71
3.4.4	The effects of irrigation on precipitation and evapotranspiration.....	75
3.5	Discussion.....	77
3.6	Conclusions .....	78
<b>4</b>	<b>THE WATER-HEAT PATTERNS AND OASIS EFFECTS IN MODS .....</b>	<b>81</b>
	<b>ABSTRACT.....</b>	<b>82</b>
4.1	Introduction .....	82
4.2	Study area .....	85
4.3	Datasets.....	85
4.3.1.	Forcing Data and In Situ Measurements.....	85
4.3.2.	Actual Land Surface Parameters.....	86
4.4	Methodology.....	86
4.4.1.	Model Description and Configuration .....	86
4.4.2.	Experimental Design.....	86
4.5	Results .....	88
4.5.1	Simulation Evaluation.....	88
4.5.2	The spatial patterns of temperature of MODS.....	92
4.5.3	The spatial patterns of humidity of MODS.....	94
4.5.4	The spatial patterns of the 10-m horizontal circulation of MODS .....	97
4.6	Comparison with previous studies and an assessment of model uncertainties.....	99
4.7	Conclusions .....	100
<b>5</b>	<b>GENERAL DISCUSSION.....</b>	<b>103</b>
5.1	Summary and discussion of research questions.....	104
	RQ1: What are the responses of the WRF performance to various actual terrestrial parameters derived from satellite products ? .....	106
	RQ2: How does the WRF coupled with a newly developed drip irrigation process perform in simulating the water-heat conditions of irrigated oasis? ....	107
	RQ3: What are the effects of drip irrigation on atmosphere structure of MODS? .....	108
	RQ4: What are the impacts of large mountains on irrigated oasis-desert interaction in a typical mountain-oasis-desert ecosystem? .....	109
5.2	Critical reflections .....	110
5.3	Recommendations for future work .....	112
5.3.1.	Future work on datasets .....	112
5.3.2.	Future work on model development .....	112
5.3.3.	Future work on research topics .....	112

---

<b>6</b>	<b>GENERAL CONCLUSIONS.....</b>	<b>115</b>
<b>7</b>	<b>APPENDIX .....</b>	<b>119</b>
7.1	namelist.wps .....	120
7.2	namelist.input .....	121
7.3	programme Wgeogrid.....	125
7.4	NCL code for updating the LU and monthly GVF in wrfinput and wrflowinp.....	127
<b>8</b>	<b>References .....</b>	<b>131</b>
	<b>SUMMARY .....</b>	<b>143</b>
	<b>SAMENVATTING (DUTCH SUMMARY) .....</b>	<b>146</b>
	<b>摘要 (CHINESE SUMMARY).....</b>	<b>149</b>
	<b>CURRICULUM VITAE (BIOGRAPHY) .....</b>	<b>151</b>

---

## LIST OF FIGURES

Figure 1-1. Schematic diagram of the interactions between an oasis and desert cited from paper (Li <i>et al.</i> , 2016a). .....	10
Figure 1-2. Central Asian circulation background.....	11
Figure 1-3. Work flow of the WRF model.....	13
Figure 1-4. (a) simulation domains of WRF-Noah and land surface elevations, meteorological sites , (b) Land use (LU) types of the study area .....	14
Figure 1-5. Work flow of study .....	23
Figure 1-6. Outline of the dissertation .....	27
Figure 2-1. Location of the northern Tianshan Mountains (NTM) in Central Asia, including land surface elevations, meteorological sites, and simulation domain over the NTM (the blue dashed line is the analysis range) .....	36
Figure 2-2. Comparison between actual LU (a), albedo (b), leaf area index (LAI) (c), and green vegetation fraction (GVF) data (d) and the corresponding default data (e–h), with differences shown in (i–l). The red line indicates the border of the key oasis areas, and the black rectangle indicates the region strongly influenced by human activities in oases and desert areas over the past 20 years. ....	40
Figure 2-3. Comparisons between observations and five simulations of hourly averaged latent heat flux (LE), and corresponding scatter diagram at S2 site in (a, b) 2010 and (c, d) 2012. The five simulations are def (using default LU, albedo, LAI and GVF), LU (using actual LU only), Alb (using actual LU and albedo datasets only), LAI (using actual LU, albedo and LAI three datasets), and VF (using all of four actual LU, albedo, LAI and GVF datasets) .....	43
Figure 2-4. Daytime spatial patterns of sensible heat flux (H) from the simulations of (a) def, (b) LU, (c) Alb, (d) LAI and (e) VF, and their differences (f) b-a, (g) c-b, (h) d-c and (i) e-d (these differences pixels are statistically significant at $p < 0.05$ ). The five simulations are def (using default LU, albedo, LAI and GVF), LU (using actual LU only), Alb (using actual LU and albedo datasets only), LAI (using actual LU, albedo and LAI three datasets), and VF (using all of four actual LU, albedo, LAI and GVF datasets). The red line represents the border of the key oasis area.....	44
Figure 2-5. Daytime spatial patterns of latent heat flux (LE) from the simulations of (a) def, (b) LU, (c) Alb, (d) LAI and (e) VF, and their differences (f) b-a, (g) c-b, (h) d-c and (i) e-d (these differences pixels are statistically significant at $p < 0.05$ ). The def is a simulation with default LU, albedo, LAI and GVF provided by WRF itself, LU is a simulation with only actual LU, Alb is a simulation with only actual LU and albedo, LAI is a simulation with actual LU, albedo and LAI, and GVF is a simulation with actual all of four terrestrial datasets. The red line represents the border of the key oasis area.....	45
Figure 2-6. Comparisons between observations and five simulations of hourly averaged 2-m air temperature(a,c,e,g,i,k), and corresponding scatter diagram at six sites(b,d,f,h,j,l). The def is a simulation with default LU, albedo, LAI and GVF provided by WRF itself, LU is a simulation with	

---

only actual LU, Alb is a simulation with only actual LU and albedo, LAI is a simulation with actual LU, albedo and LAI, and GVF is a simulation with actual all of four terrestrial datasets. ....	47
Figure 2-7. Comparisons of hourly averaged 2 m relative humidity (RH) between observations and five simulations (a, c, e, g, i, k), and corresponding scatter diagram (b, d, f, h, j, l) at six stations (S1-S6) in 2010 and 2012. The def is a simulation with default LU, albedo, LAI and GVF provided by WRF itself, LU is a simulation with only actual LU, Alb is a simulation with only actual LU and albedo, LAI is a simulation with actual LU, albedo and LAI, and GVF is a simulation with actual all of four terrestrial datasets. ....	48
Figure 2-8. Daytime spatial patterns of 2 m air temperature (T2) from the(a) def, (b) LU, (c) Alb, (d) LAI and (e) VF simulations, and their differences (f) b-a, (g) c-b, (h) d-c and (i) e-d (these difference pixels are statistically significant at $p < 0.05$ ). And corresponding patterns during the night-time, which are labelled with the corresponding daytime label and the number 1. The def is a simulation with default LU, albedo, LAI and GVF provided by WRF itself, LU is a simulation with only actual LU, Alb is a simulation with only actual LU and albedo, LAI is a simulation with actual LU, albedo and LAI, and GVF is a simulation with actual all of four terrestrial datasets. The red line represents the border of the key oasis area. ....	50
Figure 2-9. Daytime spatial patterns of 2 m specific humidity patterns (Q2, g kg <sup>-2</sup> ) from the (a) def, (b) LU, (c) Alb, (d) LAI and (e) VF simulations, and their differences (f) b-a, (g) c-b, (h) d-c and (i) e-d (these difference pixels are statistically significant at $p < 0.05$ ). And corresponding patterns during the night-time, which are labelled with the corresponding daytime label and the number 1. The def is a simulation with default LU, albedo, LAI and GVF provided by WRF itself, LU is a simulation with only actual LU, Alb is a simulation with only actual LU and albedo, LAI is a simulation with actual LU, albedo and LAI, and GVF is a simulation with actual all of four terrestrial datasets. The red line represents the border of the key oasis area. ....	51
Figure 2-10. Comparisons of hourly 10 m (a, c, e) wind speed (WS) and (b, d, f) wind direction (WD) between observations and five simulations at three stations (S1, S3, S4). ....	52
Figure 2-11. Daytime spatial patterns of 10 m wind speed (WS) and wind direction (WD) from the (a) def, (b) LU, (c) Alb, (d) LAI and (e) VF simulations, and their differences (f) b-a, (g) c-b, (h) d-c and (i) e-d (these difference pixels are statistically significant at $p < 0.05$ ). And corresponding patterns during the night-time, which are labelled with the corresponding daytime label and the number 1. The def is a simulation with default LU, albedo, LAI and GVF provided by WRF itself, LU is a simulation with only actual LU, Alb is a simulation with only actual LU and albedo, LAI is a simulation with actual LU, albedo and LAI, and GVF is a simulation with actual all of four terrestrial datasets. The red line represents the border of the key oasis area. ....	53
Figure 2-12. Average bias percentages of simulated meteorology variables at 6 meteorology stations due to using each actual terrestrial datasets: (a) T2 biases, (b) RH biases, (c) WS biases, (d) LE biases, (e) biases due to using actual LU, (f) biases due to using actual albedo, (g) biases using actual LAI, (h) biases due to using actual GVF datasets. ....	56
Figure 3-1. (a) locations of NTM in the CA, and land surface elevations, meteorological sites, simulations domains of NTM, (b) Land use (LU) types of NTM in 2012. ....	64

---

Figure 3-2. Comparisons of hourly averaged (a) 2-m air temperature (T2), (c) 2-m relative humidity (RH), (e) evapotranspiration (ET) between observations and simulations, respectively, and (b, d, f) corresponding scatter diagrams. ....	68
Figure 3-3. Comparison of the (a) monthly evapotranspiration (ET), precipitation (P) from the CON and IRR simulations and observation, and (b) irrigation amount in each month and in a year from the IRR. ....	69
Figure 3-4. Spatial patterns of averaged (a) sensible heat flux (H), (b) latent heat flux (LE), (c) 2-m air temperature (T2), and (d) 2-m specific humidity from the IRR simulation in daytime in the irrigation season, and (e, f, g, h) the difference between the IRR and CON simulations (the difference pixels are statistically significant at $p < 0.001$ ). And corresponding patterns in nighttime, which are labelled with the corresponding daytime label and the number 1. The red line represents the border of the oasis. ....	70
Figure 3-5. Vertical cross section of mean air temperature ( $^{\circ}\text{C}$ ) along the white line shown in Figure 4a from the (a, b) IRR simulation, and from the (c, d) CON simulation, and the (e, f) differences between the IRR simulation and CON simulation during daytime and nighttime, respectively. Height along y-axis is given in height (km). ....	71
Figure 3-6. Vertical cross section of mean specific humidity (g/kg) along the white line shown in Figure 4a from the (a, b) IRR simulation, and from the (c, d) CON simulation, and the (e, f) differences between the IRR simulation and CON simulation during daytime and nighttime, respectively. Height along y-axis is given in height (km). ....	72
Figure 3-7. Comparison of diurnal variation in mean planetary boundary layer height (PBLH) in irrigation season. ....	73
Figure 3-8. Mean 10-m horizontal wind speed and wind direction from the (a, b) IRR and (c, d) CON simulations, and the (e, f) differences between the IRR and CON simulations in daytime and nighttime, respectively. The red line represents the border of the oasis. ....	74
Figure 3-9. Spatial patterns of total precipitation amount (TP) from the (a, b) IRR and (c, d) CON simulations in the irrigation season, and (e, f) TP difference between the IRR and CON simulations. The red line represents the border of the oasis. ....	76
Figure 3-10. The scatter plot shows the correlation between the irrigation amount rate and (a) precipitation (P), (b) added Evapotranspiration (ET), (c) P change, and (d) ET change. ....	77
Figure 4-1. Comparisons of the observed and simulated (a) 2-m air temperature (T2), (b) 2-m relative humidity (RH) and (c) latent heat flux (LE) at the four stations (S1, S2, S3 and S4) during 16 July to 20 July. ....	89
Figure 4-2. The mean bias error (MBE), root mean squared error (RMSE) and Pearson correlation coefficient (r) between the simulated and observed (a) air temperature and (b) relative humidity at 2 m at the four stations (S1, S2, S3 and S4). ....	90
Figure 4-3. Comparison between the observed and simulated (a) wind speed (WS) and (b) wind direction (WD) from the mod and def simulations at the four stations (S1, S2, S3 and S4) during 16 July to 20 July. ....	91

---

Figure 4-4. Mean 2-m air temperatures (T2) from the (a,b) mod simulation and (c,d) the non-oasis simulation; (e,f) and the differences between the mod simulation and non-mountain simulation; and (g,h) the differences between the mod simulation and the non-oasis simulation during daytime and nighttime, respectively. The black dotted line represents the border of the oasis and the white dotted line (a) represents the location of the vertical section (longitude 85.7° E) represented in Figure 4-6. ....	92
Figure 4-5. The same as Figure 4-5 but showing for a vertical cross section of air temperature along the white line shown in Figure 4-5a. ....	94
Figure 4-6. The same as Figure 6 but for surface specific humidity Q2 (g kg <sup>-1</sup> ). ....	95
Figure 4-7. Same as Figure 6 but for the vertical section of specific humidity Q (g kg <sup>-1</sup> ) along the white line (longitude 85.7 ° E) shown in Figure 6a. ....	97
Figure 4-8. The mean diurnal WS and WD patterns (mean wind speed and direction at a height of 10 m during the daytime and nighttime) in the mod, non-oasis and non-mountain simulations and the differences between the mod and non-oasis simulations. (a) Daytime WS and WD from the mod simulation; (b) nighttime WS and WD from the mod simulation; (c) daytime WS and WD from the non-oasis simulation; (d) nighttime WS and WD from the non-oasis simulation; (e) daytime WS and WD from the non-mountain simulation; (f) nighttime WS and WD from the non-mountain simulation; (g) daytime WS and WD difference between the mod and non-oasis simulations; (h) nighttime WS and WD difference between the mod and non-oasis simulations. The red line represents the border of the oasis. ....	98
Figure 4-9. The W component difference between the mod simulation and non-oasis simulation during daytime and nighttime. ....	99

---

## LIST OF TABLES

Table 1-1 Development Process and Contents of Land Surface Process Models.....	7
Table 1-2. Physical parameterization schemes .....	15
Table 1-3. Soil moisture values for the oases and desert areas in the four Noah soil layers (Wen et al., 2012).....	15
Table 1-4. Meteorological stations' names, locations, elevations and available elements. ....	17
Table 1-5. Land use types and codes for the 2012LU.....	18
Table 1-6. Land use types and its codes in the WRF and corresponding relation with the 2012LU .....	18
Table 4-1. Statistical significance of the differences in temperature and humidity between the mod and non-oasis simulations, as assessed using the Student's t-test.....	96
Table 5-1 Overview of the contents of this dissertation.....	105





---

## ABBREVIATION LIST

AVHRR	Advanced Very High Resolution Radiometer
ALADIN	Aire Limitée Adaptation Dynamique Développement International model
AR5	the Fifth Assessment Report
ARW	Advanced Research WRF
BRDF	Bidirectional Reflectance Distribution Function
BCC_CSM	Beijing Climate Centre Climate System Model
CA	Central Asia
CFSR	Climate Forecast System Reanalysis
DOE	Department Of Energy
ERA	European ReAnalyses
ET	Evapotranspiration
GCM <sub>s</sub>	Global Climate Models
GVF	Green Vegetation Fraction
IGBP	International Geosphere-Biosphere Programme
IPCC	Intergovernmental Panel on Climate Change
JRA25	Japanese 25-year ReAnalysis
LAI	Leaf Area Index
LE	Latent heat flux
LU	Land Use
LUCC	Land Use/Cover Change
MBE	Mean Bias Error
MERRA	Modern Era Retrospective-analysis for Research and Applications
MM5	Fifth-generation Penn State/NCAR Mesoscale Model
MODIS	MODerate Resolution Imaging Spectroradiometer
MODS	Mountain-Oasis-Desert ecoSystem
NASA	National Aeronautics and Space Administration
NCAR	National Center for Atmospheric Research
NCEP	National Centers for Environmental Prediction
NDVI	Normalized Difference Vegetation Index
NOAH	NCEP, Oregon State University, Air Force and Hydrology Lab
NTM	North Tianshan Mountains
OBC	Oasis Breeze Circulation
PBLH	Planetary Boundary Layer Height
PRECIS	Providing Regional Climates for Impact Studies
RAMS	Colorado State University Regional Atmospheric Modeling System
RCA3	Rosby Centre Regional Climate model
RegCM	REGional Climate Model
RIEMS	Regional Integrated Environment Modeling System
Q2	Specific humidity at 2 m
R <sup>2</sup>	Coefficient of determination
RMSE	Root Mean Squared Error
RH	2-m Relative Humidity
RCMs	Regional Climate Models
SURFEX	SURFace EXternalisée
T2	2-m air Temperature

---

TRAMPER	Tropospheric Realtime Applied Meteorological Procedures for Environmental Research
TIL	Temperature Inversion Layer
TLR	Temperature Lapse Rate
TP	Total Precipitation
USGS	U.S. Geological Survey
GVF	Green Vegetation Fraction
WPS	WRF Preprocessing System
WPP	WRF Post-Processing
WRF	Weather Research and Forecasting model
WRF-DA	Weather Research Forecast vibrational Data Assimilation system
WS	Wind Speed
WNW	Northwest West
WD	Wind Direction

---

## ACKNOWLEDGEMENTS

Light travels like an arrow, and time like a shuttle. This year marks my 30th birthday and it coincides with my PhD graduation. Now, I can say that the 23 years educational pursuit as a student has come to an end. I would like to thank not only those who helped me during my postgraduate study, but also my parents, who have taught me perseverance “not to give up” in the face of difficulties. This is the ability and the unique inevitable factor in making key decisions in the life opportunities that I meet, and these has benefitted me immensely.

“What would I like to be?” This is the question that I have been thinking about since I was a kid. In fact, this unfounded thinking has little effect on the big decisions in my life. Because, the answer to this question lies in both subjective thinking and the objective environment. By chance, I met Prof. Mingguo Ma during my Master's study, as a researcher worked in the Cold and Arid Regions Environmental and Engineering Research Institute, Chinese Academy of Sciences. I was grateful and thankful to Mr. Ma for his great trust on me. This made me confident in scientific research, such as exploring the world that was not fully understood using GIS methodologies.

I would like to sincerely thank my supervisor, Prof. Philippe de Maeyer! I was really luck and grateful when Philippe agreed to accept me as a student in Gent University and to pursue the doctorate degree of Ugent. As one of the first trial students of the joint Ph.D. training, I benefited a lot from Professor De Maeyer’s benevolence and hands-on assistance. In research work, he not only provided me with a broad, free and inclusive learning environment, but also introduced me to the top scientists in the field of climate. These valuable efforts determined my research interests at last. In life, with him and his wife’s kindness, magnanimous, warm and tireless assistance, I felt at home in Belgium. Another kind and important professor, Alishir Kuban, should be mentioned here. It is because of his great efforts and selfless dedication that has contributed to a long-stable cooperative relationship between the Xinjiang Institute of Ecology and Geography, Chinese Academy of Sciences and the Gent University. Without his work, it is not possible for me to obtain the opportunity to peruse double Ph.D. I am also very grateful to Helga Vermeulen and Sabine Cnudde for doing all the paper work for me.

---

Greatest thanks go to my first supervisor, Prof. Geping Luo! In the past 5 years, all of his innovative ability, keen insight into scientific issues, and his meticulous attitude towards the research work have made me more respectful and prudent in my scientific work. From the selection of the topic of papers, the choice of method, the writing, modification and finalization of the papers, he led me into the PhD research step-by-step. I sincerely wish you happiness in your future life!

Many thanks go to Prof. Rafiq Hamdi, Xi Chen, Anming Bao, Tie Liu, Chi Zhang, Longhui Li, Wenqiang Xu, Xiaoyu Li, Jie Bai, Chun Chang et al. who provided valuable help for my data collection and paper writing. In particular, I would like to thank Chunhua Li, Bin Zhou, Ting Zou and Hui Li for their help and care during the past 5 years of my study.

Sincere thanks go to every colleague and friend, that have supported me in the past five years, both at home and abroad. They include Fei Wang, Qifei Han, Chaofan Li, Tureniguli Amuti, Hui Ye, Yaoliang Chen, Qi Zhang, Peng Cai, Xinxin Wang, Huili He, Nana Lv, Jianjun Li, Haiyang Shi, Hao Wang, Jean Baptiste Nsengiyumva, Friday Uchenna Ochege, Gonghuan Fang, Jiao Liu, Hao Sun, Feipeng Ye, Xiuliang Yuan, Yan Yan, Shihua Zhu, Xia Fang, Pengfei Zhang, Shikai Song, Yuan Qiu, Liangzhong Cao, Pepijn Viaene, Berdien De Roo, Britt Lonneville, Dai Liang, Zhou Xinyi, Zhang Pengdong, Zhang Long, etc.. Your companionship has made my doctorate life full of happiness. I will cherish the friendship very much.

Finally, I would like to sincerely thank my parents for their kindness, care and encouragement during the past 30 years. I am particularly grateful to my husband Pengbin for his accompany, tolerance and patience in the past 11 years. Especially during the doctoral period. He took almost all the pressure of livelihood for me, and encouraged me to concentrate on my studies and dreams.

I would like say “thank you” again to all the persons who cared and helped me again. Although It will be impossible to mention all of them here. I wish you all the best in your future endeavors.

Miao Zhang

March 2018

# CHAPTER 1

## INTRODUCTION

---

*This chapter is divided into four sections. Firstly, a general background is introduced on the topics of research status and methods, climate model and its development, climate change and land use/cover change in the North Tianshan Mountains (NTM), and oasis effects (Section 1.1). Secondly, detailed information on the study area is presented to establish why it was chosen as the case study (Section 1.2) and section 1.3 mainly introduces the Weather Research and Forecasting(WRF) model, its configuration, all of the datasets used in this dissertation (Section 1.4). Finally, the rationale and synopsis are discussed (Section 1.5)*

## 1.1 Overview

Global warming has become a definite fact based on the Fifth Assessment Report (AR5) from the United Nations Intergovernmental Panel on Climate Change (IPCC) and human activity is the primary reason of the warming (Hartmann et al., 2013). The contribution to climate change, the relation between climate change and human activities have always been the focus both at home and abroad (Pachauri *et al.*, 2014). The IPCC AR5 also stated that the average global land surface temperature increased by 0.3-4.8 °C with a rate of 0.13 °C/decades from 1986 to 2005, and the most sensitive areas to climate change were arid and semi-arid regions (IPCC, 2012). Few precipitation, seriously deficient water resources, intense potential evaporation, fragile ecological environment make arid areas sensitive to various human activities and to climate change. The Central Asia (CA), including the Xinjiang Province in China and five nations of Kazakhstan, Kyrgyzstan, Tajikistan, Turkmenistan and Uzbekistan (Hu et al., 2014; Li et al., 2015), is typical mid-latitude arid area, and has unique mountain-basin terrain structure. Precipitation in the area shows non-uniform patterns, that means the precipitation becomes drier in some areas, whilst in some areas it does not show any change, and also in some area sharply increases, such as the North Tianshan Mountains (NTM) (Chen et al., 2015). Here, the NTM, located in the hinterland of Central Asia, means the north slope of Tianshan Mountains. The boundary ranges of the NTM is from the eastern longitude 80° to 92° and the northern latitude 40° to 50° in this dissertation. The average precipitation amount in Central Asia decreased significantly with a rate of 2 mm/year. The temperature in Central Asia also significantly increased with 0.40 °C /decades from 1975 to 2015. However, both the temperature and precipitation in NTM increased significantly with a much larger rate. Horton et al. found that these (heat and water) dynamics of the regional climate change are largely independent of or potentially related to Land Use/Cover Change (LUCC) processes (Zhou et al., 2015; Horton et al., 2015; Qu et al., 2013).

The LUCC affects climate systems through altering surface biogeochemical and biogeophysical parameters, thereby influencing the energy budget and water budget (Brovkin et al., 2013). Because of the lack of water resources in the arid area, the ratio of sensible heat and latent heat exchange between the surface and the atmosphere is increasing. Moreover, the impact of energy budget and water budget on the climate is different from that in humid regions and monsoon climate regions. Due to the limitation of knowledge

and shortage of interdisciplinary cooperation, there is still lack of full understanding of the mechanism of the procedures of the climate process and how the land use changes influence the regional climate in the arid area (Feddemma et al., 2005)

#### 1.1.1. Research status and methods

The mechanism of near-surface climate change and the impact of LUCC on local/regional climate change under the background of global climate change is a complex multi-disciplinary problem, including water, soil, gas, and biomass changes and mutual feedback mechanisms. Energy balance and water cycle are two important processes that interact with each other in the climate system. According to atmospheric dynamical equations, the sensible heat and latent heat fluxes decide the atmospheric temperature and humidity (Sun, 2002), and the change of the sensible heat and latent heat flux is directly linked to the atmospheric circulation and the ascent and sinking movements. Therefore, the sensible and latent heat, as well as the corresponding temperature and humidity conditions, and changes of these elements play an important role in analysis and exploration of day, night, seasonal and long-term weather, climate change or abnormal climate system (Pitman, 2003). At present, the land-atmosphere interaction and its relationship with climate change are mainly studied by statistical analysis of observational data (Zhou et al., 2005) and numerical simulation using climate models.

A series of international cooperation projects or research projects working on climate change and human activities have been implemented to explore the relation between LUCC and climate change, such as the LUCC and Global Environmental Change, co-sponsored by the International Human Dimensions Programme on Global Environmental Change and the International Geosphere-Biosphere Programme (IGBP); the Global Energy and Water Cycle Experiment funded by the World Climate Research Programme (Coughlan and Avissar, 1996); the Heihe Watershed Allied Telemetry Experimental Research launched by the National Natural Science Foundation of China (Li et al., 2013). These experimental observations contributed a large number of raw observational data of land surface parameters in arid regions. These datasets are all devoted to revealing the relationship between different land-atmosphere interactions and changes in water-heat fluxes and climate change through water and heat budgets, and some qualitative and quantitative theories in land-atmosphere interaction process. However, due to the uneven distribution

of observation stations and limited by various natural and human factors, the tempo-spatial observational data are discontinuous, and observations cannot identify other influencing on the local/regional climate from the climate backgrounds.

Numerical simulation using climate model is another important method to reveal the mechanism and process of climate change, especially using the coupling of climate models and land surface models (Meng et al., 2015; Wen et al., 2012; Miao et al., 2011; De Troch et al., 2013), besides observation of meteorological, carbohydrate and energy fluxes (Li et al., 2016). There are studies or numerical simulations of the effects of LUCC on the climate, but there are still a lot of uncertainties in the current knowledge (Deng et al., 2013). Since there is a great difference in the physical, chemical, and biological characteristics of the land surface within different regions on the Earth, the impacts of LUCC on the regional climate systems also vary greatly. For example, arid area, where have been experiencing distinct land use changes and which is sensitive to climate change, has been significantly different from the response due to a great difference in the physical, chemical and biological characteristics of the land surface (Huang et al., 2015). On the one hand, accurate representation and retrieval of LUCC and land surface parameters is one kind of solutions to decrease the uncertainties, which relies heavily on the development of remote sensing. On the other hand, it is necessary to enhance the study of land surface process and climate processes, which not only requires mathematical physics models to effectively simulate land-atmosphere interaction, but also needs to improve the observation and understanding of surface process, thereby providing reasonable and effective initial parameters for mathematical physics modeling.

In addition, to research on the influence of LUCC on the regional climate, more attention should paid on the influence of irrigation on regional climate, especially in arid area. At present, 70% of human water is used for farmland irrigation (Douglas et al., 2009), and farmland in arid and semi-arid areas, has to be irrigated in general. So far, some simulation studies have shown that irrigation can reduce the regional temperature and daily range of temperature (Lobell et al., 2009). The change in irrigation scale and irrigation method has been expected to influence the local climate since it directly influences the soil moisture, which will further affect the land surface albedo, evaporation, regional temperature as well as precipitation. Conversely, quantitative research on how climate responds to effective drip irrigation in arid area is still rare. Moreover, the cooling effect of irrigation is obscured



due to global climate changes. For example, the temperature of irrigated oasis in the NTM has been increasing in the past 40 years according to observation. Therefore, based on numerical simulations, to distinguish the influence of large-scale oasis irrigation on local/regional climate from global climate changes in arid area is the main focus issue of oasis climate effects, which is of great significance to understanding of regional ecological oasis stability and oasis sustainable development.

### 1.1.2. Climate and land surface model development

Since the theoretical framework of Global Climate Models (GCMs) proposed by Phillips in 1956, meteorologists and ecologists from all over the world have made great achievements in modifying a dynamics framework, improving land surface schemes and parallel computing researches. On the basis of large-scale convective parameterization schemes, simpler land surface processes and a low spatial resolution (100-300 km) (Kysely et al., 2016), GCMs are normally used in big regions in order to predict climate change and are unable to resolve many important meso-microscale processes adequately, like wind patterns and precipitation due to orographic effects on a complex terrain or in mountainous areas. This deficit could be fatal in the application of GCMs to simulate the region-scale or local-scale climate. Moreover, the meteorological forcing data and basic terrestrial datasets prescribed in GCMs in mountainous regions are scarce and poor in accuracy, especially the atmospheric circulation is greatly uncertain in this region. In order to combat the low resolution of GCMs, Regional Climate Models (RCMs) have been developed due to its high spatial resolution and a better picture of the topography. RCMs incorporate more physical processes and could simulate the climate characteristics for a special terrain with a complex geomorphology better (Feser et al., 2011), including PRECIS (Providing Regional Climates for Impact Studies)(Li, 2011), RIEMS (Regional Integrated Environment Modeling System) (Cao et al., 2014), RAMS (Colorado State University Regional Atmospheric Modeling System), TRAMPER (Tropospheric Realtime Applied Meteorological Procedures for Environmental Research) (Gsella et al., 2014), MM5 (Pennsylvania State University-National Center for Atmospheric Research Mesoscale Model the 5 generation) (Gsella et al., 2014), COSMO-CLM (CCLM) (Davin et al., 2011), BCC\_CSM (Beijing Climate Centre Climate System Model) (Li, 2014) and RCA3 (Rossby Centre Regional Climate model) (Samuelsson et al., 2011), ALADIN (the Aire Limitée

Adaptation Dynamique Développement International mode) and its updated version ALARO (Hamdi et al., 2014).

The REGional Climate Model (RegCM) and the Weather Research and Forecasting model (WRF) are current widely used. The WRF model is an advanced mesoscale numerical weather prediction system designed for both climate research and numerical weather prediction (Skamarock et al., 2005). It was developed jointly by the National Center for Atmospheric Research (NCAR) and the National Centres for Environmental Prediction (NCEP). Compared to the results from RegCM3, the WRF has a relatively good performance in simulating precipitation (Miller et al., 2009).

Land-surface process schemes serve as a component of climate models to maintain the energy and moisture balance; while climate models provide initialization and boundary conditions for land-surface process. With the development of computer technology and the understanding of land surface process, people gradually come to realize the importance of the land surface process in climate predictions, and climate models are sensitive to the parameterization of land surface process after a series of numerical sensitivity experiments (Sun, 2002). An accurate and detailed land surface process scheme that describes the interaction between land and atmosphere is the key to a successful regional climate modeling (Lu et al., 2003) and is an effective way to simulate the impact of LUCC on the regional climate (Lamptey et al., 2005). Land surface process experienced below four phases (Table 1-1).

The NOAH land surface model was also developed through multi-institutional collaborative efforts among NCAR, the U.S. Air Force Weather Agency, the National Aeronautics and Space Administration (NASA) and the university community (Yin et al., 2016; Tewari et al., 2004; Chen et al., 1996). The abbreviation NOAH is composed of first letter of NCEP, the Oregon State University (Dept of Atmospheric Sciences), Air Force and the Hydrology Lab (formerly Office of Hydrology). The NOAH is a one-dimensional land surface scheme that describes soil moisture, soil temperature, surface temperature, snow depth, snow equivalent, canopy water content, and surface energy and moisture flux on the earth's surface. It was then included in the Project for the Intercomparison of Land Surface Parameters and the Global Soil Wetness Project and the Distributed Model Intercomparison Project. It can be used independently or coupled with MM5, WRF, etc. After the version

2.2, the NCEP real-time Land Data Assimilation System was added. The NOAH is good for ecological and hydrological processes simulation.

**Table 1-1 Development Process and Contents of Land Surface Process Models**

<b>Time</b>	<b>Category</b>	<b>Contents</b>	<b>Representative models</b>
1969	Bucket scheme	Near-surface layer of soil is modelled as a bucket	Evaporation and runoff occurs only when the bucket is full and the evaporation rate is a linear function of the water amount in the bucket (Manabe, 1969)
1978-1997	Soil-vegetation-atmosphere transfer scheme	Only soil, ice and lakes are described	BATS(the Biosphere-Atmosphere Transfer Scheme) (Dickinson <i>et al.</i> , 1993), SiB (Sellers <i>et al.</i> , 1986), ISBA(Interaction Sol-Biosphère-Atmosphère) (Noilhan and Mahfouf, 1996)
1990-	Biochemical scheme	Added the vegetation photosynthesis and carbon exchanges	LSM (the land-surface model) (Bonan, 1996), CoLM (Common Land Model) (Bonan <i>et al.</i> , 2011)
Recent 10 years	Comprehensive scheme	Improving urban canopy, dynamic vegetation and hydrological process	SURFEX (SURFace EXternalisée) (Le Moigne <i>et al.</i> , 2009), NOAH, NOAH-MP

### 1.1.3. Climate change and LUCC in the North Tianshan Mountains

The NTM is one of the typical geomorphological areas, which consists of a great number of complex Mountain-oasis-desert ecoSystem (MODS). Since the 1950s, the region has been experiencing distinct intense land reclamations, including grazing in the mountainous areas, but mainly oases expansion and urbanization, building dams on inland rivers and the unrestrained extraction of groundwater for irrigation in the basin areas (Hong *et al.*, 2003; Zhang *et al.*, 2017c; Jia *et al.*, 2004). As a result, the irrigated oases area expanded 4 times more than the original size (from  $121.0 \times 10^4$  hm<sup>2</sup> in the year 1949 to  $512.5 \times 10^4$  hm<sup>2</sup> in 2010), and irrigation methods changed from a large-scale traditional flood irrigation at the beginning to modern drip irrigation systems (Fan *et al.*, 2013). Thereby, a series of ecological problems appeared, such as regional desertification, soil salinization and drawdown due to groundwater withdrawal for irrigation (Sun *et al.*, 2011; Wang *et al.*, 2008). Meanwhile, recent studies indicate that the mean annual air temperature in the NTM has increased at an average rate of  $0.8$  °C decade<sup>-1</sup> (He *et al.*, 2003), which is far larger

than the average rate of the CA (i.e.  $0.39\text{ }^{\circ}\text{C decade}^{-1}$  from 1979 to 2011) and of global land areas (i.e.  $0.27\text{--}0.31\text{ }^{\circ}\text{C decade}^{-1}$  from 1979 to 2005) (Hu et al., 2014). Precipitation and the frequency of extreme precipitation show an obvious augmenting tendency in NTM at an increase rate of 11.3% (He et al., 2003; Xu et al., 2004; Lianmei, 2003), while generally, other areas in CA show a slight decrease in the average annual precipitation (Lioubimtseva and Henebry, 2009; Gessner et al., 2013). The LUCC affects change significantly surface water-heat patterns and local/regional climate. For example, it displays urban heat island effect of oasis-city comparing with oasis background, but cooler than the periphery desert due to irrigation and oasis crop effects (Lzzarini et al., 2015). The effect of LUCC on environment may be far more than that of global climate change.

#### 1.1.4. Oasis effects

As unique non-zonal landscapes on a medium-small scale, oasis systems with a relatively high primary productivity are developed on the background of deserts in mountain and basin systems in the arid area (Luo et al., 2010). Oasis is antagonistic and interactive with the desert. On the one hand, oasis is developed on the background of the desert based on the runoff from mountainous areas and irrigation based on the unrestrained extraction of groundwater. On the other hand, both oasis and desert are complex dissipative structures in MODS. In fact, many of the existing oases can be stabilized or even developed while others are degenerating. The limited water and land resources are keys to both the oasis and the desert. Although oases account for only 4-5% of the total area of the arid regions, over 90% of the population and over 95% of the social wealth are concentrated in the oases (Meng et al., 2009). Thus, oases play a vital role in the social and economic development in the dry region and it is the most essential part in MODS. The development and ecological stability of oases and the interaction between the oasis and the desert have been hot in arid areas.

In recent literatures, several studies (based on both field observations and numerical simulations) focused on the exchange of water and energy between the oases and the surrounding deserts (Li et al., 2013; Li et al., 2016b; Ling et al., 2013; Wang et al., 2016). According to the observation, the average albedo value over the oasis is approximately 0.15, which is much lower than the value of 0.25 regarding over the desert (Zhang and Hu, 2001). Shortwave radiation absorbed by the oasis surface is 16% higher than the adjacent deserts,

whereas the upward longwave radiation emitted by the surface is lower than the adjacent deserts, which ultimately results in the net radiation flux of the oasis being significantly higher than the surrounding deserts. It has been found temperature inversion over oasis and negative sensible heat fluxes of oases based on observations (Wang et al.; Rosenberg, 1969; Su and HU, 1987; Chen et al., 2005), demonstrating “oasis cold island effect” is definite (Li et al., 2016). Meanwhile, moisture inversion over the desert surface layer near oases is also observed and is called “desert effect”. These interaction between oasis and desert were explained and further studied using numerical simulations, including moisture inversion over the desert surface layer were confirmed (Gao et al., 2004; Meng et al., 2012; Meng et al., 2009; Meng et al., 2015; Chu et al., 2005; Han et al., 2010; Wen et al., 2012). During daytime, solar radiation heats the desert surface and rapidly increases the near-surface temperatures in desert areas. In contrast, the oases’ temperature is lower than that over the surrounding desert due to the intense evaporation (Li et al., 2016a), while the humidity is higher than that in the desert. The strong water-heat difference between the oasis and desert causes a local circulation between oasis and desert. The air density and pressure in the near-surface layer in the desert are lower than in the oasis. The pressure difference drives cold moist air to flow from the oasis to the desert, resulting in a moisture inversion in the desert (Liu et al., 2007). In the upper-air, the hot dry air over the desert flows toward the oasis, resulting in the oasis becoming a cold, wet island capped by a warm, dry air. This study results confirmed further the observation of temperature inversion layer and negative sensible heat fluxes in oases (Li et al., 2013; Su and Hu, 1987; Rosenberg, 1969; Wang et al., 1993). Therefore, the Oasis Breeze Circulation (OBC) caused by the significant energy and vapor differences both in horizontal and vertical directions between oasis and desert forms, maintaining development of oasis. (Figure 1-1).

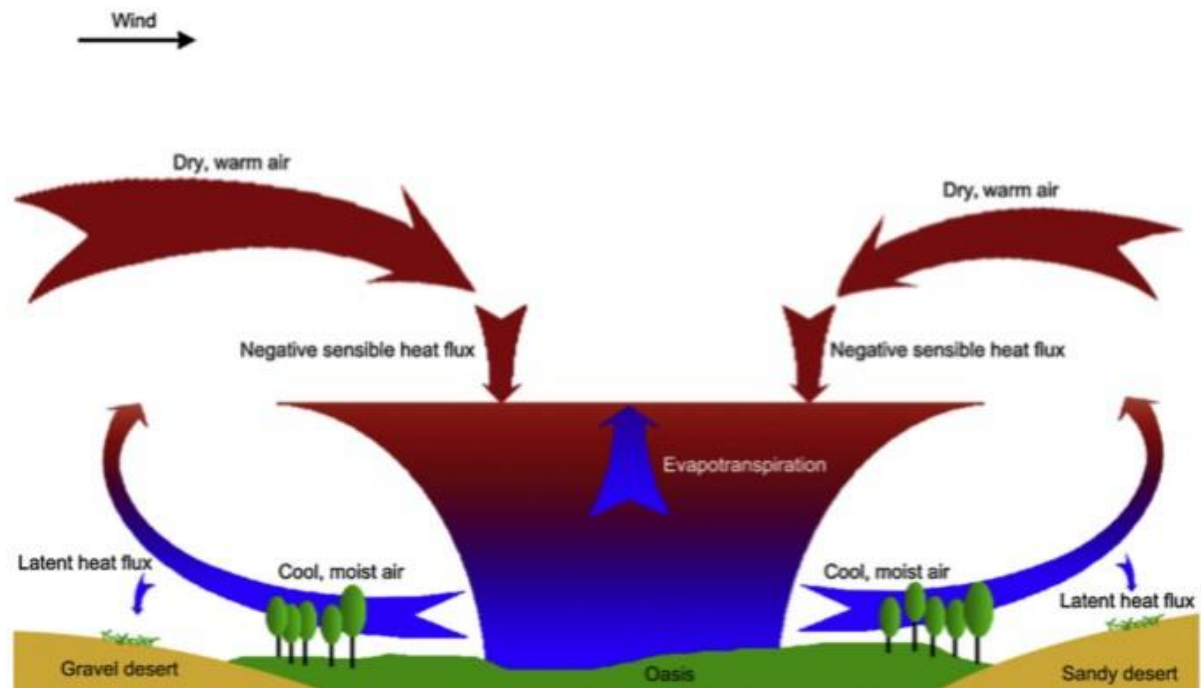


**Figure 1-1. Schematic diagram of the interactions between an oasis and desert cited from paper (Li *et al.*, 2016a).**

## 1.2 Study area

The NTM is located deep inside the CA with special geomorphology of mountain-basin structures. The water resources come only from the mountains (the Tianshan Mountains are the water towers of the CA), whose rivers are all fed by important hydrologic processes of snow and glacial melting, and precipitation from the mountain ranges (Immerzeel *et al.*, 2010), flow into artificial lakes and disappear in the desert area in the basin (Luo *et al.*, 2010). Based on the limited runoff (Bothe *et al.*, 2012) and the unrestricted groundwater exploitation (Ming jiang, 2009), oasis systems with a relatively high primary productivity are developed in the groundwater overflow zone and the surrounding deserts between the mountain and the desert (Luo *et al.*, 2010). Thus the NTM can be divided into various watersheds consisting of mountains, oases, and desert areas, called as the Mountain-Oasis-Desert ecoSystem (MODS). In general, the elevation of such typical MODS increases dramatically from a few hundred meters in the plain to over 5,000 meters above sea level in the mountainous area within a horizontal distance of less than 100 kilometers, which develops a natural vertical zone spectrum of land cover including snow/ice, alpine meadow, mid-mountain forest/meadows, low-mountain dry grasslands, alluvial plains, oases and plain deserts, etc. (Figure 1-4b).

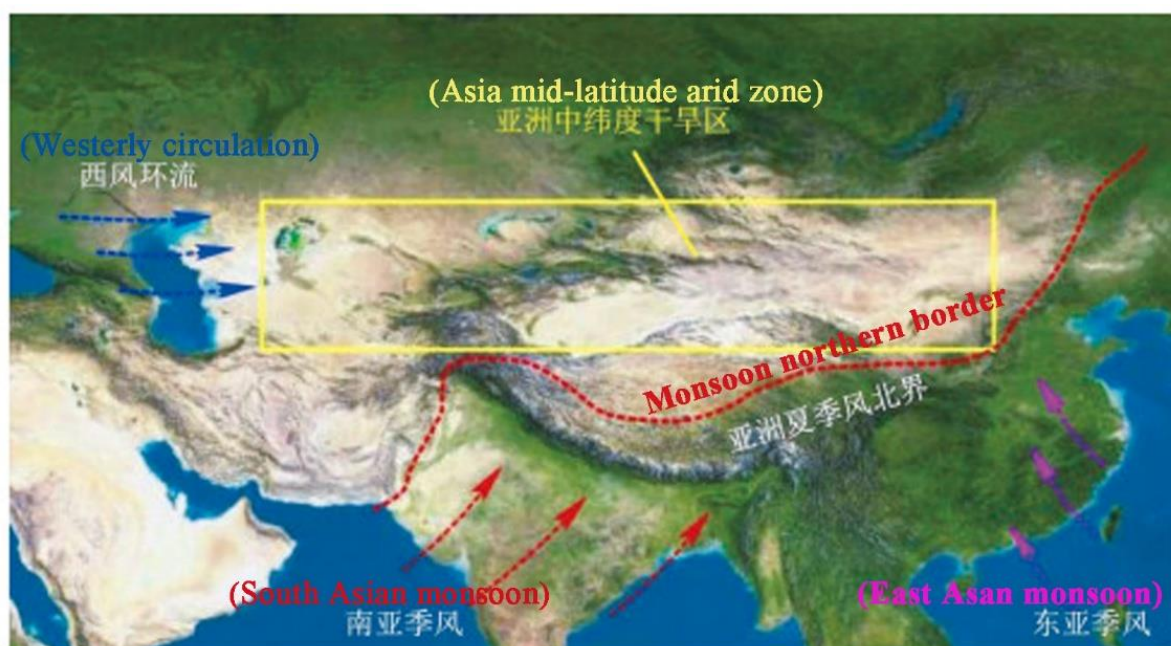


**Figure 1-2. Central Asian circulation background**

The CA is controlled by both the westerly circulation in the middle-high latitudes and monsoon from the southern and eastern Asia (Bothe et al., 2012). Since the Tianshan Mountains block the water vapor from the Pacific Ocean and the Indian Ocean, whereas faint water vapor coming from the far Arctic Ocean and the Atlantic Ocean is also concentrated in the mountains due to the topography (less than 250 mm in the basin regions and 900 mm in the mountains). The annual average temperature in this area is 6.6 °C, the average temperature is 24.8 °C in the hottest month and 16.1 °C in the coldest month, the annual extreme temperature ranges from -42.8 to 43.1 °C. The average annual temperature in the glacier region is -10.5 °C, while the mean annual temperature in the plain area is about 11.8 °C. Thus, the NTM experiences the typical arid continental climate with categories of scarce and concentrated rainfall, sufficient sunshine, large evaporation, severe temperature changes, dry climate.

### 1.3 Methodology

#### 1.3.1. WRF

The WRF is an advanced mesoscale numerical weather prediction system designed for both atmospheric research and operational forecasting needs. It is jointly administered by the National Center for Atmospheric Research and the National Centers for Environmental Prediction. The WRF model has two cores, the Advanced Research WRF (ARW) and the

Nonhydrostatic Mesoscale Model (NMM) (Skamarock et al., 2001) for research and business, respectively. There are various land surface models (LSMs) prescribed in the WRF. The NOAH is a widely used land surface process in WRF. The main input parameters for WRF-NOAH are the first-level parameters including the land use (LU) types, soil texture, slope and the second-level parameters including albedo, leaf area index (LAI), green vegetation fraction (GVF) and emission, et al.. The second level of parameters can be calculated from the first level of parameters. Before 2009, most of the terrestrial datasets in WRF-NOAH were generally derived from the Advanced Very High Resolution Radiometer (AVHRR) data, provided by the United States Geological Survey(USGS). For example, the LU data used in the WRF model are derived from the AVHRR data from 1992–1993 (Wen et al., 2012). The land surface is assigned to 24 different LU categories according the USGS classification system, whereas, the GVF datasets used in the WRF are based on multi-year averages of monthly maps derived from the AVHRR satellite data from 1985-1991 (Cao et al., 2015). The LAI and albedo are normally from a look-up table, in which the maximum and minimum constant values of the two parameters change with the LU. After the version 3.0 (Wang et al., 2012), WRF technically made great improvements on the choice of the land surface terrestrial datasets. An option of LU derived from the MODIS satellite data from January 2001 to December 2001 (Rydsee et al., 2015) using the IGBP classification system with 20 categories of land use types was added. Based on the MODIS land use types, a new look-up table “VEGPARM.TBL” with various second-level parameters could be used to update the values in the original LANDUSE.TBL. Moreover, the parameters including Albedo, LAI and GVF can use spatial data derived from MODIS. Firstly, the actual albedo, LAI and GVF data derived from MODIS products can be converted to the format that metgrid.exe processed in the WPS (WRF Preprocessing System). Secondly, setting usemonalb, sst\_update and rdlai2d in the file of “namelist.input” as “true”, then WRF can select the monthly spatial datasets of albedo, GVF and LAI from “wrflowinp”, respectively. However, the default terrestrial datasets in most RCMs (even WRF) just represent the land surface conditions in a certain period (normally outdated), which limited WRF’s ability to accurately simulate the weather and climate conditions dynamically, we can updated the spatial datasets using actual datasets from remote sensing products.



## WRF Modeling System Flow Chart

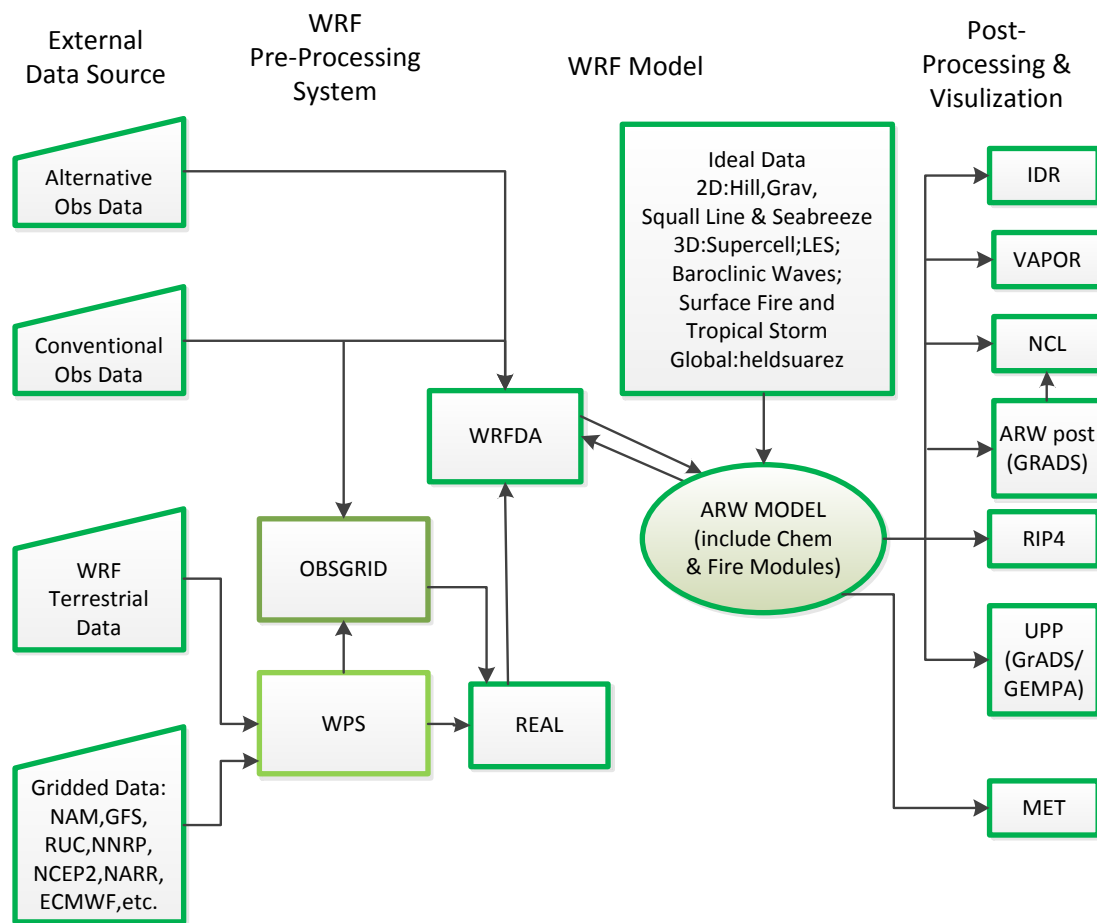


**Figure 1-3. Work flow of the WRF model**

The WRF model has the following four components including the Pre-processing System (WPS), Weather Research Forecast Vibrational Data Assimilation System (WRF-DA), Advanced Research WRF (ARW) and WRF Post-Processing (WPP) and visualization tools (Figure 1-3). The WPS's function is to transform the large-scale terrestrial and meteorological data into the format suitable for ingest by the ARW's real data pre-processor and it includes three applications: geogrid.exe, ungrib.exe, metgrid.exe, respectively. The geogrid.exe can extract interested region and interpolate large-scale terrestrial data into certain resolution; the ungrib.exe converts the grib file of raw meteorological data into the format which is suitable for the application of metgrid.exe; and the function of metgrid.exe is to combine the terrestrial and meteorological data after processing from geogrid.exe and ungrib.exe, and make them suitable for the ARW. All the three application runs are on the basis of parameters in the namelist.wps. The WRF-DA is a dynamic assimilation system that incorporates observations during the simulation (not used in this study). The core of

WRF is ARW, which includes the applications of `real.exe` and `wrf.exe`. The application of `real.exe` is the last standardized procedure that mainly generates the necessary initial conditions (`wrfinput`) and boundary files (`wrfbdy`) for `wrf.exe` running. The two applications depend on the parameters in the “`namelist.input`” file. Before performing a simulation, we used the `WRFDomainWizard` to set the WRF Domains and parameter lists of `namelist.wps` and `namelist.input` mentioned above (details can be seen in the chapter 7. Appendix). The `WRFDomainWizard` application does not belong to the WRF system and its function is to automatically generate the required domains and parameters with a visual interface. The WPP is to post-process and display the ARW simulation output data. In this study, we only used the NCL programme.

### 1.3.2. Model configurations

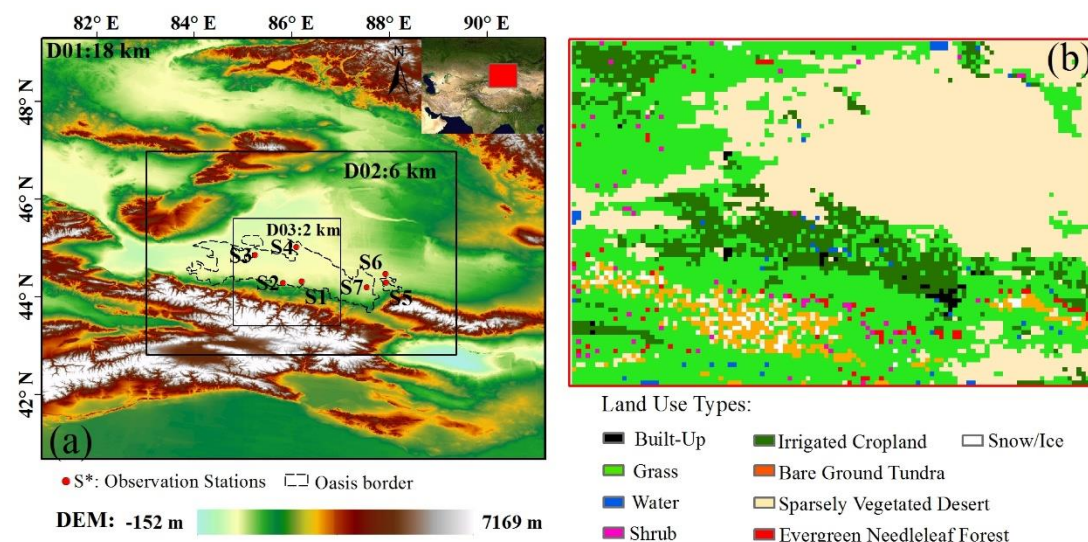


**Figure 1-4. (a) simulation domains of WRF-Noah and land surface elevations, meteorological sites, (b) Land use (LU) types of the study area**

In this study, the WRF version 3.6, which was coupled with NOAH, was used in our simulations. The NTM is functioning as the study area in this thesis because it includes many of the special characteristics of the MODS (Figure 1-4). Furthermore, the periphery of the NTM region has experienced intense human activities, such as oasis expansion, urbanization and desertification in the past 60 years (Lioubimtseva et al., 2005; Yao and Zhang, 2013). The WRF was configured for a fine-scale simulation with two nested domains in chapter 2 and 3, and three-nested domains in chapter 4 based on chapter 2 and 3 (D01, D02 and D03 in Figure 1-4). The simulation region (D01) covers the whole NTM,

captures the effects of mountainous background and spans a total area of  $890 \text{ km} \times 975 \text{ km}$  with a horizontal spatial resolution of approximately  $18 \text{ km} \times 18 \text{ km}$ ; D02 and D03 is the interest area in this study, the core area D02 has a total area of  $530 \text{ km} \times 465 \text{ km}$  with a horizontal spatial resolution measuring  $6 \text{ km} \times 6 \text{ km}$ ; the innermost domain D03 covers a total area of approximately  $330.78 \text{ km} \times 244.23 \text{ km}$  with a horizontal spatial resolution of about  $2 \text{ km} \times 2 \text{ km}$ .

**Table 1-2. Physical parameterization schemes**

Physics	Scheme	References
Boundary layer	Yonsei University (YSU)	(Song <i>et al.</i> , 2006)
Microphysics	WRF Single Moment-3 (WSM3)	(Song <i>et al.</i> , 2004)
Cumulus clouds	Kain-Fritsch Scheme	(Bretherton <i>et al.</i> , 2004)
Long-wave radiation	Community Atmospheric Model (CAM)	(Collins <i>et al.</i> , 2004)
Short-wave radiation	Community Atmospheric Model (CAM)	(Collins <i>et al.</i> , 2004)
Land surface model	Noah	(Chen and Dudhia, 2001b)

**Table 1-3. Four layer of soil moisture values for oases and desert areas in the NOAH (Wen et al., 2012)**

Land Use Type	Noah Soil Layer	Soil Moisture ( $\text{cm}^3 \text{ cm}^{-3}$ )
Oasis	0–10 cm	0.38 (at 5 cm)
	10–40 cm	0.47 (at 25 cm)
	40–100 cm	0.33 (at 70 cm)
	100–200 cm	0.26 (at 150 cm)
Desert	0–10 cm	0.07 (at 5 cm)
	10–40 cm	0.10 (at 25 cm)
	40–100 cm	0.05 (at 70 cm)
	100–200 cm	0.06 (at 150 cm)

The ERA-Interim reanalysis data provides the initial and lateral boundary conditions for simulations at 6-h intervals (detailed can be seen in section 1.3.1). The simulation results from domain D02 are stored and provide hourly lateral boundary conditions for D03. All domains ran with 35 unevenly spaced full eta levels with 15 levels below the height of 5 km from the ground surface. The model top was fixed at 50 hPa. The different parameterizations of the physical atmospheric schemes have been performed previously in

the study region by Qiu et al. (Qiu et al., 2017). We referenced the best one of WRF configurations (of physical schemes) shown in Table 1-2. The initial soil moisture and the soil boundary temperatures are derived from the forcing data; however, the soil moisture levels of the oases and desert areas are adjusted using observations (**Error! Not a valid bookmark self-reference.**).

### 1.3.3. Validation

The validation of the models is a very important part in this dissertation. The validation directly described the response of WRF to the land surface terrestrial datasets in chapter 2, and clarifies whether the newly developed irrigation scheme improves the WRF performance in simulating the water-heat conditions of irrigated oasis. We apply the coefficient of determination  $R^2$ , Mean Bias Error (MBE) and Root Mean Squared Error (RMSE) statistics in order to verify the model results on the site scale. All validation work is done using the software R. In this thesis, we also assess spatial patterns of temperature, humidity, energy, and circulation and determine the difference in their daytime and night-time values by averaging daytime simulations from 19:00 to 2:00 UTC and nocturnal simulations from 08:00 to 14:00 UTC. But the spatial patterns of precipitation in their daytime and night-time values by averaging or adding daytime simulations from 14:00 to 5:00 UTC and nocturnal simulations 06:00 to 13:00 UTC in the irrigation season

## 1.4 Datasets

### 1.4.1. Forcing data

Reanalysis data is the processes of the assimilation of all kinds of data, including the ground-based surveillance, ship/balloon/radioprobe/aircraft/satellite observations and other information, to generate a new, long-term and continuous higher spatio-temporal resolution product. At present, NCEP/NCAR (Kalnay et al., 1996), NCEP/DOE (Department Of Energy) (Kanamitsu et al., 2002), NCEP/CFSR (Climate Forecast System Reanalysis), JRA25 (Japanese 25-year ReAnalysis), ERA (European ReAnalyses) and NASA-MERRA (Modern Era Retrospective-analysis for Research and Applications) (Chen et al., 2014) constitute the most common international reanalysis datasets. The latest global atmospheric reanalysis product ERA-Interim (Dee et al., 2011) provides the initial and lateral boundary conditions for the WRF simulation in this dissertation because it

matches well with most of the local climate records, especially in the low-lying plain areas (Hu et al., 2014). These data were produced by the European Centre for Medium-Range Weather Forecasts. The reanalysis data have a spatial resolution of  $0.75^\circ \times 0.75^\circ$  and are forced over a 6-hour time interval, which are available at <http://apps.ecmwf.int/datasets/>. The boundary ranges from the eastern longitude  $80^\circ$  to  $92^\circ$  and the northern latitude  $40^\circ$  to  $50^\circ$  in this study. We used dates in the period from January 1, 2010 to December 31, 2012. We employ the fields describing the geo-potential, relative humidity, temperature, the U and V wind components on the 30 pressure levels and the surface forcing parameters, including the 10-m U and the 10-m V wind, the 2-m dew point temperature, the 2-m temperature, the mean sea level pressure, the sea surface temperature, the sea-ice cover, the skin temperature, the snow density, the snow depth, the soil temperature and the soil water contents in 4 different layers.

#### 1.4.2. Station-based data

**Table 1-4. Meteorological stations' names, locations, elevations and available elements.**

ID	Longitude/ $^\circ$ E	Latitude/ $^\circ$ N	Altitude/m	LU	Elements	Time
S1	86.20	44.32	473.10	Crop/Urban	T2, P, RH, WS, WD	2012
S2	85.82	44.28	469.30	Crop	T2, RH, SW, LW, LE	2010, 2012
S3	85.25	44.85	338.10	Crop	T2, P, RH, WS, WD	2012
S4	86.10	45.02	347.80	Crop	T2, P, RH, WS, WD	2012
S5	87.93	44.29	476	Desert	T2, RH	2010, 2012
S6	87.92	44.48	466	Desert	T2, RH,	2010, 2012
S7	87.53	44.20	440.50	Crop	T2, RH	2010,2012

In-situ observations from seven meteorological stations within domain D02 (Figure 1-4) are applied to validate the simulation results and these four stations are distributed in oasis areas with diverse LU types including irrigated crops, urban areas and combinations of the both (Table 1-4). The T2 represents the 2-m air temperature, the RH stands for the 2-m relative humidity, LE represents the latent heat flux, WS and WD are the wind speed and direction at 10 m; SW and LW demonstrate the downward shortwave and longwave radiation, respectively in the table. The observations from 2012 and 2010 constitute the hourly and daily data. In addition, observations of the latent heat and downward shortwave and longwave radiation from an eddy covariance system at station S2 are also utilized. Due to a damaged radiation sensor, observations of the sensible heat flux are not available.

## 1.4.3. Land use (LU) types datasets

**Table 1-5. Land use types and codes for the 2012LU**

First level code	Categories	Sub-level code	Subcategories		
1	Cropland	11	Irrigated crops (rice, lotus and other aquatic crops)		
		12	Non-irrigated crops (rainfed croplands)		
2	Forestland	21	Closed (> 30%) natural and artificial forests		
		22	Closed (> 40%) shrub		
		23	Closed (10%~30%) woodland		
		24	Other woodland (orchards, mulberry)		
3	Grassland	31	Closed (>50%) grassland		
		32	Closed- to-open 20%~50% grassland		
		33	Open 5%~20% grassland		
4	Water and Wetland	41	Rivers and canals		
		42	Lakes		
		43	Reservoir ponds		
		44	Snow and ice		
		45	Intertidal		
		46	Floodplain		
		5	Settlements	51	Cities and towns
				51	Villages
53	Other construction lands				
6	Others	61	Sandy land		
		62	Gobi		
		63	Saline		
		64	Marsh		
		65	Bare		
		66	Bare rock		
		67	others		

The default LU data (included in the WRF model) stem originally from the USGS, which classifies LU into 24 categories (**Error! Not a valid bookmark self-reference.**) (Wen et al., 2012). A high-resolution LU image was produced for 2012 (2012LU) using visual interpretations based on Landsat images and a 1:1,000,000 scale topographic map. This image was generated by the Xinjiang Institute of Ecology and Geography, Chinese Academy of Sciences (Chen, 2008). The 2012LU has a spatial resolution of 30 m and adopts a hierarchical classification system with a spatial resolution of 30 m, including 6 categories and 25 subcategories (

Table 1-5). We converted it into the USGS classification system according to the corresponding relations shown in the

Table 1-5. We studied the uncertainties on conversion of LU data using different classification systems in MODIS, and found that the uncertainties decreased quickly from high to low levels of aggregation (Zhang et al, 2017). The actual LU has spatial resolution of 30 m and more detailed categories, the conversion in fact, is a process of aggregation from high-level to lower level of both thematic and spatial resolution, thus, the uncertainties could be ignored.

**Table 1-6. Land use types and its codes in the WRF and corresponding relation with the 2012LU**

Land use types	WRF	2013LU
Urban and Built-Up Land	1	51
Dryland Cropland and Pasture	2	
Irrigated Cropland and Pasture	3	11, 12, 52, 21 (if DEM < 1,500)
Mixed Dryland/Irrigated Cropland and Pasture	4	
Cropland/Grassland Mosaic	5	
Cropland/Woodland Mosaic	6	
Grassland	7	31 (if DEM ≥ 1,000), 32 (if DEM ≥ 1,000), 33 (if DEM ≥ 1,000)
Shrubland	8	23, 22 (if DEM < 1,500)
Mixed Shrubland/Grassland	9	
Savanna	10	
Deciduous Broadleaf Forest	11	
Deciduous Needleleaf Forest	12	
Evergreen Broadleaf Forest	13	
Evergreen Needleleaf Forest	14	21 (if DEM ≥ 1,500), 22 (if DEM ≥ 1,500)
Mixed Forest	15	
Water Bodies	16	41, 42, 43, 46,
Herbaceous Wetland	17	
Wooded Wetland	18	
Barren or Sparsely Vegetated	19	61, 62, 63, 65, 67, 66 (if DEM < 3,400), 31 (if DEM < 1,000), 32 (if DEM < 1,000), 33 (if DEM < 1,000)
Herbaceous Tundra	20	
Wooded Tundra	21	
Mixed Tundra	22	
Bare Ground Tundra	23	66 (if DEM ≥ 3,400)
Snow or Ice	24	44

#### 1.4.4. Land surface terrestrial datasets from MODIS

##### Albedo product

The MODIS Bidirectional Distribution Reflectance Model (BRDF) 16-Day surface albedo standard products have been validated through comparisons with in situ measurements (Cescatti et al., 2012; Stroeve et al., 2013). The high-quality primary algorithm for the MODIS standard albedo product (MCD43) has also been shown to produce consistent global quantities over a variety of land surface types and snow-covered conditions (Román et al., 2013). We used the nadir BRDF-adjusted reflectance MCD43A4 (MODIS Terra+Aqua Nadir BRDF-Adjusted Reflectance 16-Day L3 Global 500-m SIN Grid V005), which is computed for each MODIS spectral band (1-7) at the mean solar zenith angle. MCD43A4 images were downloaded from <https://modis.gsfc.nasa.gov/data> with strip numbers of h23v04 and h24v04 for every month in 2010 and 2012. We reprocessed them using the same coordinate systems and resolutions via numerical simulations.

### **LAI product (MYD15A2)**

The MODIS global LAI product has been validated to the Committee on Earth Observation Satellites Stage 2 (Yan et al., 2016a; Yan et al., 2016b), and determined to have a strong continuity and consistency for all biome types. On global and regional scales, earth observation-based estimates of LAI serve as valuable inputs for climate and hydrologic modelling (Fensholt et al., 2004). In this study, the level-4 MODIS global LAI MYD15A2 (MODIS/Terra+Aqua LAI/FPAR 8-Day L3 Global 1-km SIN Grid V005) was utilized.

### **GVF data from the MODIS Vegetation Indices (MOD13A2)**

Validation to stage 3 has currently been achieved for the MODIS vegetation indices (MOD13) and analyses produced by various airborne and field validation campaigns demonstrate that over most biomes, the MODIS near-nadir satellite vegetation indices shows a strong agreement with the top-of-canopy nadir vegetation indices and the land surface biophysical properties (Sesnie et al., 2012; Sims et al., 2011). Using this qualified MODIS NDVI (Normalized Difference Vegetation Index), the GVF can be calculated as (Yin et al., 2016; Miller et al., 2006; Seungbum et al., 2009),

$$\text{GVF} = \frac{\text{NDVI} - \text{NDVI}_s}{\text{NDVI}_v - \text{NDVI}_s} \quad (1)$$

where NDVI denotes the NDVI value for each pixel from the MODIS NDVI,  $\text{NDVI}_s$  is the NDVI value for a sparsely vegetated or barren vegetation area, and  $\text{NDVI}_v$  represents the NDVI value corresponding to a full vegetation cover type. Both  $\text{NDVI}_v$  and  $\text{NDVI}_s$  are



constant, allowing the pixel-level GVF to reach theoretical values of 0.0 to 1.0 for any LU. In reference to the previous paper (Zeng et al., 2000; Gutman and Ignatov, 1998; Jiang et al., 2010; Li and Zhang, 2016),  $NDVI_S$  and  $NDVI_V$  were empirically determined to be 0.05 and 0.87, respectively. These two parameters serve as global bounds to ensure that the derived GVFs vary from 0.0 to 1.0 (i.e.  $GVF = 1.0$  when  $NDVI > 0.87$  and  $GVF = 0.0$  when  $NDVI < 0.05$  in Eq. (1)). The MOD13A2 (Didan, 2015) Version 6 product (MODIS/Terra VI 16-Day L3 Global 1-km Grid SIN V006) was dealt with in this dissertation.

## 1.5 Rationale and synopsis

### 1.5.1. Research objectives and questions

The climate of the NTM changes obviously from the warm-dry to the warm-wet trend with the year 1987 as a turning point, while the change range of other arid regions in CA is less intense and develops toward a warm-dry trend. At the same time, the NTM experienced intense human activities in the past 60 years and irrigated oasis increased with 4 times more than its original size. Based on the literature review and background in section 1.1, the cold-wet island effects of oasis were assumed and the interaction between oasis and desert is believed to play an important role in maintaining the existence of oases over time. Thus, the abnormal regional or local climate change in NTM may be likely to respond to the rapid oases expansion and intensive irrigation in the MODS. In the context of the LUCC's impact on the climate, this dissertation studied the local climate of a typical MODS in the CA (a microcosm of the terrain and climate of CA) and the effect of irrigated oasis on the climate in the NTM using WRF model. In order to answer the research questions above, the research workflow in Figure 1-5 followed. Firstly, related data were collected and used to construct an comprehensive database. They include meteorological observation, LUCC, biophysical and terrestrial parameters from satellite products over the study area (including surface albedo, LAI and GVF, land surface temperature and NDVI) and forcing datasets. Secondly, the regional climate model WRF was localized with updating outdated terrestrial datasets by actual satellite products and with adding a drip irrigation process in the simulation. Thirdly, the localized models are applied for simulating and exploring effects of mountain, oasis, and desert on water-heat patterns of the whole MODS, and the mutual interaction of each subsystems among MODS. All of the works aim to explore the relationship between irrigated oasis and regional climate change in complex MODS. The

answer will provide useful information for further investigation of the impacts of LUCC on climate changes under global climate change in CA. Moreover, it can deliver the scientific support to the oasis water resources management and it is essential to the sustainable development and ecological stability of oases. Four detailed key scientific issues were answered.

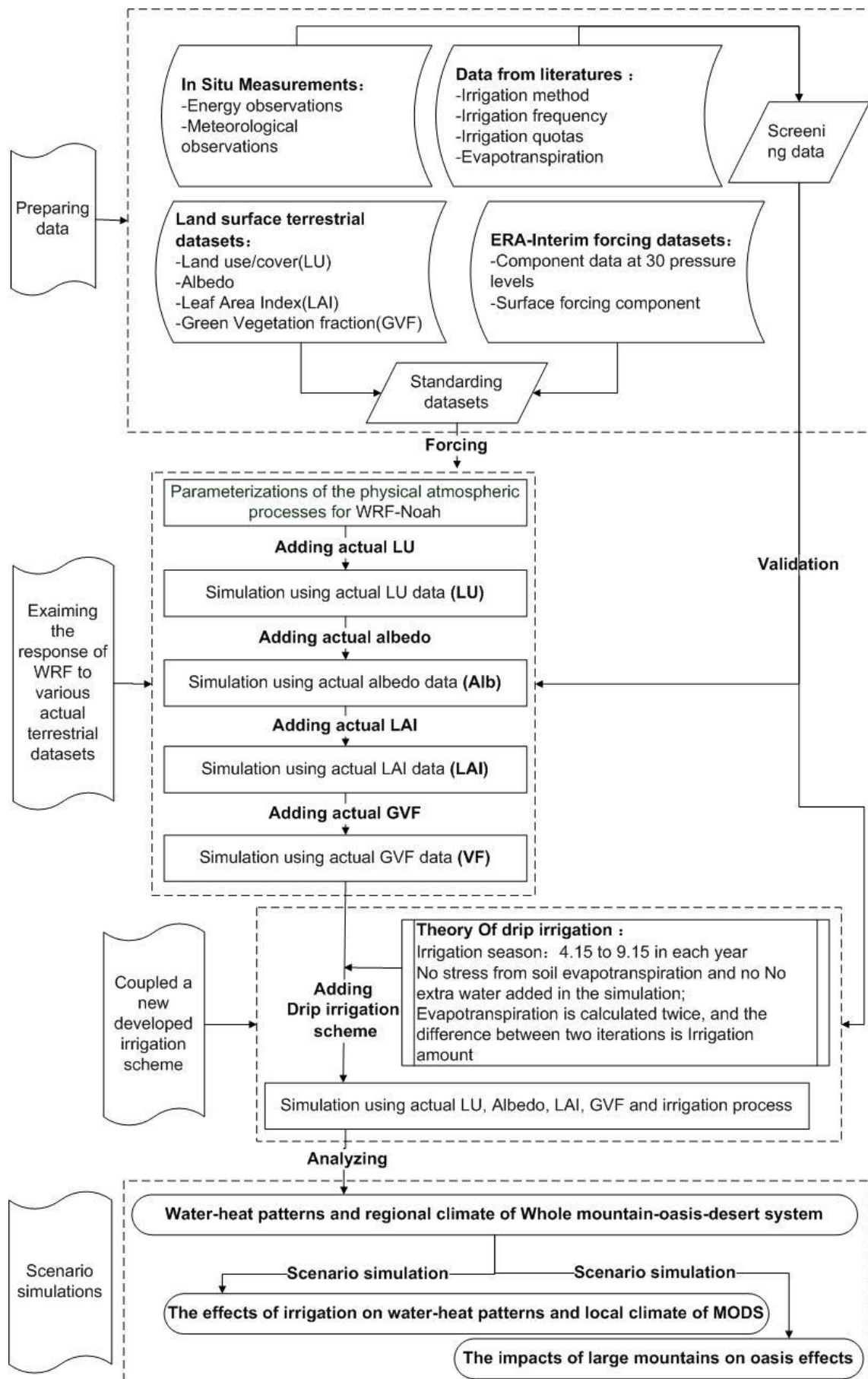


Figure 1-5. Work flow of study

***Question 1: What are the responses of the WRF performance to various actual terrestrial parameters derived from satellite products ?***

On this small-scale climate research, WRF's performance in simulating the water-heat condition of complex MODS are the key issue. The default terrestrial datasets in the WRF, even most RCMs in the world, are generally derived from the AVHRR data in the 1990s and only represent one certain period of land surface conditions. The insufficiency of outdated terrestrial datasets and the inability to implement a dynamic change of terrestrial datasets makes the ability of WRF to accurately simulate the weather and climate conditions limited. Using actual terrestrial datasets from satellite products to update the outdated terrestrial datasets in the WRF is the only possible solution to the insufficiency and the MODIS products provide partly actual datasets (albedo, LAI and GVF) after 2000, (Cao et al., 2015; Deng et al., 2015; Yin et al., 2016; Wen et al., 2012; Xu et al., 2015; Meng et al., 2009). However, these terrestrial datasets from satellite products were scarce before 2000 and field measurements are temporally and spatially limited, especially in complex MODS. These limitation makes updating default datasets in the WRF using real-time, even monthly, actual various satellite terrestrial datasets very time- and labour-consuming. Whether simulations using WRF with updating several key observed datasets are meeting expected results in various applications whilst reducing the time and labour cost, especially for land surface modeling or climate modeling, and also partly overcome the limitation of scarce observations and satellite products in such a complex region ? This is a very meaningful work in the arid CA, which is characterized by typical MODS and is known for climatic change.

***Question 2: How does the WRF coupled with a newly developed drip irrigation process perform in simulating the water-heat conditions of irrigated oasis?***

Since the 1950s, drip irrigation under plastic film, as an effective farmland management method, has been used so as to conserve the limited water resources in the NTM (Fan et al., 2013), and oases cannot survive without irrigation in the NTM in arid area. However, there were no irrigation schemes implemented in the accompanying NOAA in the official releases of WRF (Chen and Dudhia, 2001b; Chen and Dudhia, 2001a), also in most of the other RCMs. Most model improvement methods for irrigation from literature reviews include initialized irrigated crops with a high soil moisture without additional water (Jiang

et al., 2014; Qu et al., 2013; Cao et al., 2015; Deng et al., 2015; Kueppers and Snyder, 2012) or regarding irrigation as precipitation (Ozdogan et al., 2007) or letting soil moisture continuous saturation (Pei et al., 2016; Evans and Zaitchik, 2008; Zaitchik et al., 2005; Meng et al., 2009; Zeng et al., 2017; Branch et al., 2014). These descriptions for irrigation are not suitable for the current oasis management in arid area. We examine whether simulations using WRF with a new developed drip irrigation realistically simulate the heat-water conditions of such drip-irrigated oases in the NTM, which is the premise to study historic contribution of irrigation and the oasis evolution on regional climate change.

***Question 3: What are the effects of drip irrigation on atmosphere structure of MODS?***

Water is a particularly scarce and valuable good for both human livelihoods and ecosystems in the NTM (Gessner et al., 2013) because the water resources only come from the mountains (Sorg et al., 2012), whose rivers are all fed by important hydrologic processes of snow and glacial melting, and precipitation from the mountain ranges (Immerzeel et al., 2010), flow into artificial lakes, disappear in the desert area's basin (Luo et al., 2010). Based on literature reviews regarding the climate effects of irrigation, it shows that irrigation could be an important component of climate change. Irrigation results in an increase of the latent heat flux and a decrease in the sensible heat flux, thereby leading to a decrease in temperature (Kueppers and Snyder, 2012; Jiang et al., 2014). However, how does the typical drip irrigation influence the water-heat patterns and atmospheric structure in complex MODS? The answer to this question is still unclear and very significant for a regional sustainable development under the limited water and soil conditions in the arid NTM.

***Question 4: What are the impacts of large mountains on irrigated oasis-desert interaction in a typical mountain-oasis-desert ecosystem?***

Oasis effects are thought to play an important role in maintaining the existence of oases over time. Most oases researches believe that the cold-wet island effects of oases and the OBC between the oases and the desert maintain the oases' ecological stability by reducing heat and moisture exchanges between oases and the surrounding desert areas, called the "self-supporting mechanism of the oasis". However, oasis cannot survive without water supply from the nearby large mountains in a MOD and land surface-atmosphere interactions are complex and depend on many factors. The background of the circulation is

a complex system (Song et al., 2004). Therefore, studies should explore the oasis effects (i.e. the oasis-desert interactions) under impacts of these surrounding mountains rather than focusing only on the oasis and desert areas (Chu et al., 2005; Gao et al., 2004; Han et al., 2010; Liu et al., 2007; Lv et al., 2005; Meng et al., 2015; Meng et al., 2012; Meng et al., 2009; Nnamchi, 2011; Wen et al., 2012). Failing to consider the impact of the mountains may result in an incorrect or incomplete understanding of the oasis-desert interactions within MODS. For example, what are the spatial patterns of water and heat throughout the MODS? Do intense mountain-valley winds occur within the current MODSs (Zardi and Whiteman, 2013; Helgason and Pomeroy, 2012) ? Finally, how does the mountain-valley wind, if present, influence the oasis effects and OBC ? The answers to these questions are unclear and deserve additional and comprehensive investigation.

Question 1 aims at the model performance in the simulation of climate elements in MODS using actual terrestrial datasets. Question 2 focuses on examining whether the WRF performance coupled with a newly developed drip irrigation scheme realistically represents the water-heat conditions of irrigated oasis in the NTM. And at the same time, we analyzed the climate effects of irrigation on the atmospheric structure and the conditions of the relatively closed MODS in Question 3. According to the understanding of the first three questions, Question 4 analyzes the water-heat of MODS comprehensively, distinguishes the contribution of oases and mountains to these conditions, and explores the interaction mechanism between the mountains, oasis and desert.

#### 1.5.2. Dissertation outline

The research questions stated above are addressed in the following chapters of this dissertation. All the chapters are connected by logical relationship diagrammed in a framework (Figure 1-6). The chapter design corresponds to the research questions, and all of chapters contribute so as to clarify the primary objective. The localization of the WRF in Chapter 2 and 3 constitute the foundation for the following questions addressed in Chapter 4. Chapters 2 through 4 correspond to papers, which are published or prepared for publication in international peer-reviewed journals.

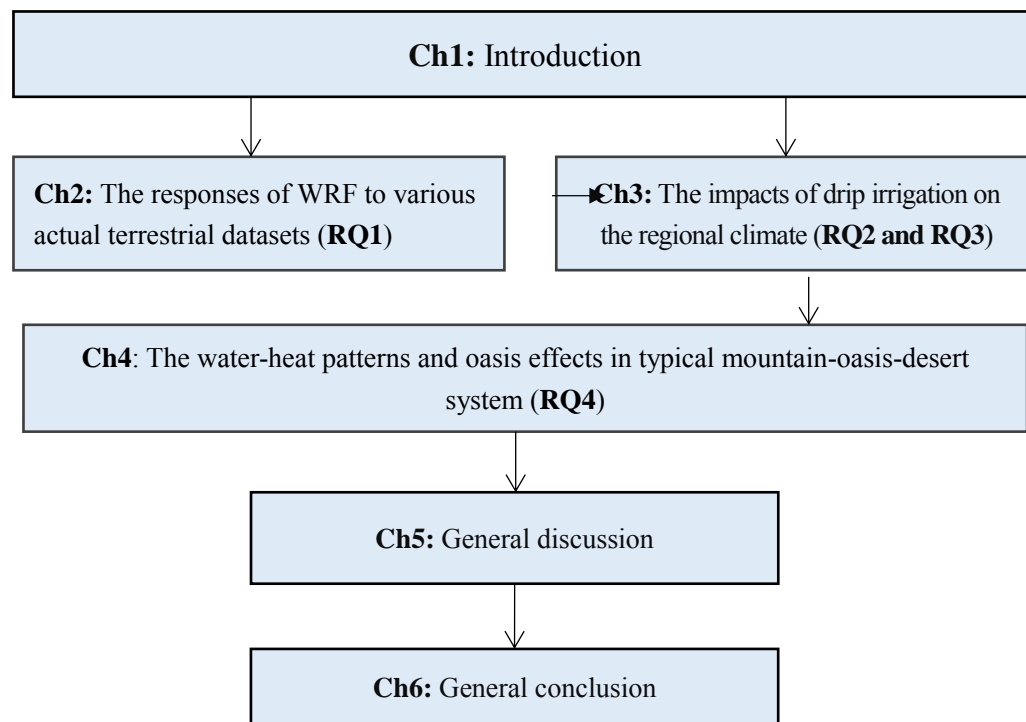


**Figure 1-6.** Outline of the dissertation

***Chapter 2. The response of WRF to various actual terrestrial datasets.***

This chapter, which contents were published in Remote Sensing (Zhang et al., 2017a), describes the impact of using the actual LU, albedo, LAI and GVF data from satellite products in WRF on the model performance. Firstly, we compared the differences between the actual terrestrial datasets from the satellite images and the default datasets in the WRF. Secondly, five simulations were conducted by updating LU, albedo, LAI and VF gradually with the same meteorological forcing data and model schemes: def (using the default LU, albedo, LAI and VF data), LU (using the actual LU data only), Alb (using the actual LU and albedo data only), LAI (using the actual LU, albedo, and LAI), and VF (using all of the actual LU, albedo, LAI, and GVF together). Finally, we analyzed the spatial pattern's differences of T2, RH, LE and WS of MODS from five simulations and quantify which actual terrestrial datasets the WRF was most sensitive to.

***Chapter 3. The impacts of drip irrigation on the atmospheric structure and the local climate.***

Chapter 3 (Zhang et al., 2017, submitted) explores the impacts of drip irrigation on energy balances, temperature, precipitation and atmospheric structure in MODS, using WRF with a new irrigation process. Firstly, we developed a new drip irrigation scheme in line with

the current irrigation scenarios in arid MODS. Then, we conducted two simulations with and without a drip irrigation scheme with updating LU and GVF in the WRF based on the configuration in the Chapter 2. By validation on a site level, we examine whether the newly developed irrigation scheme is improving the performance of the WRF in the simulation of the water-heat conditions of irrigated oasis. Finally, the spatial and temporal distinctions of the two simulations show the climate effects of irrigation in MODS.

#### ***Chapter 4. The water-heat patterns and oasis effects in typical mountain-oasis-desert system***

Chapter 4, which was published in the atmosphere (Zhang et al., 2017b), investigated the temperature, humidity and regional circulation patterns of the complete MODS in the NTM and the oasis effects within the MODS using the WRF. Firstly, three numerical simulations were performed with the same configuration as in chapter 3 but only in July, 2012. The mod simulation applies actual LU and GVF from satellite products and coupled a new irrigation scheme. The non-oasis simulation is a scenario simulation in which oasis areas are replaced by desert conditions, while all other conditions are the same as in the mod simulation. Finally, the non-mountain simulation is a scenario simulation in which the elevation values of all grids are set to a constant value of 300 m, while all other conditions are the same as in the mod simulation. The differences between the mod simulation and the non-oasis simulation and the differences between the mod simulation and the non-mountain simulation were used to quantitatively investigate the effects of oases and mountains, respectively, on the temperature, humidity and circulation features within complete MODS.

Chapter 5 and Chapter 6 summarize and discuss the results of the previous chapters and also present several important points for future research. A general discussion on the initial research questions and their results is given in Chapter 5. Chapter 6 summarizes the main conclusions of this dissertation.

#### 1.5.3. Out of scope

Not all aspects of this topic can be included in a given research study and this gap always drives future investigations. Although we added an irrigation scheme to the WRF, the effects of plastic mulching are still not considered in the simulation. Moreover, we only examine the impacts of LU, albedo, LAI and GVF on the WRF performance. Other



parameters such as emission, rough length of the land surface et al. might have a great impact in this region. We only performed a short-term simulation in our study, a long-term simulation (more than 35 years) will be performed to quantitatively explain the climate effects of the historical oases' expansion on the regional climate.

In addition, more energy observation data with a different underlying surface in MODIS would definitely be better so as to validate the simulation work of WRF. For example, there are no observations available on the sensible heat flux of the irrigated oasis, not to mention observational data on the energy balance in the desert. The limited observations for energy reduce our grasp of the physical reality, which potentially adds uncertainty to the WRF modeling.



# CHAPTER 2

## THE RESPONSES OF WRF TO VARIOUS ACTUAL TERRESTRIAL DATASETS

---

*Modified from: Miao Zhang, Geping Luo, Philippe De Maeyer, Peng Cai, 2017. Improved Atmospheric Modelling of the Oasis-Desert System in Central Asia Using WRF with Actual Satellite Products. Remote Sensing, 2017. 9(12): 1273; doi:10.3390/rs9121273.*

## ABSTRACT

Because of the use of outdated terrestrial datasets, regional climate models (RCMs) have a limited ability to accurately simulate weather and climate conditions over heterogeneous oasis-desert systems, especially near large mountains. Using actual terrestrial datasets from satellite products for RCMs is the only possible solution to the limitation; however, it is impractical for long-period simulations due to the limited satellite products available before 2000 and the extremely time- and labor-consuming processes involved. In this study, we used the Weather Research and Forecasting (WRF) model with observed estimates of land use (LU), albedo, Leaf Area Index (LAI), and Green Vegetation Fraction (GVF) datasets from satellite products to examine which terrestrial datasets have a great impact on simulating water and heat conditions over heterogeneous oasis-desert systems in the northern Tianshan Mountains. Five simulations were conducted for 1–31 July in both 2010 and 2012. The decrease in the root mean squared error and increase in the coefficient of determination for the 2 m temperature (T2), humidity (RH), latent heat flux (LE), and wind speed (WS) suggest that these datasets improve the performance of WRF in both years; in particular, oasis effects are more realistically simulated. Using actual satellite-derived fractional vegetation coverage data has a much greater effect on the simulation of T2, RH, and LE than the other parameters, resulting in mean error correction values of 62%, 87%, and 92%, respectively. LU data is the primary parameter because it strongly influences other secondary land surface parameters, such as LAI and albedo. We conclude that actual LU and VF data should be used in the WRF for both weather and climate simulations.

**Key words:** MODIS; Weather Research and Forecasting model; oasis-desert system; oasis effects; Northern Tianshan Mountains; Central Asia

### 2.1 Introduction

The arid region of Central Asia (CA), which includes Kazakhstan, Kyrgyzstan, Tajikistan, Turkmenistan, Uzbekistan, and the Xinjiang Province of China (Hu et al., 2014; Li et al., 2015), is located deep inside the continent and has unique geomorphological characteristics, including mountain–basin systems. In this area, elevations can increase dramatically, from a few hundred meters above sea level in the basin areas to over 5000 m above sea level in the mountainous areas, over a horizontal distance of less than 200 km; thus, there is high

heterogeneity in land cover types (Zhang et al., 2004). Water is scarce and is valuable for both human livelihoods and ecosystems in CA (Gessner et al., 2013); water resources are largely derived from the mountainous areas, whose rivers are fed by hydrologic processes of snow and glacial melt and precipitation (Immerzeel et al., 2010). These rivers flow into artificial lakes and then disappear into the desert areas in the basin (Luo et al., 2010). Given the limited amount of runoff (Bothe et al., 2012) and unrestricted groundwater exploitation in the area (Deng, 2009), oases form at the foothills of large mountains (Souza et al., 2006; Smith et al., 2007; Soltan, 1999; Li et al., 2007; Luo et al., 2010). The geographical and ecological characteristics differ significantly between these oases and the surrounding deserts, causing significant differences in energy budgets, the exchange rate of momentum, and water vapor levels. These differences produce typical oasis effects (Liu et al., 2007) such as the “cold–wet” island effects of oases (an oasis is a wet, cold island capped by warm–dry air), and the thermal differences between oases and the surrounding deserts result in oasis breeze circulation (OBC). Such oasis effects increase in complexity both in and near mountain ranges. Although oases account for only a small proportion of the land surface (e.g., a proportion of 4–5% in Xinjiang, a typical region of the hinterland of the CA), more than 90% of the population and 95% of the socioeconomic wealth are concentrated there (Meng et al., 2009). Therefore, CA, because of its large elevation differences and the importance of oases, can be divided into mountainous region, oases, and desert areas, often named the Mountain–Oasis–Desert ecoSystem (MODS).

The northern Tianshan Mountains (NTM), the core section of the Silk Road, is a typical geomorphological part of CA; it is also sensitive to climate change (Sorg et al., 2012). Recent studies have indicated that annual mean air temperature in the NTM has been increasing at an average rate of  $0.8\text{ }^{\circ}\text{C decade}^{-1}$  (He et al., 2003), which is greater than the average rate in CA ( $0.39\text{ }^{\circ}\text{C decade}^{-1}$  from 1979 to 2011) and the global land surface ( $0.27\text{--}0.31\text{ }^{\circ}\text{C decade}^{-1}$  from 1979 to 2005) (Hu et al., 2014). Precipitation and the frequency of extreme precipitation show a rate of 11.3% in the NTM (He et al., 2003) amid a longer-term drying trend (Xuand Wei, 2004; Lianmei, 2003). Other areas in CA generally show a slight decrease in average annual precipitation (Lioubimtseva and Henebry, 2009; Gessner et al., 2013). Additionally, the region has been experiencing distinct intense oases expansion since the 1950s (Hong et al., 2003; Zhang et al., 2017b; Jia et al., 2004). Oases have expanded more than 400% in the past 60 years (from  $121.0 \times 10^4$  ha in 1949 to  $512.5$

$\times 10^4$  ha in 2010). A series of ecological problems have appeared as a result, including soil salinization, oasis degradation, and desertification (Sun et al., 2011; Wang et al., 2008; Lioubimtseva et al., 2005; Yao and Zhang, 2013). Horton (Zhou et al., 2015; Horton et al., 2015; Qu et al., 2013) found that regional climate change was largely independent or potentially related to land cover change processes. The abnormal regional temperature and precipitation changes in the NTM may be due to the rapid oases expansion. Therefore, understanding the mechanisms of oasis effects and quantitatively investigating the climate effects of oases expansion on the regional climate are important for ensuring the sustainable development and ecological stability of oases, and will also provide useful information for regional climate change assessments (Yan et al., 2014).

Numerical simulation using regional climate models (RCMs) is the most effective method to explore both oasis effects and climatic effects of the oases expansion in the complex mountain–basin systems of CA because RCMs can account for climatic mechanisms not included in field measurements (Yu et al., 2006; Li et al., 2013) and Global Circulation Models (GCMs) (Seungbum et al., 2009; Seneviratne et al., 2006). GCMs are unable to adequately resolve many important meso-microscale processes, like wind patterns and precipitation due to orographic effects based on large-scale convective parameterization schemes, and simpler land surface processes (Kyselý et al., 2016). The Weather Research and Forecasting model (WRF) is an RCM that has been widely used to simulate regional climatic patterns, particularly over the past 10 years (Branch et al., 2014; Cao et al., 2015). Because the default terrestrial datasets in RCMs are generally derived from Advanced Very High Resolution Radiometer (AVHRR) data from 1992–1993, the ability of RCMs to accurately simulate weather and climate conditions is limited by the use of these outdated terrestrial datasets (Lenderink et al., 2007; Vidale et al., 2007). Integrating actual terrestrial datasets from satellite products or observation in the model simulations is a novel way to overcome these limitations. Many numerical simulations have used MODerate resolution Imaging Spectro radiometer (MODIS) products, including land use (LU), albedo, leaf area index (LAI), and green vegetation fraction (VF), to improve the boundary layer meteorology simulation and to explore the climatic effects of land use cover change (LUCC) (Cao et al., 2015; Deng et al., 2015; Yin et al., 2016; Wen et al., 2012; Xu et al., 2015; Meng et al., 2009). The results from the simulations using actual albedo, LAI, and VF indicated that LUCC led to local cooling of 1 °C in the summer and local warming

exceeding 0.8 °C in the winter. By contrast, simulations using default terrestrial datasets showed random changes in temperature. However, these actual datasets mainly came online in the early 2000s; most numerical simulations, especially long-period simulations (many years, even hundreds of years) (Deng et al., 2015) and downscaled GCM runs, have to be performed using (Qiu et al., 2017) default terrestrial datasets provided by RCMs. This choice is motivated by the fact that terrestrial datasets from satellite products are scarce and field measurements are temporally and spatially limited, especially in complex terrain. In addition, simulations using real-time, even monthly, actual various satellite terrestrial datasets in RCMs are very time- and labor-consuming processes. The question remains as to whether simulations using RCMs that update several key observed datasets can meet expected results in various applications, especially for land surface modelling or climate modelling, while reducing the time and labor cost, and also partly overcome the limitation of scarce observations and satellite products in such a complex region.

Therefore, this study aims both to quantitatively examine which actual terrestrial datasets (including LU, albedo, LAI, and GVF) have a great impact on WRF performance, and to improve the simulation of weather and climate conditions over complex and heterogeneous oasis–desert systems near to large mountains. Our specific research objectives are as follows: (1) to compare the differences between the actual LU, albedo, LAI, and GVF datasets and the corresponding default terrestrial datasets over MODS; (2) to quantitatively examine the impacts of using each actual terrestrial dataset on WRF performance and to determine which is key for the WRF simulations with a complex underlying surface; and (3) to comprehensively assess oasis effects including temperature, humidity, energy flux, and circulation patterns.

## 2.2 Study area

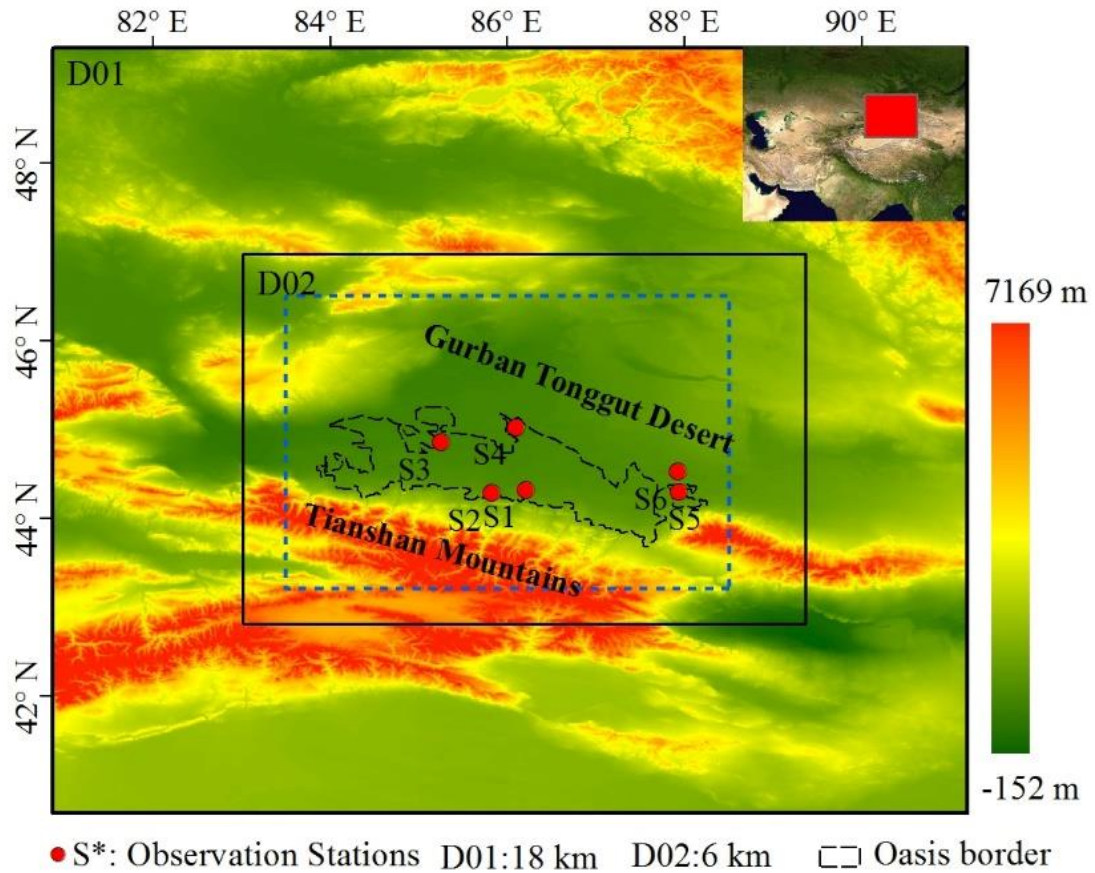


**Figure 2-1. Location of the northern Tianshan Mountains (NTM) in Central Asia, including land surface elevations, meteorological sites, and simulation domain over the NTM (the blue dashed line is the analysis range)**

The information of NTM has been introduced in the section 1.2 and We only used the outer two domain simulation in this chapter (Figure 2-1). Detailed domain information can be seen in section 1.3.2.

## 2.3 Data

### 2.3.1. Forcing data and in situ measurements

The detailed elements and information of ERA-Interim can be seen in section 1.4.1.

We selected observation from meteorological stations of S1-S6 to validate simulation results (Table 1-4). The qualified T2, RH at 2 m, WS, WD at 10 m and precipitation in July at hourly scale in 2012 and at daily scale in 2010 were retrieved. Regretfully, there is no



surface energy observations are available for desert area, we only validated temperature and relative humidity over desert area.

### 2.3.2. Land use data

The detailed information of actual LU (Table 1-5) and corresponding converting relations (The default LU data (included in the WRF model) stem originally from the USGS, which classifies LU into 24 categories (Wen et al., 2012). A high-resolution LU image was produced for 2012 (2012LU) using visual interpretations based on Landsat images and a 1:1,000,000 scale topographic map. This image was generated by the Xinjiang Institute of Ecology and Geography, Chinese Academy of Sciences (Chen, 2008). The 2012LU has a spatial resolution of 30 m and adopts a hierarchical classification system with a spatial resolution of 30 m, including 6 categories and 25 subcategories (Table 1-5).

We converted it into the USGS classification system according to the corresponding relations shown in the Table 1-5.

We studied the uncertainties on conversion of LU data using different classification systems in MODIS, and found that the uncertainties decreased quickly from high to low levels of aggregation (Zhang et al, 2017). The actual LU has spatial resolution of 30 m and more detailed categories, the conversion in fact, is a process of aggregation from high-level to lower level of both thematic and spatial resolution, thus, the uncertainties could be ignored.

Table 1-6) can be seen in section 1.4.3.

### 2.3.3. Albedo product (MCD43A4)

The MODIS albedo product has been introduced in section 1.4.4, we only used two scenes for July 3, 2012, respectively, in this chapter.

### 2.3.4. LAI product (MYD15A2)

The MODIS LAI product has been introduced in section 1.4.4, we only used two scenes for July 3, 2012, respectively, in this chapter.

### 2.3.5. GVF data from the MODIS Vegetation Indices (MOD13A2)

The MODIS NDVI product has been introduced in section 1.4.4, we only used two scenes for July 3, 2012, respectively, in this chapter.

## 2.4 Methodology

### 2.4.1 Model configuration

The detailed WRF configuration has been introduced in section 1.3.2.

### 2.4.2 Experimental design

We designed five sets of numerical experiments to investigate using the impact of each of actual LU, albedo, LAI, and GVF on model results for 2010 and 2012. The experiments were as follows: the def simulation used default LU, albedo, LAI, and GVF provided by the WRF itself; the LU simulation using only actual 2012LU (Chen, 2008); the Alb simulation used actual LU and albedo datasets; the LAI simulation used actual LU, albedo, and LAI datasets; and the VF simulation used all of actual LU, albedo, LAI, and GVF data. The model simulation was initialized from 00:00 UTC on 1 July to 18:00 UTC on 31 July in each year. During this period, the interaction of water and energy between oases and deserts are often the strongest, and oasis crops are at their growth peak. The simulation results were stored hourly with a 60 s time step for integration. Generally, in the absence of accurate, gridded initial soil moisture conditions, a spin-up period is needed to allow the soil moisture within Noah to approach equilibrium within the hydrological cycle (Branch et al., 2014). The optimal spin-up period for any particular application is uncertain and may require years to reach equilibrium (Lim et al., 2012). In this study, the soil moisture values of oasis and desert areas were initialized via interpolation from observed soil moisture data from similar oasis and desert regions referenced in a previous paper (Wen et al., 2012) (Table 2). In addition, following previous simulations that were similar for mesoscale water, surface energy, and circulation (Chu et al., 2005; Meng et al., 2012; Meng et al., 2009), the simulation results for the first 21 days were discarded as spin-up, and only simulations for 19:00 UTC on 22 July to 18:00 UTC on 31 July were used for the analysis. According to observation and simulations, 22–31 July were with anticyclonic and clear-sky conditions (Figure S1); thus, the effects of cloud distribution on results were excluded.

## 2.5 Results

### 2.5.1. Differences between the actual terrestrial datasets and the defaults

We first examined the differences between the actual LU, albedo, LAI, and GVF data and the corresponding default datasets one by one. Both the defaults and the actual satellite images showed generally correct land surface information for MODS. However, there were significant differences, especially in oasis and desert areas, that were strongly impacted by human activities.

Large areas of cropland and barren desert in oases and north-eastern desert areas are apparent in the actual LU data (Figure 2-2a), while the default data show grassland and shrubland in these oases and desert areas. The default LU data in WRF is based on AVHRR satellite data for 1992–1993 (Wen et al., 2012), which represents the original oasis and desert land cover. There has been a large expansion in urban areas and irrigated cropland in the NTM at the expense of sparse shrubland during the last 20 years (Fan et al., 2013). In addition, the default LU data shows a large area of forest in the Ili River basin and did not indicate that ice was found on the mountaintops. These areas are misclassified, because dense grassland and cultivated lands have accounted for the largest areal proportion in this river basin over the past 40 years (Zhu et al., 2010), and glaciers are common at the mountaintops in CA. The spatial consistency was only 38.42% between the actual and default LU data using a rough pixel-by-pixel comparison (Figure 2-2i) (Zhang et al., 2017a).

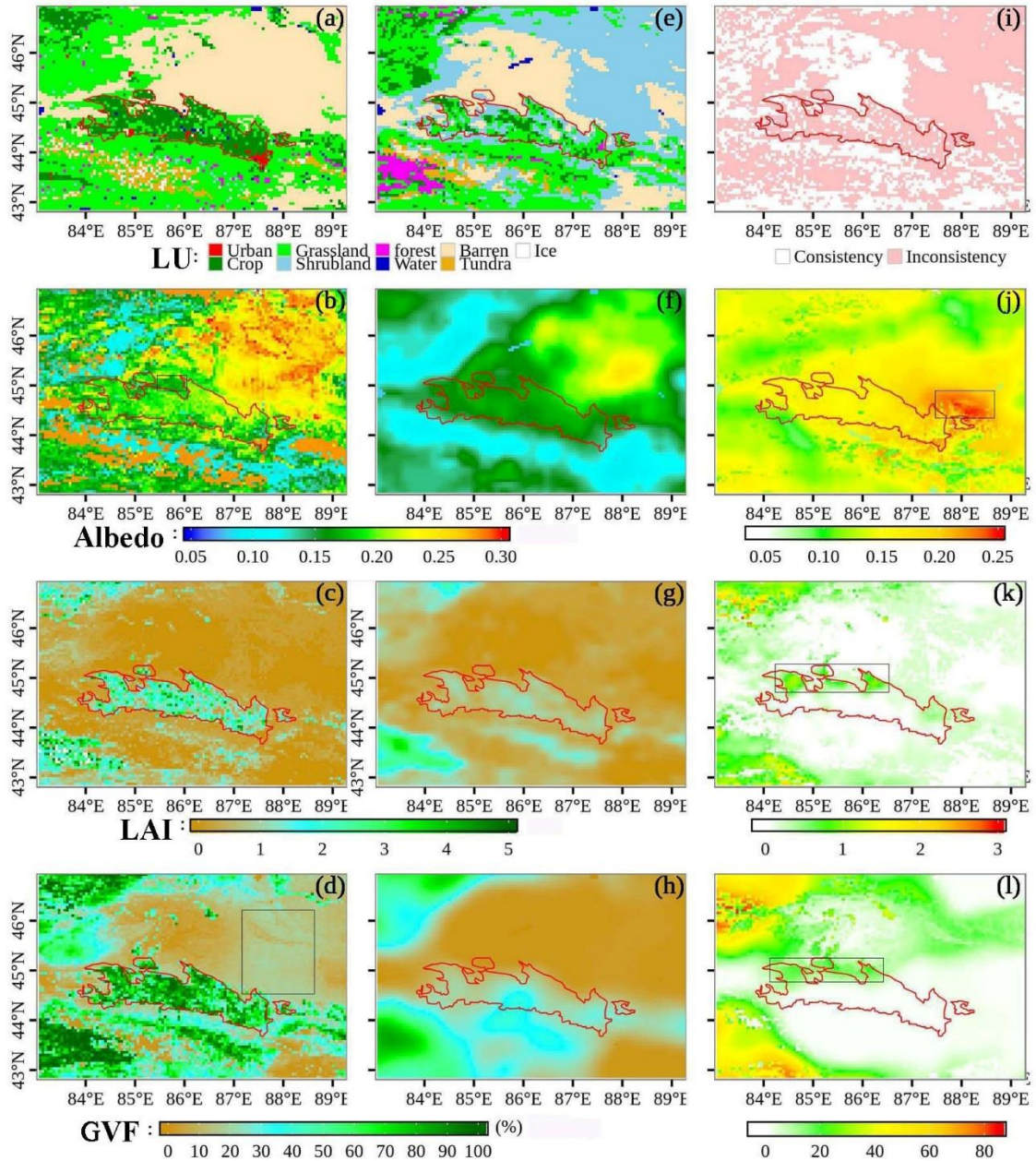


**Figure 2-2. Comparison between actual LU (a), albedo (b), leaf area index (LAI) (c), and green vegetation fraction (GVF) data (d) and the corresponding default data (e–h), with differences shown in (i–l). The red line indicates the border of the key oasis areas, and the black rectangle indicates the region strongly influenced by human activities in oases and desert areas over the past 20 years.**

The default albedo, LAI, and GVF datasets are based on inter-annual averages of monthly climatology for 1986–1991 (Kumar et al., 2014). Figures 2-2b, f, j respectively show the spatial distributions of the actual and default albedo data and the difference between the two. The actual albedo level is overall higher than the default data, ranging from 0.05–0.25

(Figure 2-2j); the difference between the two datasets mainly occurs in the oasis areas and the northern desert areas (Figure 2-2b, black rectangle). There is also a slight difference in the values of approximately 0.10 occurring at mountaintops. It is difficult to explain why albedo would be greater in the actual image than in the default dataset; we would expect albedo to decrease with an increase in crop cover. Albedo is influenced by multiple factors, including LU, GVF, dynamic roughness lengths, solar elevation angle, soil color, and humidity (Zhang et al., 2015). The difference in albedo in the oasis area could be related to the severe salinization caused by irrigation (Litan et al., 2011; Zhang et al., 2013) as well as the expansion of plastic-mulched areas (Liu and Tian, 2005) over the past 20 years. The greater albedo in the northern desert area (black rectangle) in Figure 2-2j can be attributed to the degradation of the desert flora following drawdown of groundwater levels in the oasis–desert transition zone (Sun et al., 2011; Wang et al., 2008), which implies that land reclamation and groundwater extraction have led to serious ecological problems in CA oases. In addition, the albedo over crops in the actual image is higher than over the surrounding northern desert area (black rectangle in Figure 2-2b), but this is not the case for the default data. This indirectly confirms our speculation that oasis salinization and larger areas with plastic mulching could increase the actual albedo levels. The possible reason for slight differences at the mountaintops between the actual and default albedo is that the surface reflectance estimation from different satellite images has large uncertainties over rugged terrain (Wen et al., 2014; Wen et al., 2017; Wen et al., 2015; Wen et al., 2012; Wen et al., 2009b; Wen et al., 2009a). The spatial distributions of the actual versus default LAI and GVF data, as well as the differences between them, are shown in Figures 2-2c,d,g,h,k,l, respectively. The differences between actual LAI and GVF data and the corresponding default data range from 0 to 3 and from 0 to 85%, respectively. Major differences are evident across the basin, especially near the Ili River basin and the northern oasis border (black rectangle in Figures 2-2k,l), consistent with the expanded oasis region. There are few differences in the desert and mountainous areas between the actual and default LAI data. In contrast, there are noticeable differences between the actual and default GVF data in the desert area, indicating that the default data do not realistically represent GVF conditions in this region. Field verification shows that there are sparse desert plants (e.g., *Haloxylon* and *Tamarix ramosissima*) with a coverage of approximately 20%. The

differences between the actual and default terrestrial datasets confirm that the default datasets are outdated and are less representative of land surface information.

### 2.5.2. Impacts of the actual terrestrial datasets on the surface energy fluxes

Figure 2-3 shows the WRF performance in simulating LE from five simulations over cropland at S2 in 2010 and 2012. The daily average LE from five simulations correctly reproduces the overall shape of the observations (Figures 2-3a,c), and a strong linear relationship is obtained from all of simulations with coefficients of determination ( $R^2$ ) larger than 0.73 ( $p < 0.05$ ) (Figures 2-3b,d). The difference between the five simulations and observations mainly occurs during daytime from 17:00 to 6:00 UTC. The observed daily average maximum value in LE is 244.67  $W/m^2$  in 2010, while the peak values of LE from the def, LU, Alb, LAI, and VF simulations are 158.78  $W/m^2$ , 161.81  $W/m^2$ , 150.63  $W/m^2$ , 176.70  $W/m^2$ , and 355.06  $W/m^2$ , respectively (Figure 2-3a). In 2012, the daily average maximum value of LE from observation and the def, LU, Alb, LAI, and VF simulations are 371.50  $W/m^2$ , 192.50  $W/m^2$ , 191.51  $W/m^2$ , 182.74  $W/m^2$ , 211.46  $W/m^2$ , and 427.27  $W/m^2$ , respectively (Figure 2-3c). The VF simulation slightly overestimates LE and the other four simulations underestimate LE during the daytime in both of the two years. However, the RMSE value of the simulations decreases and  $R^2$  increases in the following order: def, LU, Alb, LAI, and VF simulations. The  $R^2$  increased from 0.73 to 0.74 in 2010 (Figure 2-3b) and from 0.92 to 0.94 in 2012 (Figure 2-3d). The RMSE reduced from 75.81 to 69.05  $W/m^2$  in 2010 (Figure 2-3b) and from 87.64 to 53.52  $W/m^2$  in 2012 (Figure 2-3d). These results indicate that the performance of WRF is improved in simulating the surface energy budget by the inclusion of actual LU, albedo, LAI, and VF data in the model. The VF simulation in particular shows considerable improvements in both years; the daily maximum LE value has a much closer resemblance to observations after approximately 1:00 UTC. The VF simulation may have overestimated LE because plastic mulching resulted in lower evaporation (Wang et al., 2003; Li et al., 2004). This process is not considered in the simulations (Wen et al., 2012; Meng et al., 2009).

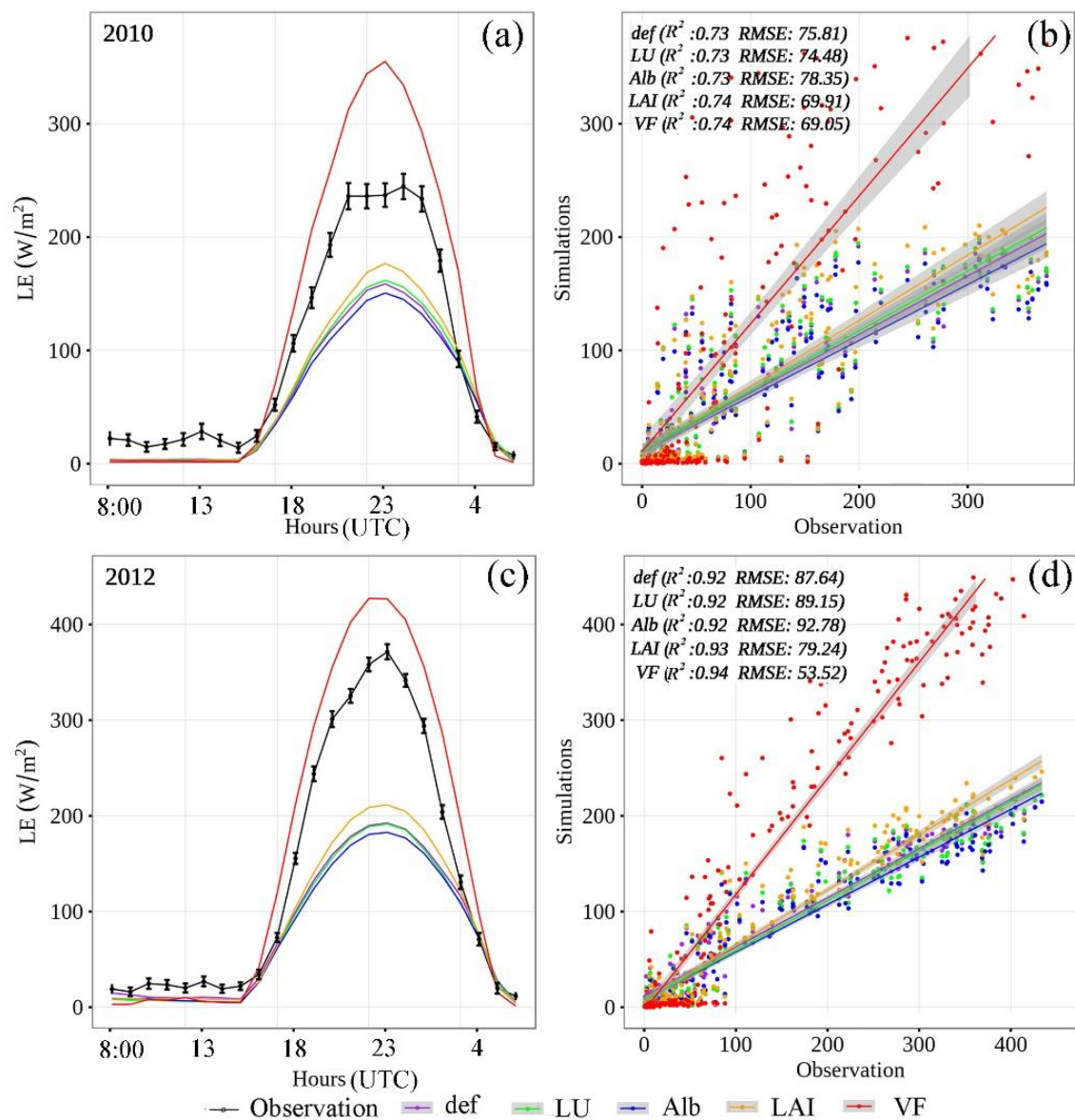


**Figure 2-3. Comparisons between observations and five simulations of hourly averaged latent heat flux (LE), and corresponding scatter diagram at S2 site in (a, b) 2010 and (c, d) 2012. The five simulations are def (using default LU, albedo, LAI and GVF), LU (using actual LU only), Alb (using actual LU and albedo datasets only), LAI (using actual LU, albedo and LAI three datasets), and VF (using all of four actual LU, albedo, LAI and GVF datasets)**

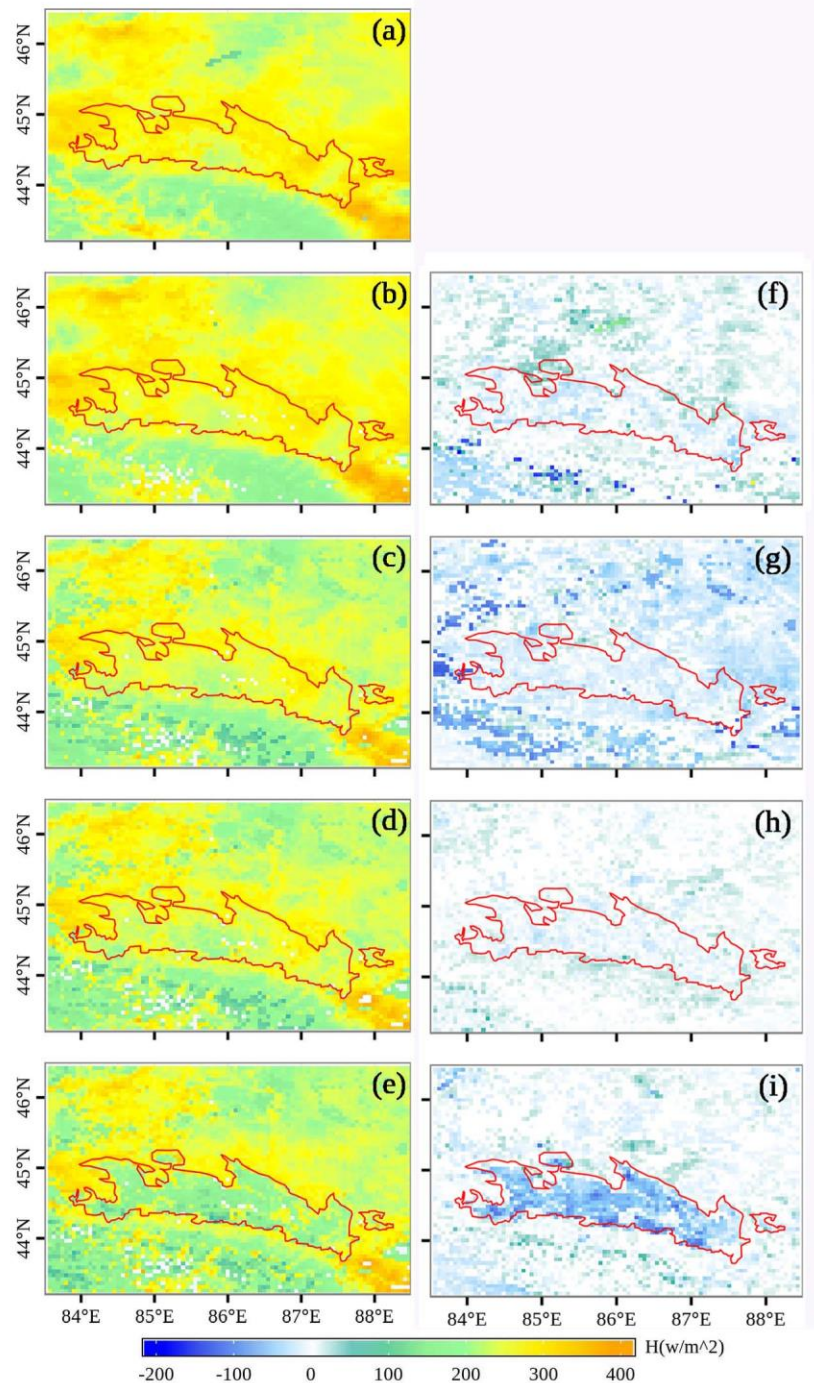


**Figure 2-4. Daytime spatial patterns of sensible heat flux ( $H$ ) from the simulations of (a) def, (b) LU, (c) Alb, (d) LAI and (e) VF, and their differences (f) b-a, (g) c-b, (h) d-c and (i) e-d (these differences pixels are statistically significant at  $p < 0.05$ ). The five simulations are def (using default LU, albedo, LAI and GVF), LU (using actual LU only), Alb (using actual LU and albedo datasets only), LAI (using actual LU, albedo and LAI three datasets), and VF (using all of four actual LU, albedo, LAI and GVF datasets). The red line represents the border of the key oasis area.**



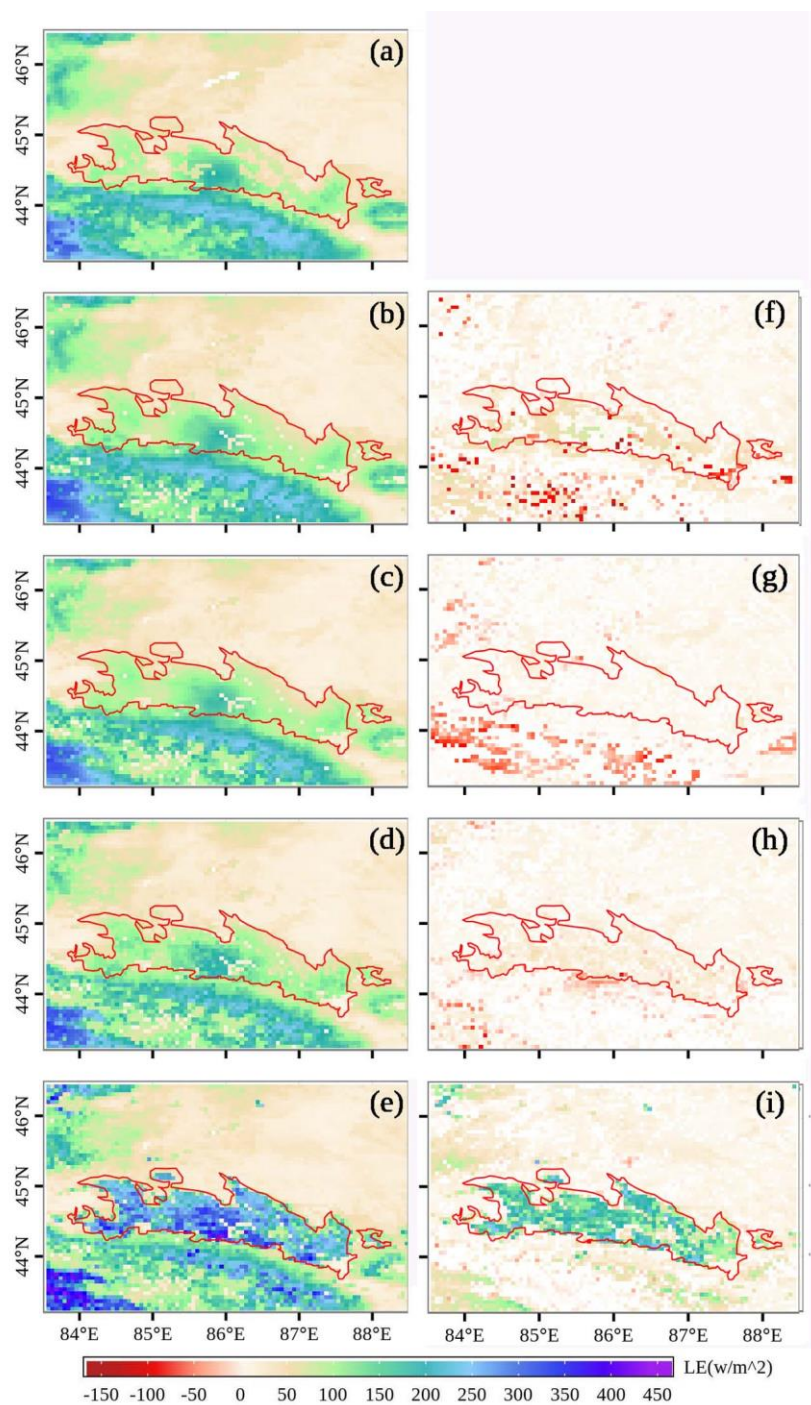


**Figure 2-5. Daytime spatial patterns of latent heat flux (LE) from the simulations of (a) def, (b) LU, (c) Alb, (d) LAI and (e) VF, and their differences (f) b-a, (g) c-b, (h) d-c and (i) e-d (these differences pixels are statistically significant at  $p < 0.05$ ). The def is a simulation with default LU, albedo, LAI and GVF provided by WRF itself, LU is a simulation with only actual LU, Alb is a simulation with only actual LU and albedo, LAI is a simulation with actual LU, albedo and LAI, and GVF is a simulation with actual all of four terrestrial datasets. The red line represents the border of the key oasis area.**

Using the actual LU, albedo, LAI, and GVF datasets during the night-time results in similar spatial patterns of average sensible heat (H) flux. Thus, Figures 2-4 and 2-5 only show the daytime spatial patterns of average H and LE from the def, LU, Alb, LAI, and VF simulations and the differences of H and LE resulting from using each of the actual LU, albedo, LAI, and VF datasets. The VF simulation (Figures 2-4 and 2-5e) indicates an obvious difference in spatial patterns of H and LE in the basin, compared with that from the other four simulations (Figures 2-4 and 2-5a–d). Since evident differences with values of 0–85% are across the Ili River basin and the oases areas between the actual and default GVF (Figure 2-2l), the VF simulation considerably decreases simulation of H by a value of approximately 50–150 W/m<sup>2</sup> (Figure 2-4i) and considerably increases LE by approximately 90–270 W/m<sup>2</sup> (Figure 2-5i) over these areas. Although the def, LU, Alb, and LAI simulations present relatively similar overall spatial patterns of H and LE, some detailed differences have to be noted. Since there is no urban representation in the default LU (Figure 2-2e), the value of H (LE) is obviously underestimated (overestimated) by approximately 100–150 W/m<sup>2</sup> (Figures 2-4 and 2-5f) over corresponding grids in the def simulation. Since the default LU data includes a large area of shrubland over the oasis region, and forest in the Ili River valley rather than cropland in the actual LU data, the misclassification results in the def simulation overestimating (underestimating) LE (H) by approximately 50 W/m<sup>2</sup> over the corresponding grids (Figures 2-4 and 2-5f). In addition, since there is no ice found in the default LU compared with the actual LU, the def simulation overestimates (underestimates) H (LE) in the corresponding areas. These results indicate that the outdated default LU results in an incorrect energy response, especially over the oasis area, the Ili River valley basin, and the glacier region. Realistic representation of LU is important for energy budget simulation, since it determines secondary parameters such as LAI, albedo, emissivity, and surface roughness length. Given that the actual albedo values are slightly greater than the default values, ranging from 0.05–0.25 (Figure 2-2j), this decreases H and LE in the Alb simulation compared with the LU simulation (Figures 2-4 and 2-5c), especially in mountainous areas. Slight differences in H and LE result from using the actual LAI data, with the most obvious differences in the Ili River basin and the northern oasis border (black rectangle in Figures 2-2k,l).

## 2.5.3. Impacts of the actual terrestrial datasets on 2-m air temperature, humidity

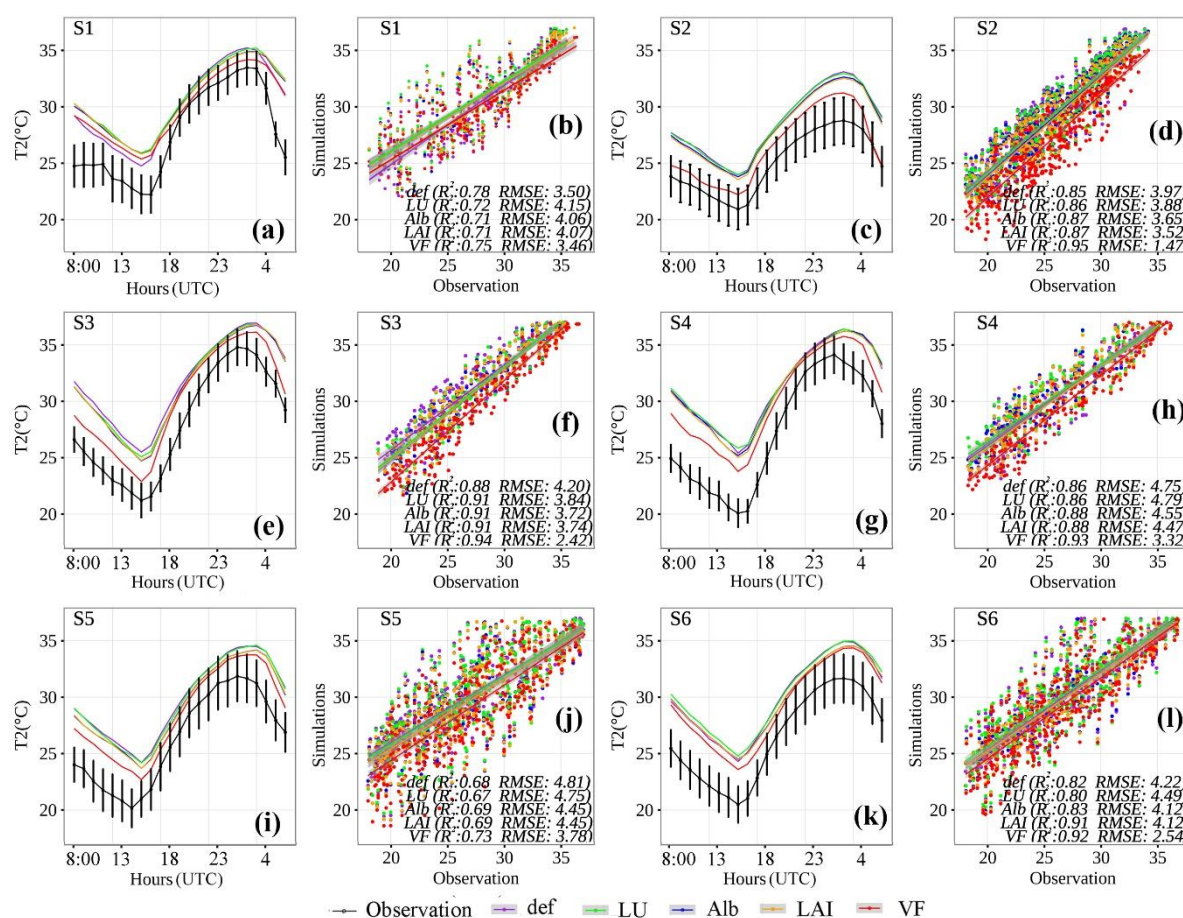


**Figure 2-6. Comparisons between observations and five simulations of hourly averaged 2-m air temperature (a,c,e,g,i,k), and corresponding scatter diagram at six sites (b,d,f,h,j,l). The def is a simulation with default LU, albedo, LAI and GVF provided by WRF itself, LU is a simulation with only actual LU, Alb is a simulation with only actual LU and albedo, LAI is a simulation with actual LU, albedo and LAI, and GVF is a simulation with actual all of four terrestrial datasets.**

Figures 2-6 and 2-7 show aspects of the WRF performance in simulating  $T_2$  and RH, respectively, from the five simulations. All of the def, LU, Alb, LAI, and VF simulations reproduce the shape and peak of  $T_2$  and RH, and produce a strong linear relationship of  $T_2$  and a relatively moderate relationship of RH with the observations at six stations in the two years. The  $R^2$  of  $T_2$  ranges between 0.71 and 0.95 ( $p < 0.05$ ), and that of RH ranges between 0.44 and 0.75 ( $p < 0.05$ ) obtained from all of the five simulations. Although the  $T_2$  (RH) from all of the simulations, compared with the observations, is overestimated (underestimated) over both cropland sites (S1, S2, S3, and S4) and over desert sites (S5 and

S6) throughout all times of the day, a stronger relationship (increasing  $R^2$  progressively) and similar magnitudes of T2 and RH (decreasing RMSE progressively) are observed when each of actual LU, albedo, LAI, and GVF datasets was used in the simulations. In particular, at S2, S3, and S4, the bias of temperature was corrected by up to 0.35–2.25 °C and that of relative humidity was corrected by up to 8.85%. Thus, using actual terrestrial datasets improves the WRF performance.

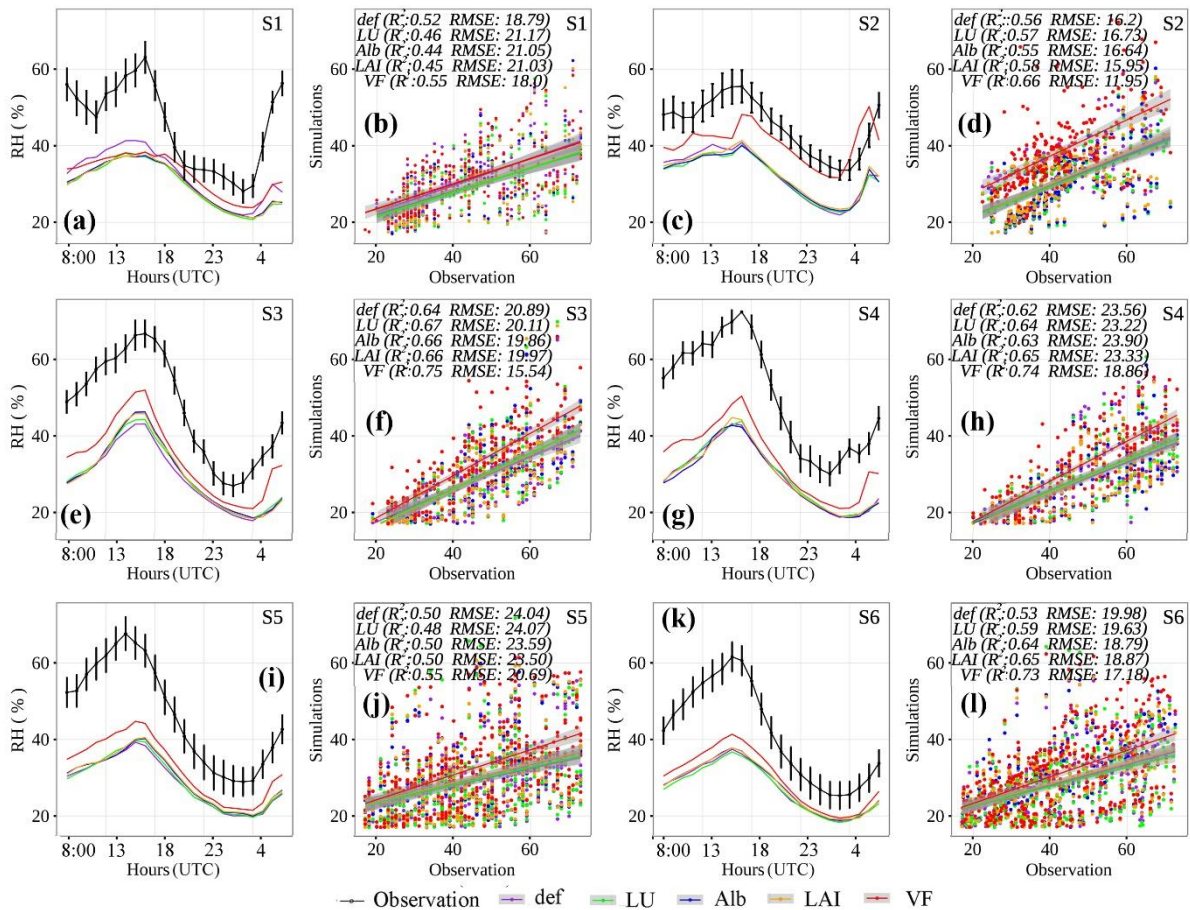


**Figure 2-7. Comparisons of hourly averaged 2 m relative humidity (RH) between observations and five simulations (a, c, e, g, i, k), and corresponding scatter diagram (b, d, f, h, j, l) at six stations (S1-S6) in 2010 and 2012. The def is a simulation with default LU, albedo, LAI and GVF provided by WRF itself, LU is a simulation with only actual LU, Alb is a simulation with only actual LU and albedo, LAI is a simulation with actual LU, albedo and LAI, and GVF is a simulation with actual all of four terrestrial datasets.**

Note that the improvements are relatively smaller at station S1 compared with those at stations S2, S3, and S4. This can be attributed to the fact that the S1 station is located in an urban area, so using actual vegetation parameters such as the LAI or GVF does not affect

the performance of the WRF model in these areas. The overestimations of T2 and underestimations of RH over oasis areas could be attributed to the cooling or wetting effects of soil evaporation from irrigation; these cannot be simulated by lake irrigation schemes in WRF. All five simulations (the def, LU, Alb, LAI, and GVF) captured the rain event that occurred on 28 July 2012 at S1, S3, and S4 (not shown). However, it is difficult to determine whether the use of actual LU, albedo, LAI, and GVF data improved the simulation of precipitation due to the limited statistics.

Figures 2-8 and 2-9 present spatial patterns of T2 and Q2 from the def, LU, Alb, LAI, and VF simulations, and their differences (the differences of pixels are statistically significant at  $p < 0.05$ ) using each of actual LU, albedo, LAI, and GVF data, respectively. Overall, all of the simulations (the def, LU, Alb, LAI, and GVF) generally suggest continuous stripe like T2 increases from the mountainous areas to the basin due to the lapse rate of temperature resulting from the elevation gradient difference. In addition, the simulations show lower Q2 in the mountainous regions as compared to basin areas due to the large difference of temperature in each. Focusing on the difference between oases and desert regions, in accordance with spatial patterns of H and LE, the spatial patterns of T2 and Q2 from the def (Figures 2-8 and 2-9a,a1) and VF (Figures 2-8 and 2-9e,e1) simulations differ from the LU, Alb, and LAI simulations during the daytime (Figures 2-8 and 2-9b–d) and night-time (Figures 2-8 and 2-9b1–d1).

Specifically, as indicated by the difference of T2 and Q2 between the LU and def simulations (Figures 2-8 and 2-9f,f1), the averaged T2 differences over the oasis area and Ili River valley from the LU simulation decrease up to approximately  $-0.5^{\circ}\text{C}$  in the daytime (Figure 2-8f) and  $-1.2^{\circ}\text{C}$  at night-time (Figure 2-8f1), and the averaged Q2 over these areas increases (decreases)  $0.25\text{ g kg}^{-1}$  during the daytime (in night-time) when actual LU data is used in the WRF model (Figures 2-9f,f1). The differences most likely result from the fact that the default LU over these areas includes sparse shrubland and forest, while the actual LU data show cropland. Since the default LU data do not include urban areas or ice (Figure 2-2b), there are also large differences in T2 and Q2 over these grids. In addition, there are also obvious differences in T2 and Q2 in the northeast desert when actual LU data was used. Although the LU, Alb, and LAI simulations can simulate the cold–wet island effects of the area during the daytime, this effect is more intense in the VF simulation than in the other three simulations. Using actual GVF data results in a significant decrease in T2

of  $-0.5$  to  $-1.5^{\circ}\text{C}$  during the day (Figure 2-8i) and  $-0.5$  to  $-4.5^{\circ}\text{C}$  (Figure 2-8i1) at night; similarly, there is a large increase in Q2 by  $0.5$ – $2.5\text{ g kg}^{-1}$  during the day (Figure 2-9i) and a decrease of  $1.0\text{ g kg}^{-1}$  at night (Figure 2-9i1) over the oasis area and Ili River Valley. Using actual albedo data results in a slight decrease in T2 of approximately  $-0.45^{\circ}\text{C}$  (Figure 2-8g1) and a decrease in Q2 of approximately  $0.5\text{ g kg}^{-1}$  (Figure 2-9g1) over the north-eastern desert at night, as shown by the difference between the Alb and LU simulations. Using actual LAI data results in a slight decrease in T2 by approximately  $-0.15^{\circ}\text{C}$  (Figures 2-8h, h1), and an increase in Q2 by approximately  $0.25\text{ g kg}^{-1}$  over the oasis region for the whole day (Figures 2-9h,h1). Overall, actual LU and GVF data strongly influence the simulations of T2 and Q2 patterns in the oasis–desert system, while albedo and LAI have a lesser impact.

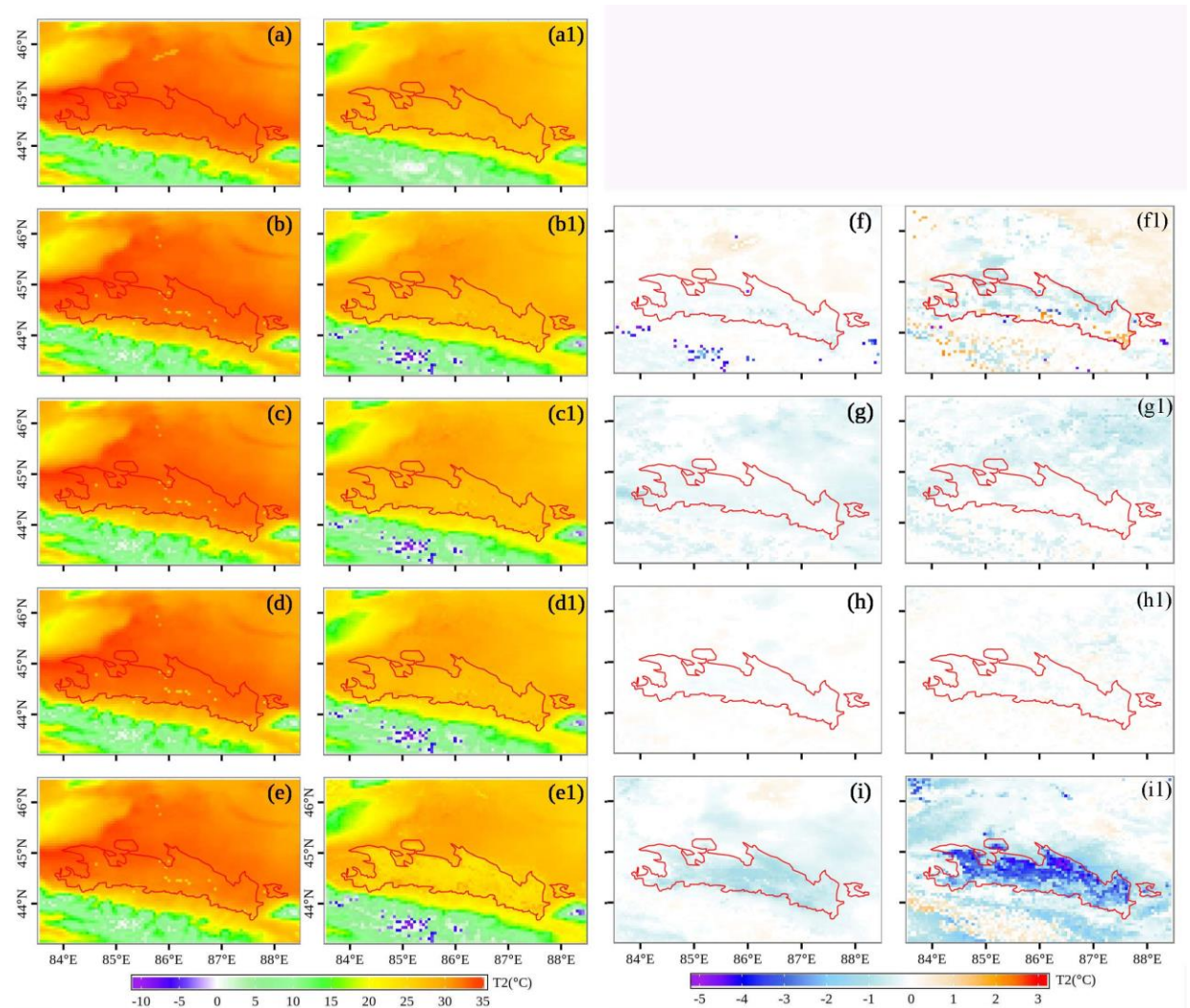


**Figure 2-8.** Daytime spatial patterns of 2 m air temperature (T2) from the(a) def, (b) LU, (c) Alb, (d) LAI and (e) VF simulations, and their differences (f) b–a, (g) c–b, (h) d–c and (i) e–d (these

difference pixels are statistically significant at  $p < 0.05$ ). And corresponding patterns during the night-time, which are labelled with the corresponding daytime label and the number 1. The def is a simulation with default LU, albedo, LAI and GVF provided by WRF itself, LU is a simulation with only actual LU, Alb is a simulation with only actual LU and albedo, LAI is a simulation with actual LU, albedo and LAI, and GVF is a simulation with actual all of four terrestrial datasets. The red line represents the border of the key oasis area.

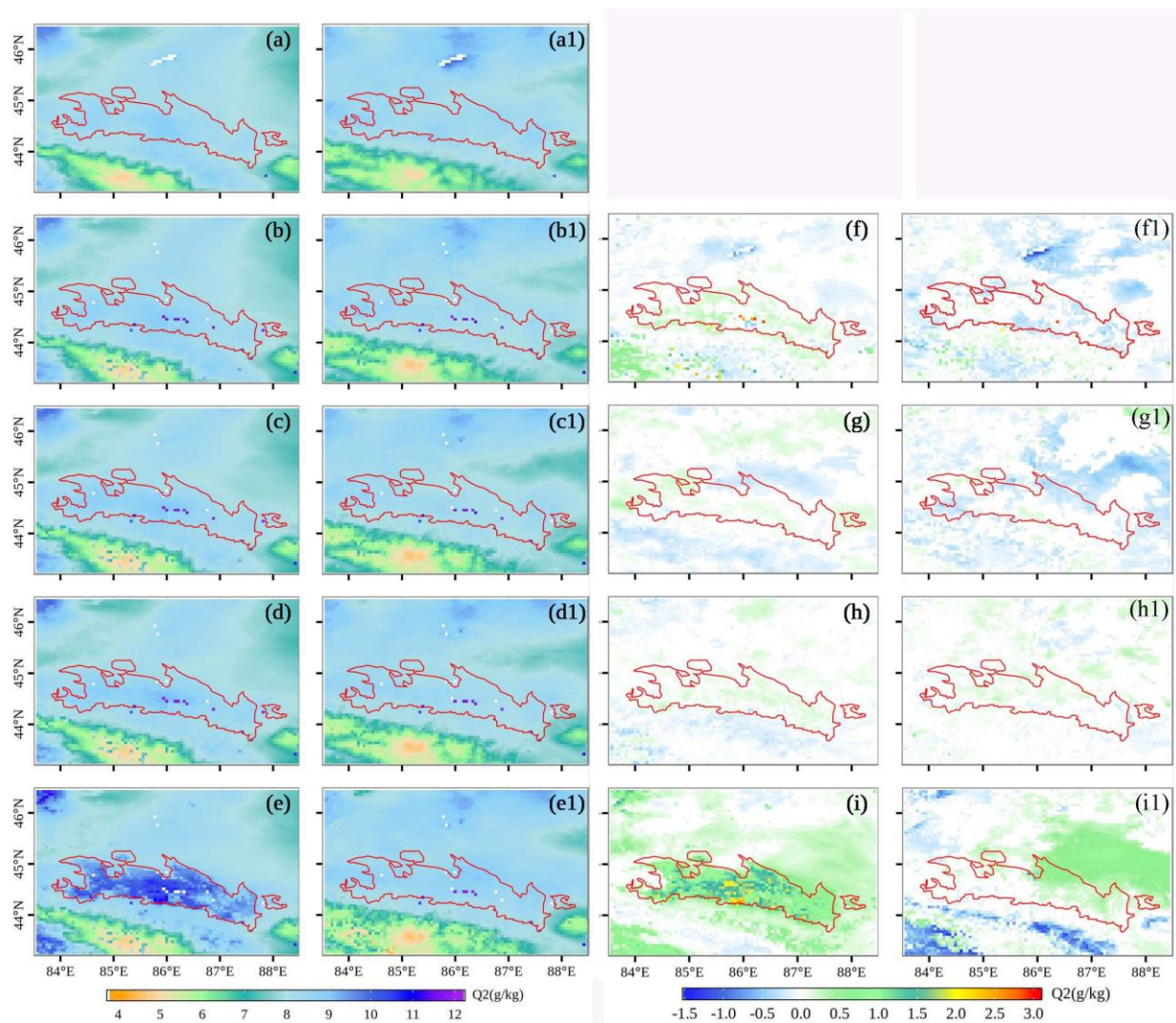


**Figure 2-9.** Daytime spatial patterns of 2 m specific humidity patterns ( $Q_2$ ,  $\text{g kg}^{-2}$ ) from the (a) def, (b) LU, (c) Alb, (d) LAI and (e) VF simulations, and their differences (f) b-a, (g) c-b, (h) d-c and (i) e-d (these difference pixels are statistically significant at  $p < 0.05$ ). And corresponding patterns during the night-time, which are labelled with the corresponding daytime label and the number 1. The caption of def, LU, Alb, LAI and VF simulations is same with the figure 2-8.

2.5.4. Impacts of the actual terrestrial datasets on the surface circulation

Figure 2-10 shows comparisons of the simulated 10 m horizontal WS and WD from the def, LU, Alb, LAI, and VF simulations with observations at three meteorological stations over cropland. Station S1 is located in the upper part of the oasis, near its southern border, and stations S3 and S4 are located in the lower part of the oasis, near its northern border. Although the RMSE ( $R^2$ ) of the WS decreases slightly (increases) as actual data are added in the def, LU, Alb, LAI, and VF simulations, most of the simulated WS values are higher than the observed values by approximately 2 m/s; 60% of the simulated WS range from 2–6 m/s, whereas the observed values range from 2–4 m/s. The reason for this bias in WS is that the uncertainty of randomized turbulence processes results in difficulties in the accurate simulation of wind patterns (Hanna and Yang, 2001). The trends in WD are consistent with the observations. The dominant WD is WNW or NW during the daytime and WSW or SW during the night-time for all stations; these directions are observed in all simulations and in the observations, and reflect the circulation characteristics in a mountain–valley region.

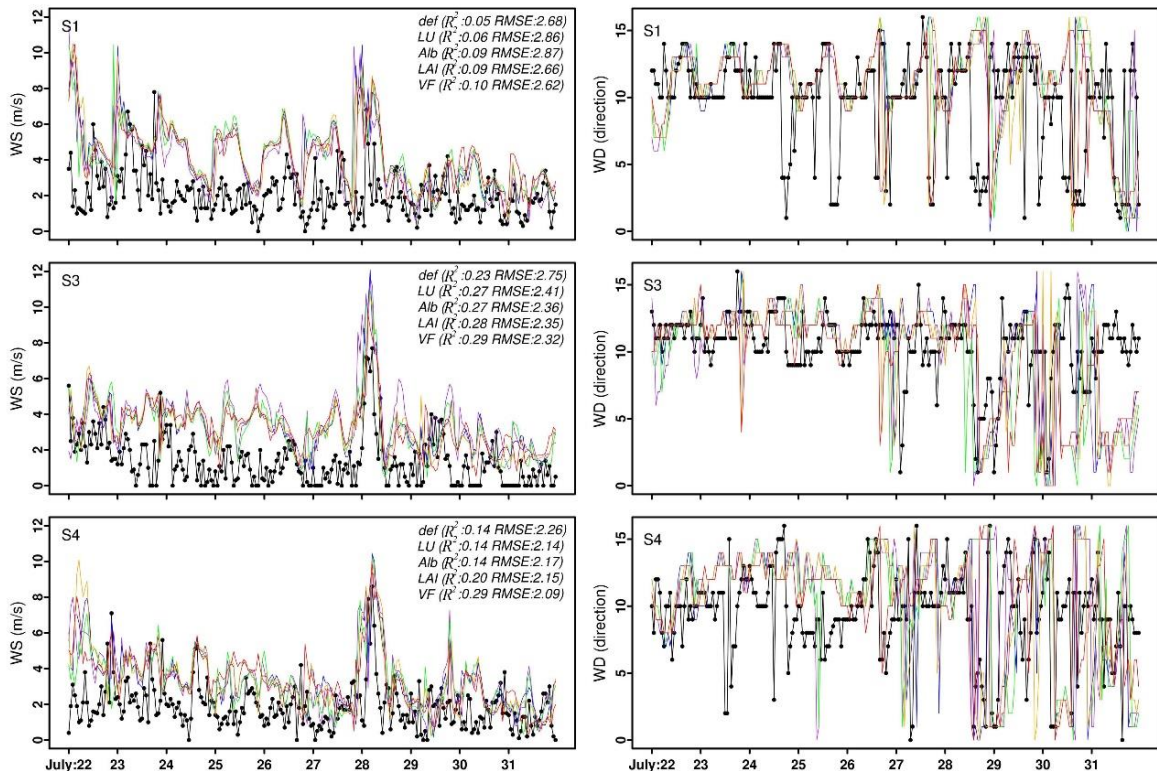
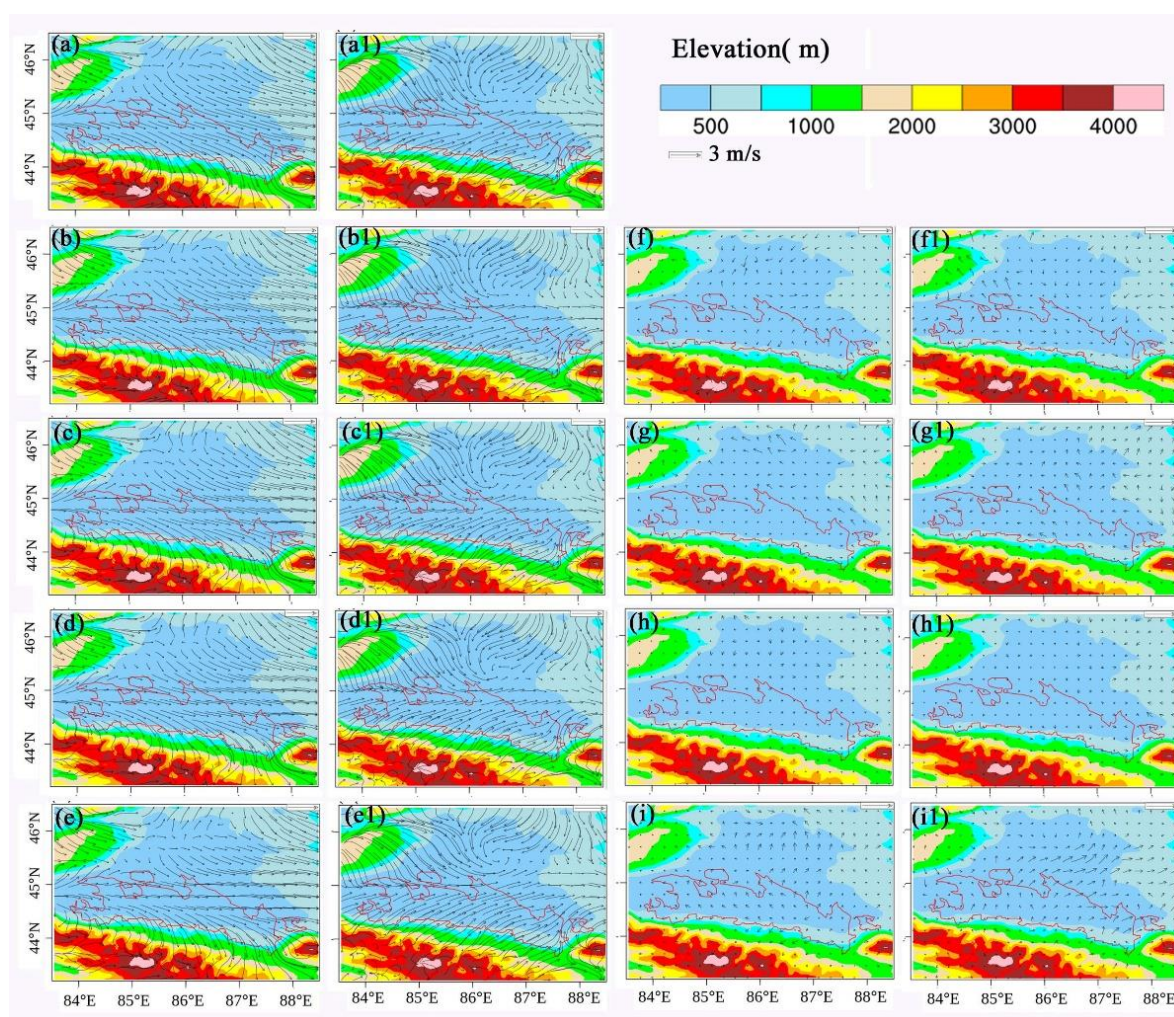


Figure 2-10. Comparisons of hourly 10 m (a, c, e) wind speed (WS) and (b, d, f) wind direction (WD) between observations and five simulations at three stations (S1, S3, S4)





**Figure 2-11. Daytime spatial patterns of 10 m wind speed (WS) and wind direction (WD) from the (a) def, (b) LU, (c) Alb, (d) LAI and (e) VF simulations, and their differences (f) b–a, (g) c–b, (h) d–c and (i) e–d (these difference pixels are statistically significant at  $p < 0.05$ ). And corresponding patterns during the night-time, which are labelled with the corresponding daytime label and the number 1. The def is a simulation with default LU, albedo, LAI and GVF provided by WRF itself, LU is a simulation with only actual LU, Alb is a simulation with only actual LU and albedo, LAI is a simulation with actual LU, albedo and LAI, and GVF is a simulation with actual all of four terrestrial datasets. The red line represents the border of the key oasis area.**

Figure 2-11 shows the WS and WD patterns from the def, LU, Alb, LAI, and VF simulations and the differences caused by using each of the actual LU, albedo, LAI, and VF datasets. Overall, the simulations (def, LU, Alb, LAI, and VF) reflect the characteristics of mountain–valley winds, which have WDs to the WNW or NW during the day and to the WSW or SW at night. Using actual LU, albedo, and LAI data has very little impact on the

spatial patterns of WD (Figures 2-11f–h, f1–h1), but using actual VF data causes slight differences in the oasis center and the surrounding desert (Figures 2-11i, i1). These results suggest that using actual VF data increases the intensity of oasis effects (cold–wet island effects, and OBC).

#### 2.5.5. Response of WRF to various actual terrestrial datasets

To quantitatively discern which terrestrial datasets have the strongest influence on the meteorological elements simulated in this region, the bias percentage was calculated as the general regional influence index, following the approach in (Gao et al., 2008). After land surface parameters are replaced, the equation is as follows:

$$BP_i = \frac{\frac{1}{n} \sum_{i=1}^n (Y_{sim(j)} - Y_{sim(j-1)})}{\frac{1}{n} \sum_{i=1}^n Y_{obs}}$$

In the current study,  $n$  is the number of stations,  $Y_{sim(j)}$  is the simulated meteorological variables (e.g., temperature) with updated actual land surface parameters from experiment  $j$ , and  $Y_{obs}$  is the observed value at each station. Four modelled predictors (T2, RH, WS, and LE) are analyzed.

Figure 2-12 presents the bias percentage of the simulated T2, RH, WS, and LE due to using each actual dataset. The y axis shows the mean bias percentage for 2010 and 2012, which represents the impact of using each actual dataset on atmospheric simulations. Using actual LAI and GVF data mainly affects the LE (Figures 2-12g,h), while using actual LU and albedo data affects the WS (Figures 2-12c,f). T2 (RH) decreases (increases) by a total of  $-3.5\%$  ( $10.2\%$ ) from using actual LU, albedo, LAI, and GVF data. In total,  $-2.26\%$  ( $8.85\%$ ) of the change in T2 (RH) is contributed by using actual GVF data, and the remainder comes from using actual data for albedo and the other two parameters (Figures 2-12a,b). The WS decreases by  $-13.31\%$  when actual LU, albedo, LAI, and GVF data are used; of that total, LU and albedo contribute  $-5.51\%$  and  $-4.47\%$ , respectively—far more than the other two parameters (Figure 2-12c). The LE first decreases due to the use of actual LU and albedo data and then increases with the addition of actual LAI and GVF data; the total change is  $58.19\%$ , of which VF contributes  $54.94\%$ , which is far more than the other three parameters (Figure 2-12d). In general, using actual land surface parameters alters the near-surface

meteorology simulation in the lower atmospheric layer (Figures 2-12e–h). Using actual GVF data has a large influence on the simulation of T2, RH, and LE in the oasis–desert system, which contributes to error correction values of 62%, 87%, and 92%. Thus, using actual VF data is very important for simulating near-surface meteorology. Using actual LU is the principal parameter for near-surface water and heat simulation, since it determines the value of secondary parameters such as LAI, albedo, emissivity, and surface roughness length.

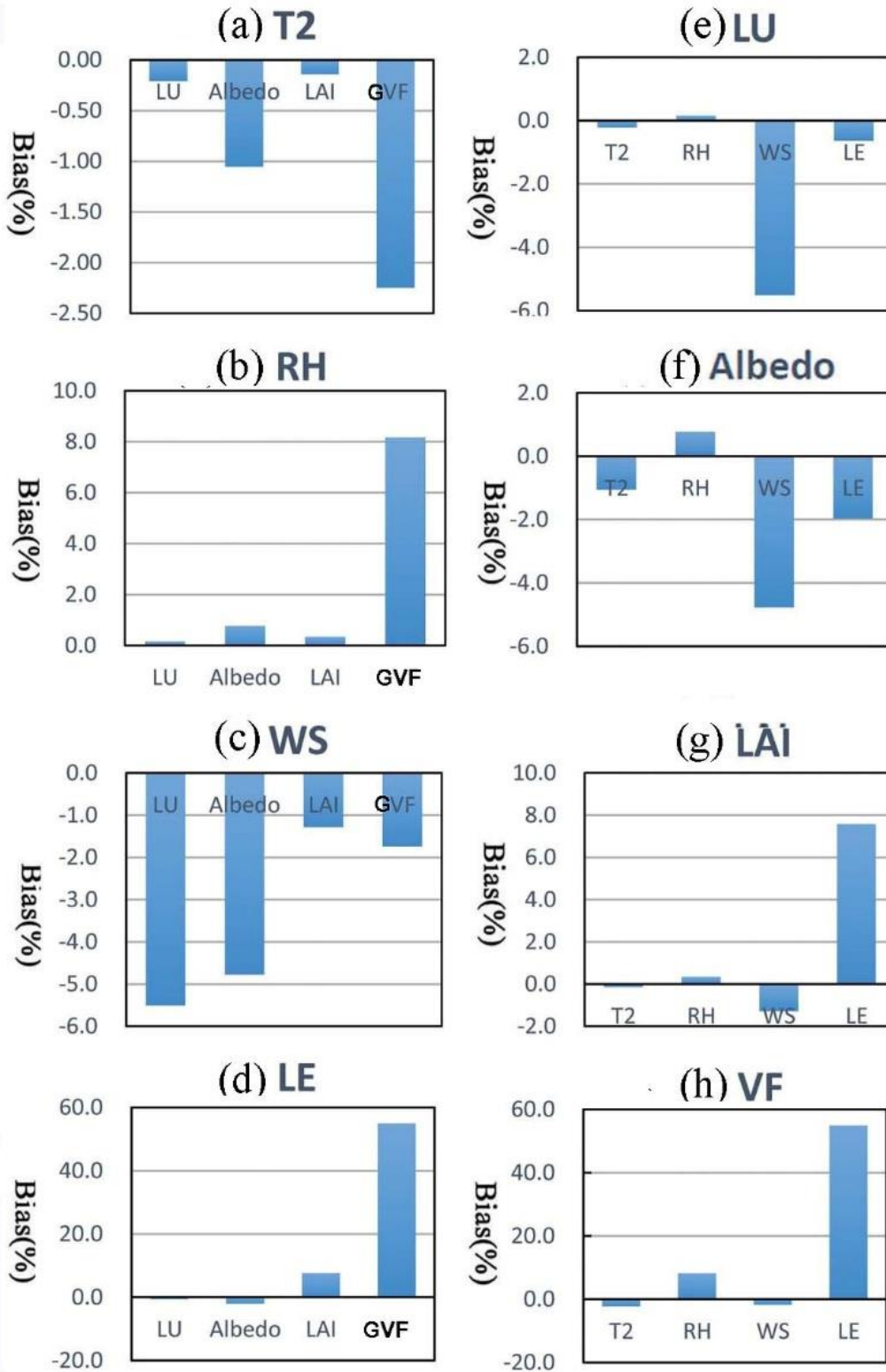


Figure 2-12. Average bias percentages of simulated meteorology variables at 6 meteorology stations due to using each actual terrestrial datasets: (a) T2 biases, (b) RH biases, (c) WS biases, (d) LE biases, (e) biases due to using actual LU, (f) biases due to using actual albedo, (g) biases using actual LAI, (h) biases due to using actual GVF datasets.

## 2.6 Discussion

Outdated default terrestrial datasets in WRF, including LU, albedo, LAI, and VF, limit this model's ability to accurately simulate the meteorological characteristics of the complex oasis–desert system in NTM. In this study, we examined the impact of using actual LU, albedo, LAI, and GVF data from satellite products in WRF on the model performance. Five simulations were conducted with the same meteorological forcing data and model schemes: def (using default LU, albedo, LAI, and GVF data), LU (using actual LU data only), Alb (using actual LU and albedo data only), LAI (using actual LU, albedo, and LAI), and VF (using all of actual LU, albedo, LAI, and GVF together).

WRF simulations of temperature, humidity, energy, and WS are improved by the incorporation of actual LU, albedo, LAI, and GVF into the model, as evidenced by the decrease in RMSE values and increase in  $R^2$  in both 2010 and 2012. Using actual VF data greatly affects the simulation of T2, RH, and LE in the oasis–desert system, contributing to error correction values of 62%, 87%, and 92%, respectively. LU data is a primary parameter and it determines the values of many secondary parameters. Although all of the simulations conducted in this study produce the characteristic of the “wet–cold” island effect over the oasis area, as reported previously (Kumar et al., 2014; Zhang et al., 2015; Meng et al., 2009), WRF can more accurately reflect the intensity of the oasis cold–wet effects when using all actual LU, albedo, LAI, and GVF data. The results of this study contribute to a greater knowledge of the impacts of land surface parameters on the performance of WRF (Wen et al., 2012), which is beneficial for various applications, especially for land surface and climate modelling. Our results are also critical to accurately understanding the intensity of cold–wet effects of oases and the OBC.

We note that our simulations have several limitations. For example, overall, we found that the simulations overestimated (underestimated) T2 (RH), and the VF simulation overestimates the LE relative to the observations. These errors can be attributed to the fact that soil evaporation resulting from irrigation and plastic mulching effects are not considered in the simulations of WRF (Wen et al., 2012; Meng et al., 2009). Adding irrigation and plastic mulching schemes may help to correct these errors.

## 2.7 Conclusions

The current study used WRF with actual LU, albedo, LAI, and GVF data derived from satellite products to improve the simulation of weather and climate conditions in the oasis–desert system of the NTM in 2010 and 2012. Model evaluations for temperature, humidity, and energy demonstrated that our simulations, which were performed using actual terrestrial datasets, improved the performance of WRF, as evidenced by the decrease in RMSE and the increase in  $R^2$ . All of the simulations exhibit the “wet–cold” island effects of the oases. However, the intensity of the wet–cold effect varies depending on the use of actual LU, albedo, LAI, and VF data. Using actual GVF data results in error correction values of 62%, 87% and 92%, respectively, for simulated T2, RH, and LE in the oasis–desert system. Using actual LU data is crucial for near-surface water and heat simulation, since it determines the values of additional secondary parameters. We conclude that it is important to use, at least, actual LU and GVF data for weather and climate simulations in WRF.

# CHAPTER 3

## THE IMPACT OF DRIP IRRIGATION ON THE ATMOSPHERIC STRUCTURE AND THE LOCAL CLIMATE

---

*Modified from: Miao Zhang, Geping Luo, Philippe De Maeyer, Rafiq Hamdi, Hui Ye, Huili He, Peng Cai. 2017. The effect of drip irrigation on water-heat patterns in a mountain-oasis-desert ecosystem in the north Tianshan Mountains. JGR-Atmosphere.submitted.*

## ABSTRACT

Exploring irrigation's effects on water and heat patterns of complex mountain-oasis-desert ecosystem is very significant for regional sustainable development under the limited water and soil conditions in the north Tianshan Mountains (NTM). A drip irrigation scheme was incorporated into the weather research and forecasting (WRF) in order to realistically represent water and heat conditions of artificial oasis across the NTM. Two simulations were conducted with drip irrigation (IRR) and without irrigation (CON) from January 1st, 2011 to September 31st, 2012. Model evaluation further reveals that this new irrigation approach can generate irrigation water amounts that are in close agreement with the actual irrigation water amounts across the NTM, and surface energy, temperature and humidity conditions have been substantially altered with the new irrigation process. No significant effects of the irrigation on water-heat conditions of oasis were observed in the non-irrigation season, however, irrigation increases the latent heat flux (LE)  $80.81 \text{ W/m}^2$  and decreases the sensible heat flux (H)  $63.03 \text{ W/m}^2$  over oasis, thereby strengthening cold-wet island effects of oasis and intensity of oasis breeze circulation (OBC) during the irrigation season. In addition, our modeling results show that the impacts of irrigation on temperature, H and LE were mainly restricted over oasis, but the impact on humidity spread to across whole NTM. Moreover, irrigation increased precipitation amount in upwind mountains areas with elevation approximately 1000-2000 m in daytime and northern desert area in nighttime. That the impacting range of irrigation on humidity and precipitation spreads to non-irrigation area might be relevant to mountain-valley winds, which implied that irrigation might accelerate the hydrological cycle in MODS.

**Key words:** MODIS; Weather Research and Forecasting model; Oasis-Desert system; Oasis effects; North Tianshan Mountains; Central Asia

### 3.1 Introduction

Central Asia arid area (CA), including Kazakhstan, Kyrgyzstan, Tajikistan, Turkmenistan, Uzbekistan, and the Xinjiang Province of China (Hu *et al.*, 2014; Li *et al.*, 2015), is located deep inside the continent with special geomorphology of mountain-basin systems, known to climate change (Sorg *et al.*, 2012b). Water is a particularly scarce and valuable good for both human livelihoods and ecosystems here (Gessner *et al.*, 2013), because the water



resources are only from Mountains (The Tianshan mountains, located in the hinterland of Central Asia, acts as the “water tower of Central Asia”(Sorg *et al.*, 2012a)), whose rivers all are fed by important hydrologic processes of snow and glacial melt, and precipitation from mountain ranges (Immerzeel *et al.*, 2010), flow into artificial lakes, disappear in the desert area in the basin (Luo *et al.*, 2010). Based on limited runoff (Bothe *et al.*, 2012) and unrestricted groundwater exploitation (Ming-jiang, 2009), oases are widespread embedded in the desert and Gobi background by irrigation (Souza *et al.*, 2006; Smith *et al.*, 2007; Soltan, 1999; Li *et al.*, 2007; Luo *et al.*, 2010). Accordingly, CA can be divided into various watersheds consisting of mountain, oasis, and desert areas, named as Mountain-Oasis-Desert ecoSystem (MODS). The north Tianshan Mountains (NTM) is one of such typical geomorphology areas, which consists of a great number of complex MODS. Since 1950s, the region has been experiencing intense oases expansion (from  $121.0 \times 10^4$  ha in the year of 1949 to  $512.5 \times 10^4$  ha in 2010) based on unrestrained extraction of groundwater for irrigation (Hong *et al.*, 2003; Zhang *et al.*, 2017c; Jia *et al.*, 2004). As a result, a series of ecological problems appear, such as regional desertification, soil salinization and drawdown of groundwater levels due to irrigation (Sun *et al.*, 2011; Wang *et al.*, 2008). Meanwhile, recent studies indicate that annual mean air temperature in the NTM have been increasing at an average rate of  $0.8 \text{ }^\circ\text{C decade}^{-1}$  (He *et al.*, 2003), which is far larger than the average rate for CA (i.e.,  $0.39 \text{ }^\circ\text{C decade}^{-1}$  from 1979 to 2011) and for global land areas (i.e.,  $0.27\text{-}0.31 \text{ }^\circ\text{C decade}^{-1}$  from 1979 to 2005) (Hu *et al.*, 2014). Precipitation and frequency of extreme precipitation have an obvious increasing tendency in NTM at an increase rate of 11.3% (He *et al.*, 2003), but climate shows drying tendency (Xu *et al.*, 2004; Lianmei, 2003). While other arid areas in the CA show generally a slight decrease of average annual precipitation (Lioubimtseva and Henebry, 2009; Gessner *et al.*, 2013). Horton, et al. found these heat and water dynamic contributions for regional climate change are largely independent of or potentially related to land cover change processes (Zhou *et al.*, 2015; Horton *et al.*, 2015; Qu *et al.*, 2013). The abnormal regional temperature and precipitation change in the NTM may be likely to respond to the rapid oases expansion and intensive irrigation in such relatively close mountain-basin structures.

Numerical simulation using regional climate models (RCMs) is the most effective method to explore the local water and surface energy dynamics of such irrigated oases systems and climate effects of its evolution on regional climate change in such complex mountain-basin

landscape, because RCMs can account for climatic mechanisms not included in field measurements (Yu *et al.*, 2006; Li *et al.*, 2013) and Global Circulation Models (GCMs) (Seungbum *et al.*, 2009; Seneviratne *et al.*, 2006). GCMs are unable to adequately resolve many important meso-microscale processes, like wind patterns and precipitation due to orographic effects based on large-scale convective parameterization schemes, and simpler land surface processes (Kysely *et al.*, 2016). Emerging RCMs include the Canadian RCM (Caya *et al.*, 1999), Fifth-generation Mesoscale Model (MM5) (Grell *et al.*, 1994), the Regional Climate Model version 3 (Giorgi *et al.*, 1993a; Giorgi *et al.*, 1993b; Pal *et al.*, 2007), Regional Atmospheric Modeling System (RAMS), NCAR regional climate model (RegCM) (Evans and Zaitchik, 2008) and ALARO (Hamdi *et al.*, 2013; De Troch *et al.*, 2013) and the Weather Research and Forecasting model (WRF) (Skamarock *et al.*, 2005). As the next generation of climate model MM5, WRF coupled to a sophisticated land surface scheme Noah (WRF-Noah) is currently widely used and preferable to simulate regional climate in past 10 years (Branch *et al.*, 2014; Cao *et al.*, 2015). Many numerical simulations have been conducted to examine heat and water conditions of oases and effects of irrigation using WRF. For example, the “cold-wet island” effects of oasis (oasis becoming a cold, wet island capped by warm, dry air) and Oasis Breeze Circulation (OBC) between irrigated oases and deserts are driven by the significant horizontal and vertical differences of energy and vapor between them (Chu *et al.*, 2005; Liu *et al.*, 2007; Lv *et al.*, 2005; Meng *et al.*, 2015; Meng *et al.*, 2012; Meng *et al.*, 2009; Wen *et al.*, 2012). Many researchers proposed that such oasis has altered regional climate with widespread reduction in summer temperature due to reduced sensible heat flux and increased latent heat fluxes at the same times, leading to modified large-scale atmospheric circulations and boundary layer height based on simulations (Pei *et al.*, 2016; Jiang *et al.*, 2014; Qu *et al.*, 2013; Cao *et al.*, 2015; Deng *et al.*, 2015; Kueppers and Snyder, 2012; Evans and Zaitchik, 2008; Zaitchik *et al.*, 2005; Meng *et al.*, 2009; Zeng *et al.*, 2017; Branch *et al.*, 2014).

However, there were no irrigation schemes implemented in the accompanying NOAH in official releases of WRF (Chen and Dudhia, 2001b; Chen and Dudhia, 2001a), also in most of others RCMs, and an oasis cannot survive without irrigation in the CA. The climate effects of irrigation in the CA are neglected or idealized in most of climate researches (Sacks *et al.*, 2009). Some studies initialized irrigated crops with high soil moisture distinguished from dry land crop in default WRF- NOAH (Jiang *et al.*, 2014; Qu *et al.*,

2013; Cao *et al.*, 2015; Deng *et al.*, 2015; Kueppers and Snyder, 2012), but no additional water was introduced during the simulation. This may be appropriate for 2-3 days weather simulations, but for studies of climate some modification may be required. Some simulations were done to mimic sprinkler irrigation as precipitation (Ozdogan *et al.*, 2007), which is typical for cash crops in the United States, but relatively uncommon in such oases in the CA. Others were trying to let soil moisture continuous saturation at every time step to describe an ideal flood irrigation status (Pei *et al.*, 2016; Evans and Zaitchik, 2008; Zaitchik *et al.*, 2005; Meng *et al.*, 2009; Zeng *et al.*, 2017; Branch *et al.*, 2014). The ideal irrigation schemes may be helpful to understand the potential climate effects of irrigated crop, however in reality, irrigation usually occurs when the soil moisture drops to a low level threatening the crop growth, especially the irrigation would be largely constrained by the shortage of water resources in the CA. Using drip irrigation under plastic film since 1995 is effective method to conserve the limited water resources in this region (Fan *et al.*, 2013). The premise of studying historic contribution of irrigation and oasis evolution on regional climate change is to realistically simulate heat and water conditions of such drip-irrigated oases. If the water-heat conditions of the drip-irrigated crop surface is realistically represented, we can then go on to assess the impacts of such irrigated oases evolution on historical regional climate change, mesoscale impacts such as convection initiation and water resources in MODS in CA arid area.

Our ultimate goal in this paper is to examine the performance of WRF with adding a drip irrigation scheme proposed by Evans (Evans and Zaitchik, 2008) realistically represent water-heat conditions (surface energy budgets, temperature and humidity, planetary boundary layer height (PBLH), atmospheric structure and dynamics) of oasis in the CA, and show the effects of the drip irrigation on the water-heat conditions in relatively close mountain-basin systems, which is a prerequisite to further examine effects of historical irrigated oases evolution on regional climate change in the CA. This paper is organized as follows. The study area, datasets, methods are introduced in section 2; the validation and simulated results are presented in section 3; the comparisons between this study and previous studies and the associated uncertainties are discussed in section 4. Finally the conclusions are summarized in section 5.

## 3.2 Study area and Data

### 3.2.1. Study area and its climate

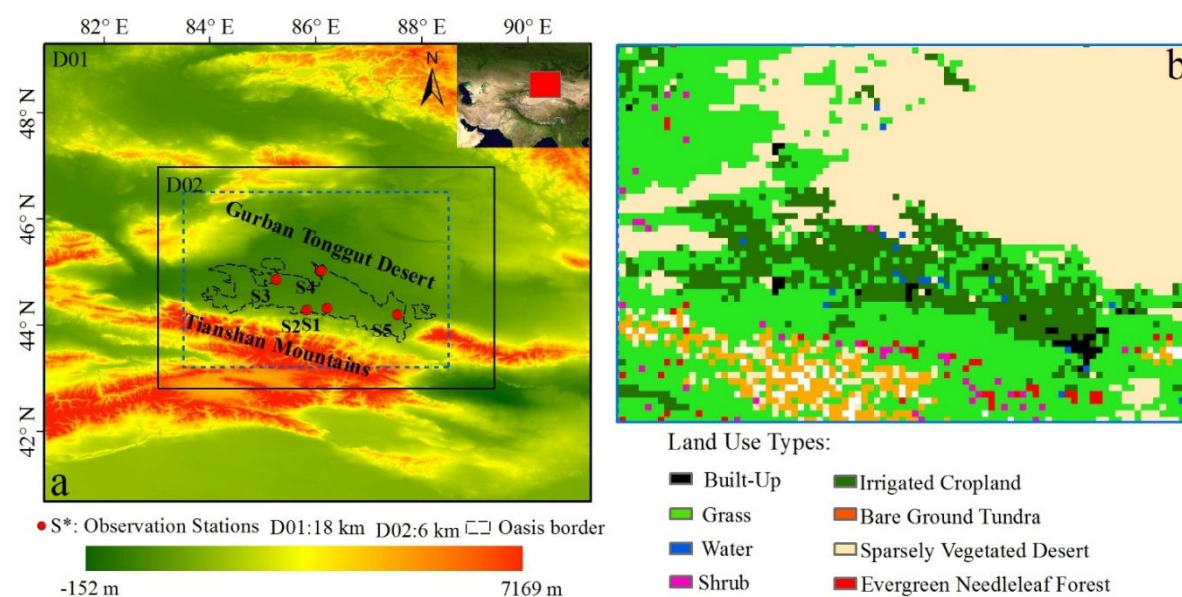


**Figure 3-1. (a) locations of NTM in the CA, and land surface elevations, meteorological sites, simulations domains of NTM, (b) Land use (LU) types of NTM in 2012**

The information of NTM has been introduced in the section 1.2 and the oasis expansion situation has also been introduced in the section 1.1.1. We only used the outer two domain simulation in this chapter (Figure 3-1). Detailed domain information can be seen in section 1.3.2.

### 3.2.2. Forcing data and in situ measurements

The detailed elements and information of ERA-Interim are seen in section 1.4.1. We select hourly observation in 2012 at meteorological stations S1, S2, S3, S4 and S7 to validate simulation results (Table 1-4), because the five stations are distributed in irrigated oasis areas. Hourly climate elements were retrieved to validate the simulation results.

## 3.3 Methodology

### 3.3.1. Model description and configuration

We only used the two outer domain simulation in this chapter (Figure 3-1). Detailed domain information and configuration can be seen in section 1.3.2.

Because of the use of these outdated terrestrial datasets, WRF have a limited ability to accurately simulate weather and climate conditions over such heterogeneous and complex oasis-desert systems, especially near large mountains (Lenderink et al., 2007; Vidale et al., 2007). We used actual LU and GVF datasets in 12 months, which are generated by the Xinjiang Institute of Ecology and Geography, Chinese Academy of Sciences, based on Landsat images and a 1:1,000,000 scale topographic map (Chen, 2008) and from MODIS vegetation indices (MOD13A2), respectively. Because LU and GVF account for 70% more influence on simulation results compared with others terrestrial datasets (Zhang et al., 2017a; Zhang et al., 2017b). The updated LUs and GVF provided a substantially more realistic map of summertime irrigated crops and associated vegetation density.

### 3.3.2. Irrigation in WRF-NOAH

In WRF-NOAH, there were no official releases of WRF with irrigation schemes implemented in the accompanying Noah or the newer Noah-MP land surface models, and grid cells classified as irrigated crops are initialized at 100% soil moisture, but no additional water is introduced during the simulation. This may be appropriate for 2-3 d weather simulations, but for studies of climate response of oases evolution in arid area some modification is required. In this study, a drip irrigation scheme proposed by previous researcher (Evans and Zaitchik, 2008) were incorporated into WRF-NOAH. The irrigation season was set as from 15<sup>th</sup> April and closed on 15<sup>th</sup> September in accordance with average irrigation patterns over oases region in the CA (Fan et al., 2013). Since the crop here was irrigated by drip water into root and most of crop was under plastic film. Moreover the water is scarce here. Our assumed that the irrigated crops always have enough moisture to transpire without being stressed but no excess water is added, and that very little moisture reached 25 cm away from the drip radially on the basis of detailed field experiment (Fernández et al., 2006a; Fernandez et al., 2006b). Thus this scheme makes sure there is always enough water available for the vegetation to transpire without water limitations, even though the mean soil moisture of grid cell may continue to decrease.

In NOAH, the soil moisture effects on evapotranspiration (ET) through the canopy resistance,  $R_c$ , given by (Chen and Dudhia, 2001b; Chen et al., 1996; Niu et al., 2011; Yang et al., 2011)

$$E_t = \sigma_f E_p B_c \left[ 1 - \sqrt{\frac{W_c}{S}} \right]$$

Where  $\sigma_f$  is the green vegetation fraction,  $E_p$  is the potential evaporation,  $B_c$  is a function of the canopy resistance given below,  $W_c$  is the intercepted canopy water,  $S$  is the maximum canopy water storage.

$$B_c = \frac{1 + \frac{\Delta}{R_r}}{1 + R_c C_h + \frac{\Delta}{R_r}}$$

Where  $C_h$  is the surface exchange coefficient for heat and moisture,  $\Delta$  depends on the slope of the saturation specific humidity curve,  $R_r$  is a function of the surface air temperature, surface pressure and  $C_h$ .

$$R_c = \frac{R_{cmin}}{LAI \times F_1 \times F_2 \times F_3 \times F_4}$$

where  $R_{cmin}$  is the minimum canopy resistance, LAI is the leaf area index,  $F_1$  is the solar radiation effect (amount of PAR),  $F_2$  is the vapor pressure deficit effect (air humidity: dry air stress),  $F_3$  is the air temperature effect (air temperature: heat stress) and  $F_4$  is the soil moisture effect. All  $F$  factors vary between 0 and 1, with 1 represents the least canopy resistance to transpiration. In our drip irrigation process, we calculated the canopy resistance twice. Once given the current soil moisture status, and another once with  $F_4$  is set to 1 for grid cells classified as irrigated crops, ensuring that there is no soil moisture stress (Evans et al., 2008). The first value is used to calculate the amount of current soil moisture used for ET, while the second value is used to calculate the ET that occurs if there is no soil moisture stress. The difference between the two gives the amount of irrigation amount that must be added to a grid cell to avoid any soil moisture stress under drip irrigation.

### 3.3.3. Experiment design

To carry out this study, we first incorporated drip irrigation scheme (Evans and Zaitchik, 2008) into WRF model. Second, two simulations were performed from January 1st, 2011 to December 31st, 2012. The first run is the control simulation using default WRF without irrigation processes (CON); the second run is the scenario simulation adding drip irrigation scheme into the WRF (IRR). The simulated results were compared to observations at five meteorological stations (Figure 1a) to examine whether the water and heat conditions of oases were realistically represented. Finally, we present the effects of irrigation on the

surface energy budget, temperature, humidity and precipitation, as well as atmospheric structure in MODS. Generally, in the absence of accurate, gridded, initial soil moisture conditions, a spin-up period is needed to allow soil moisture within Noah to approach equilibrium within the hydrological cycle (Branch et al., 2014), and the optimal spin-up period may require considerable periods, possibly even years to reach equilibrium (Lim et al., 2012). In this study, following similar simulations (Liu et al., 2007; Lv et al., 2005; Meng et al., 2015; Meng et al., 2012; Meng et al., 2009), the simulation results for the first year were discarded as spin-up. The simulated results in the 2012 were used as analysis.

### 3.4 Results

#### 3.4.1 Validation

Figure 3-2 shows aspects of the WRF performance in simulating T2, RH and ET, respectively from the CON and IRR simulations. The two simulations reproduce the similar shape and peak of T2, RH and ET, but the IRR produces a stronger linear relationship and similar magnitudes of T2, RH and ET. Drip irrigation in this region did not impact simulations of T2, RH and ET in non-irrigation season based on scarce difference between CON and IRR simulations (not shown). In the irrigation season, The  $R^2$  of T2 obtained from CON and IRR simulations are 0.92 and 0.92 ( $p < 0.001$ ), that of RH ranges from 0.52 to 0.54 ( $p < 0.001$ ), and that of ET ranges from 0.37 to 0.84 ( $p < 0.001$ ) respectively. The bias of temperature was corrected by up to 0.35 °C in each hour, that of relative humidity was corrected by up to 2.84% in each hour, and that of evapotranspiration was corrected by up to 0.61 mm/day. Although errors can still be seen in the two simulations mentioned above, the improvement of bias and RMSE is statistically extremely significant, and coefficients of determination are remarkably increased from the IRR, which indicates that adding drip irrigation scheme improves performance of the WRF in simulating water and heat patterns in the MODS in the irrigation season.

Figure 3-3 shows the monthly ET and precipitation(P) from the CON and IRR simulations and observation, respectively, and total irrigation amount and P in each month in irrigation season. The ET is far more than the P in this region from both simulations and observation, indicating typical arid climate features in this region (Figure 3-3a). The ET values from the IRR simulation is closer to the observations (Figure 3-3a). The IRR simulation shows that the annual irrigation amount is 475.67 mm in 2012. Such a simulated irrigation amount is

comparable to the climatological irrigation consumption of 477 mm estimated from ground measurements (Li Fuxian 2002) and the irrigation quota of approximately 397.5-487.14 mm (ZHOU et al., 2013; MA Jinlong et al., 2015).

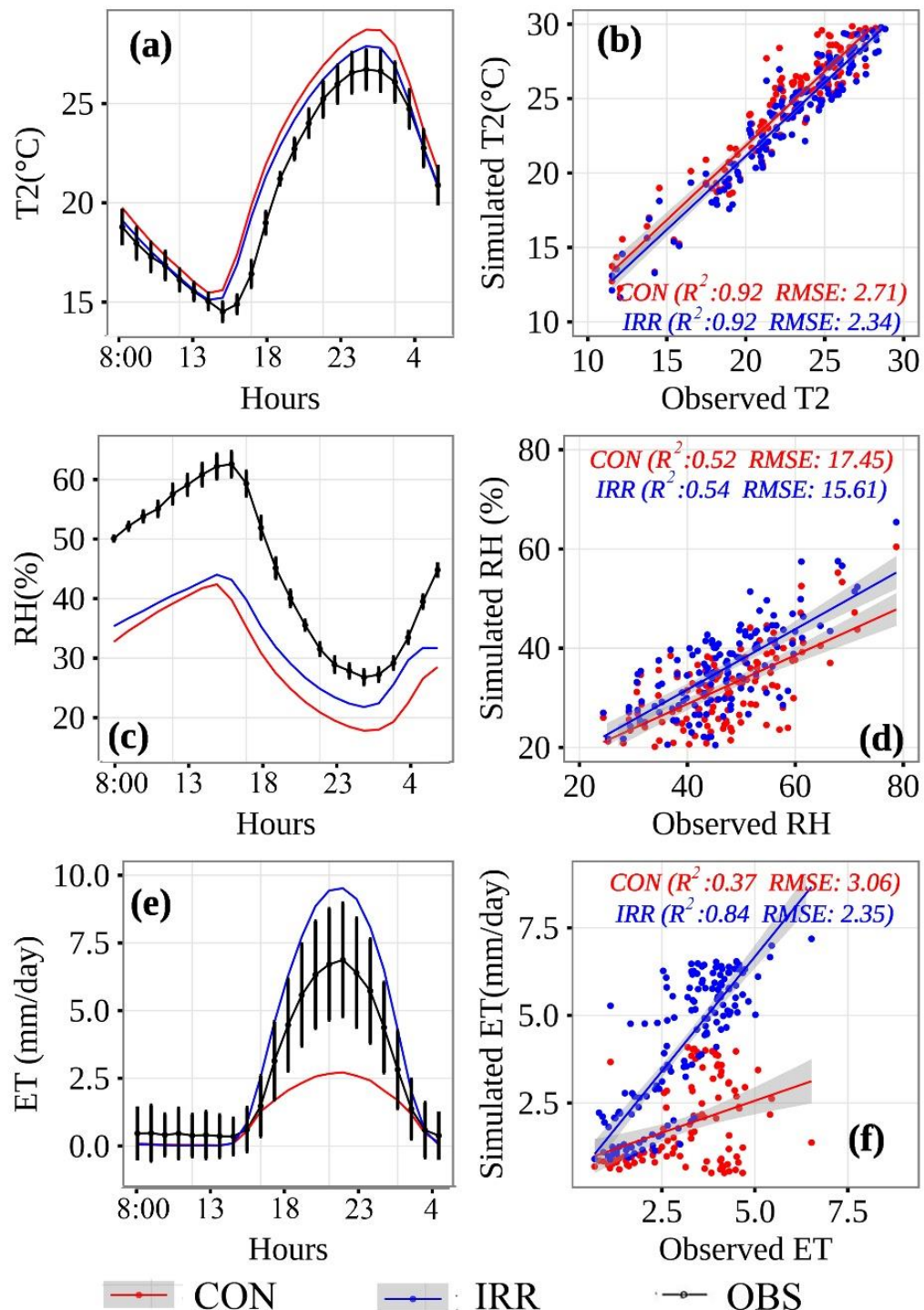
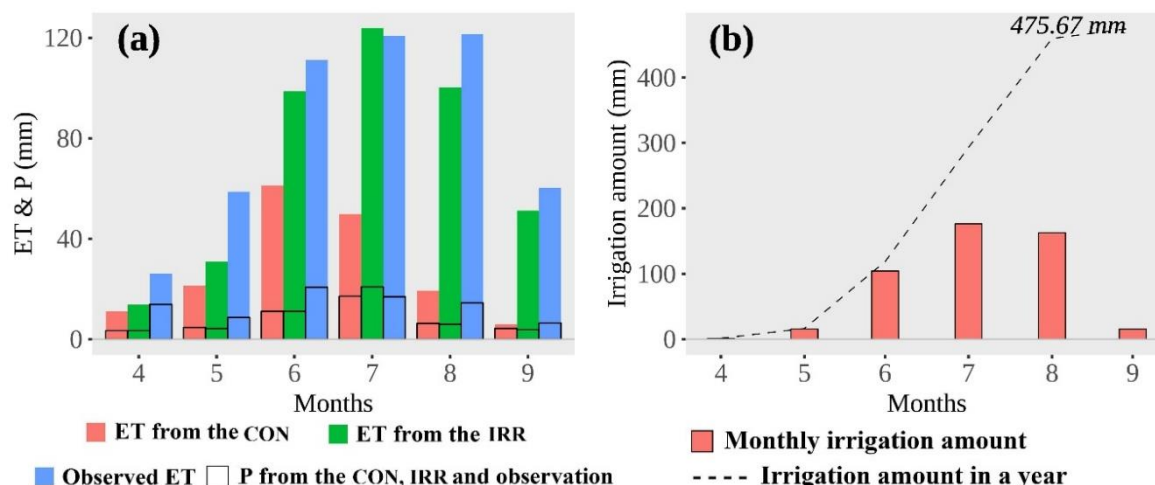


Figure 3-2. Comparisons of hourly averaged (a) 2-m air temperature (T2), (c) 2-m relative humidity (RH), (e) evapotranspiration (ET) between observations and simulations, respectively, and (b, d, f) corresponding scatter diagrams.





**Figure 3-3. Comparison of the (a) monthly evapotranspiration (ET), precipitation (P) from the CON and IRR simulations and observation, and (b) irrigation amount in each month and in a year from the IRR.**

### 3.4.2 The effects of irrigation on the near-surface climate elements

The patterns and partition of heat fluxes are directly associated with radiation budget and rising-sinking motions, which determines local, even wider range atmospheric circulation and local climate (Gu et al., 2006; Wang and Bouzeid, 2012). H and LE are directional parameters, their values are positive when the direction is upward. The spatial patterns of H, LE, T2 and Q2 in daytime and night time from the IRR simulation, and the effects of drip irrigation on these patterns are shown in Figure 3-4. In an overall look, the spatial patterns of H, LE, T2 and Q2 in daytime and nighttime generally exhibit continuous stripe-like increases from the mountainous areas to the oasis areas and to the desert areas (Figure 3-4a, b, c, d, c1, d1), except for H and LE patterns in nighttime (Figure 3-4a1, b1). The stripe-like change indicates that the near surface water-heat patterns of MODS are not only impacted by various underlying LU differences of mountain, oasis and desert, but are controlled by temperature lapse rate (TLR) caused by elevation difference. An obvious gradient line is observed along the northern boundary of the oasis and desert, indicating irrigated oasis region obviously disturb the stripe-like tendency of the water-heat patterns in the NTM. There is no effects of drip irrigation on patterns of H and LE at nighttime, but, in daytime, the mean all irrigated grid H and LE difference between the IRR and CON are  $-63.03 \text{ W/m}^2$  (ranges from  $-231.55$  to  $15.69 \text{ W/m}^2$ , the difference pixels are statistically significant at  $p < 0.001$ ) and  $80.81 \text{ W/m}^2$  (ranges from  $-12.9$  to  $286.2 \text{ W/m}^2$ , the difference

pixels are statistically significant at  $p < 0.001$ ), respectively, indicating that drip irrigation decreased H and increase LE over oasis region. We also noticed that the drip irrigation resulted in a decrease of near-surface air temperatures of mean all irrigated grid as large as  $-0.61\text{ }^{\circ}\text{C}$  (ranges from  $-1.71\text{ }^{\circ}\text{C}$  to  $0\text{ }^{\circ}\text{C}$ ) in daytime and as large as  $-0.35\text{ }^{\circ}\text{C}$  (ranges from  $-1.01\text{ }^{\circ}\text{C}$  to  $0.29\text{ }^{\circ}\text{C}$ ) at night over the oasis. While the irrigation increased Q2 over oasis  $0.68\text{ g/kg}$  in daytime and  $0.04\text{ g/kg}$  at nighttime, and the impacts of the irrigation on Q2 are distributed over the whole basin rather than over oasis itself.

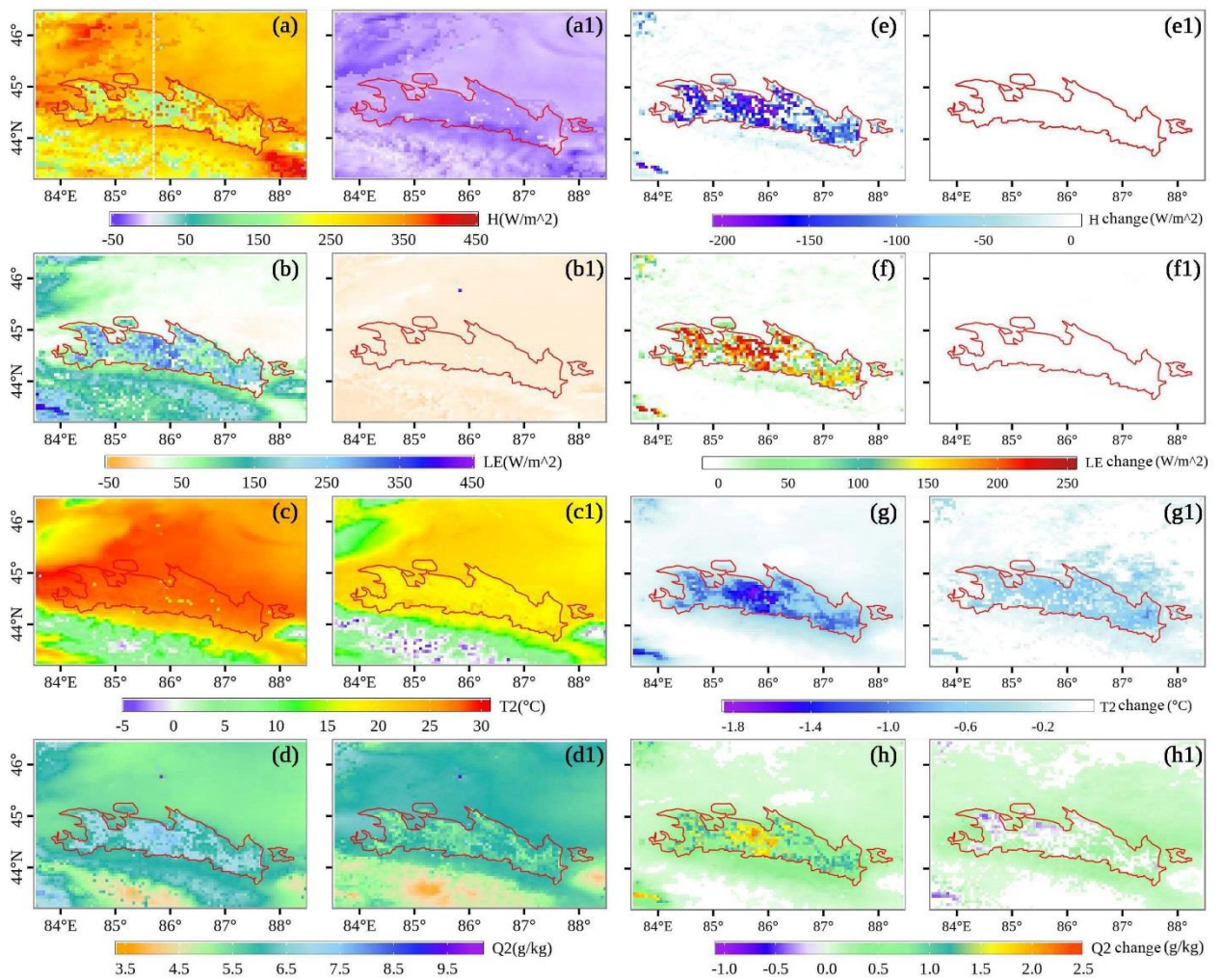


**Figure 3-4.** Spatial patterns of averaged (a) sensible heat flux (H), (b) latent heat flux (LE), (c) 2-m air temperature (T2), and (d) 2-m specific humidity from the IRR simulation in daytime in the irrigation season, and (e, f, g, h) the difference between the IRR and CON simulations (the difference pixels are statistically significant at  $p < 0.001$ ). And corresponding patterns in nighttime, which are labelled with the corresponding daytime label and the number 1. The red line represents the border of the oasis.

### 3.4.3 The effects of irrigation on the atmospheric structure and dynamics (humidity, temperature and PBLH)

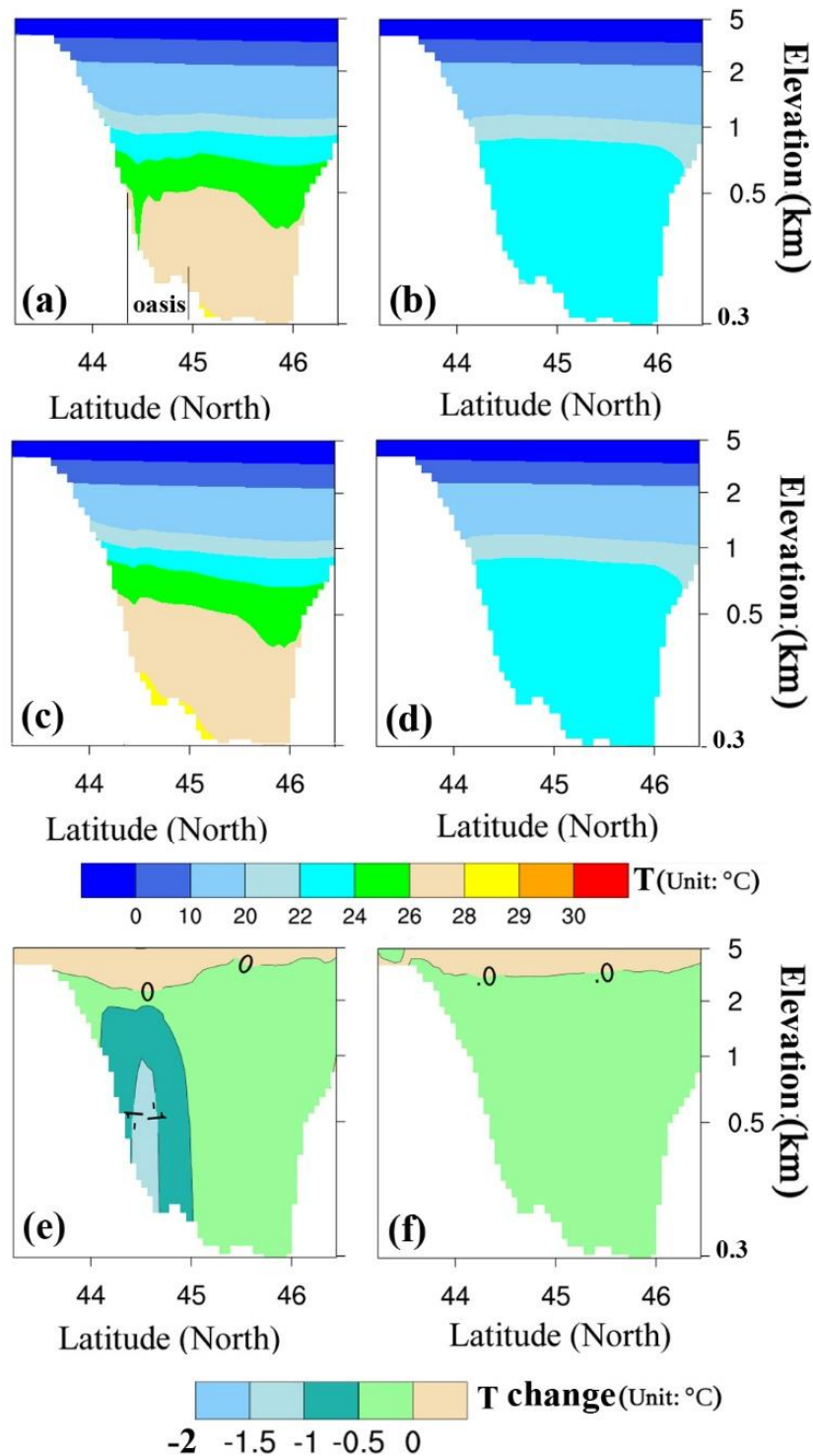
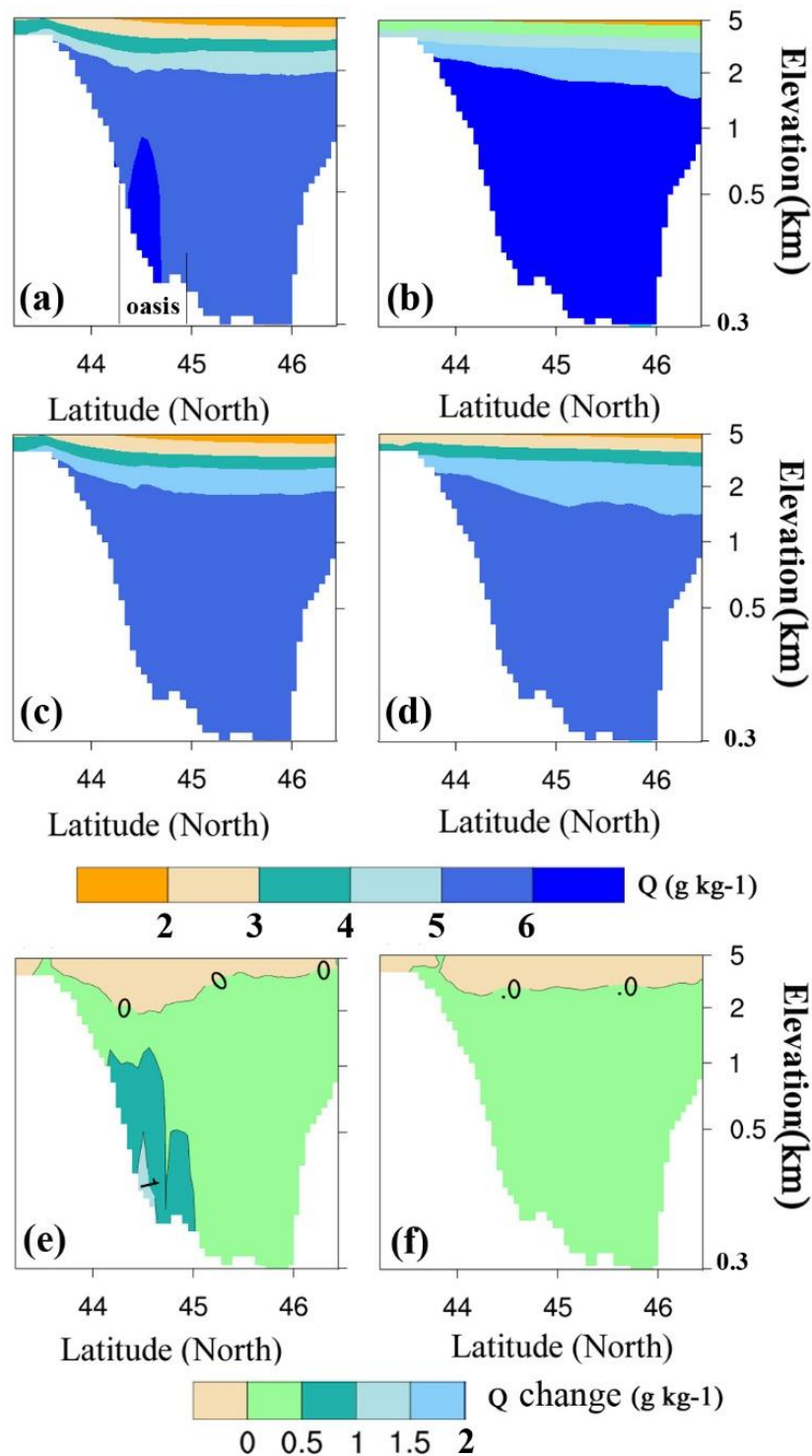


Figure 3-5. Vertical cross section of mean air temperature ( $^{\circ}\text{C}$ ) along the white line shown in Figure 4a from the (a, b) IRR simulation, and from the (c, d) CON simulation, and the (e, f) differences between the IRR simulation and CON simulation during daytime and nighttime, respectively. Height along y-axis is given in height (km).



**Figure 3-6. Vertical cross section of mean specific humidity (g/kg) along the white line shown in Figure 4a from the (a, b) IRR simulation, and from the (c, d) CON simulation, and the (e, f) differences between the IRR simulation and CON simulation during daytime and nighttime, respectively. Height along y-axis is given in height (km).**

Figure 3-5 and Figure 3-6 present the vertical section of mean air temperature ( $^{\circ}\text{C}$ ) and specific humidity (g/kg) from the IRR and CON simulations, and the effects of drip

irrigation on the vertical temperature and humidity patterns. Although both the IRR and CON simulations show continuous stripe-like increasing temperature and decreasing humidity patterns from earth surface to its above (Figure 3-5 and Figure 3-6a, b, c, d), the air temperatures (specific humidity) over the oasis area are clearly lower (higher) at the same altitude of approximately 1500 m from the IRR simulation compared with the CON simulation with n-shaped difference patterns of air temperature and humidity (Figure 3-5 and Figure 3-6e). These show that drip irrigation has a cooling and wetting effects on the atmospheric temperature and humidity in MODS, with values up to 0- -2 °C and 0-2 g/kg from near surface to approximately 1.5 km over the irrigated oasis region. These results indicates irrigation enhance the clod-wet island effects of oasis.

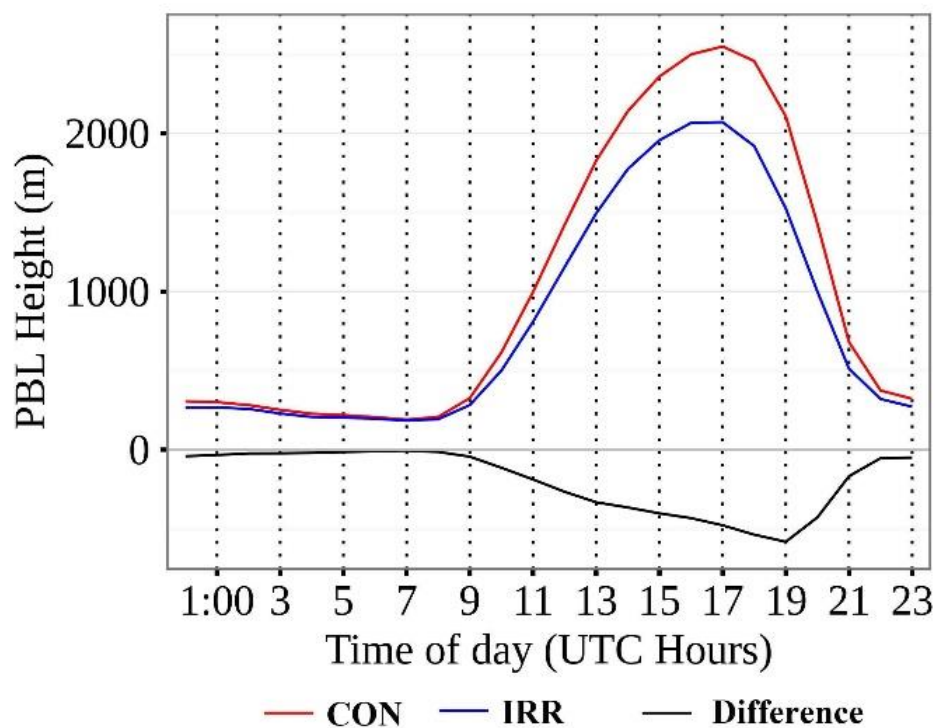


**Figure 3-7. Comparison of diurnal variation in mean planetary boundary layer height (PBLH) in irrigation season.**

The planetary boundary layer (PBL) generally refers to the bottom layer of atmosphere which is very close to the ground and is greatly influenced by the ground. Its thickness varies with weather conditions, terrain, roughness and biophysical properties of the ground, and provides the energy required to initiate local convective processes, such as precipitation, storms and circulation. Thus examining the relationship between PBLH and irrigation plays an important role in exploring the effects of irrigation on local water-heat states and

precipitation. The PBL height is lower over irrigated areas in a day (from 9:00 to 22:00 UTC time) based on the difference between IRR and CON simulations (Figure 3-7), indicating that the air mass over the oasis tends to be more stable when irrigation happened in the MODS.

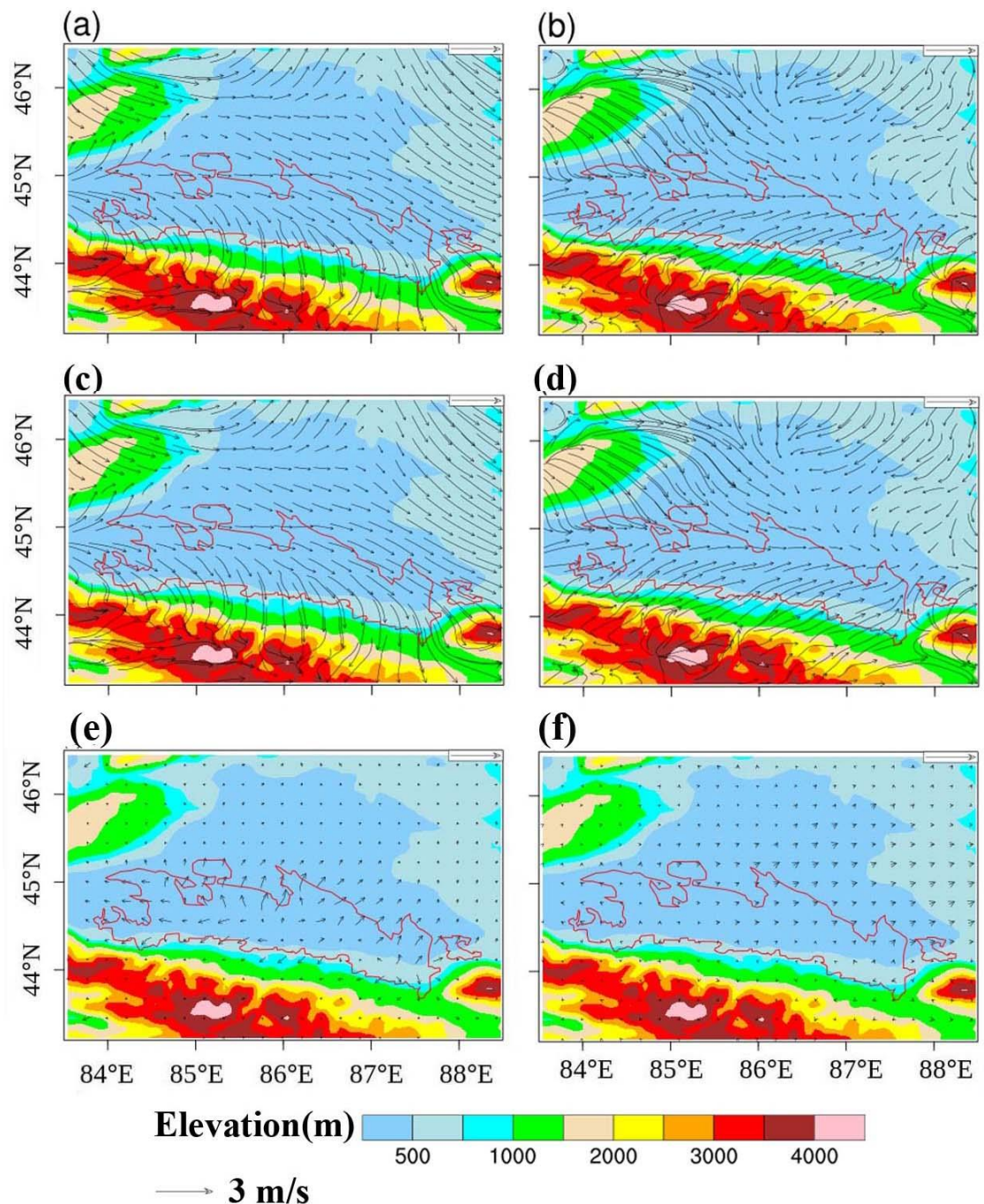


**Figure 3-8.** Mean 10-m horizontal wind speed and wind direction from the (a, b)IRR and (c, d)CON simulations, and the (e, f)differences between the IRR and CON simulations in daytime and nighttime, respectively. The red line represents the border of the oasis.

Figure 3-8 shows the diurnal mean WS and WD patterns from the IRR and CON simulations, and the effects of drip irrigation on circulation. In the context of the prevailing westerly wind, a wind direction of WNW with a wind speed of approximately 3 m/s occurs during the daytime (Figure 3-8a,c), whereas a wind direction of SW with a wind speed of approximately 4 m/s occurs at night (Figure 3-8b,d) covering the NTM, as observed from both the IRR and CON simulations. The diurnal change in the wind direction from WNW to SW in the IRR simulation demonstrates the typical characteristics of mountain-valley winds in the MODS. The drip irrigation produced a weak divergent wind blowing from the center of the oasis area to the surrounding desert with a speed of less than approximately 0.5 m/s at a height of 10 m (Figure 3-8c) in daytime, indicating drip irrigation increased the intensity of OBC (Chu et al., 2005; X Deng et al., 2015; X Meng et al., 2012; X H Meng et al., 2009). Almost no impacts of irrigation on circulation are observed at nighttime (Figure 8d).

#### 3.4.4 The effects of irrigation on precipitation and evapotranspiration

Local precipitation in this region is relevant to special geomorphology of mountain-basin systems (Luo et al., 2011), and both IRR and CON simulations show similar precipitation patterns in daytime and nighttime, that precipitation processes mainly concentrated on the mountains areas with elevation value greater than 1000 m (Figure 3-9a, b, c, d). However, total precipitation amount seems obviously increased in upwind mountains areas with elevation value of approximately 1000-2000 m, and decreased at the mountain top with elevation value greater than approximately 2000 m in daytime (Figure 3-9e and f). Meanwhile, all grids averaged P in the domain are 3.75 mm and 2.48 mm in daytime and nighttime, respectively, which implies that P might be overall increased due to irrigation. The change of precipitation might be relevant to terrain and mountain-valley winds. The airflow with increased moisture because of irrigation over oasis is brought to mountains areas with elevation approximately 1000-2000 m by intense valley wind in daytime (Zhang et al., 2017b), and forms precipitation due to adiabatic cooling and condensation in this region. Meanwhile intense mountain wind bring increased moisture because of irrigation over oasis to extend into the surrounding desert area at night, which may produce wet conditions favorable for desert plants in the oasis-desert transition zone (Zhang et al., 2017b).

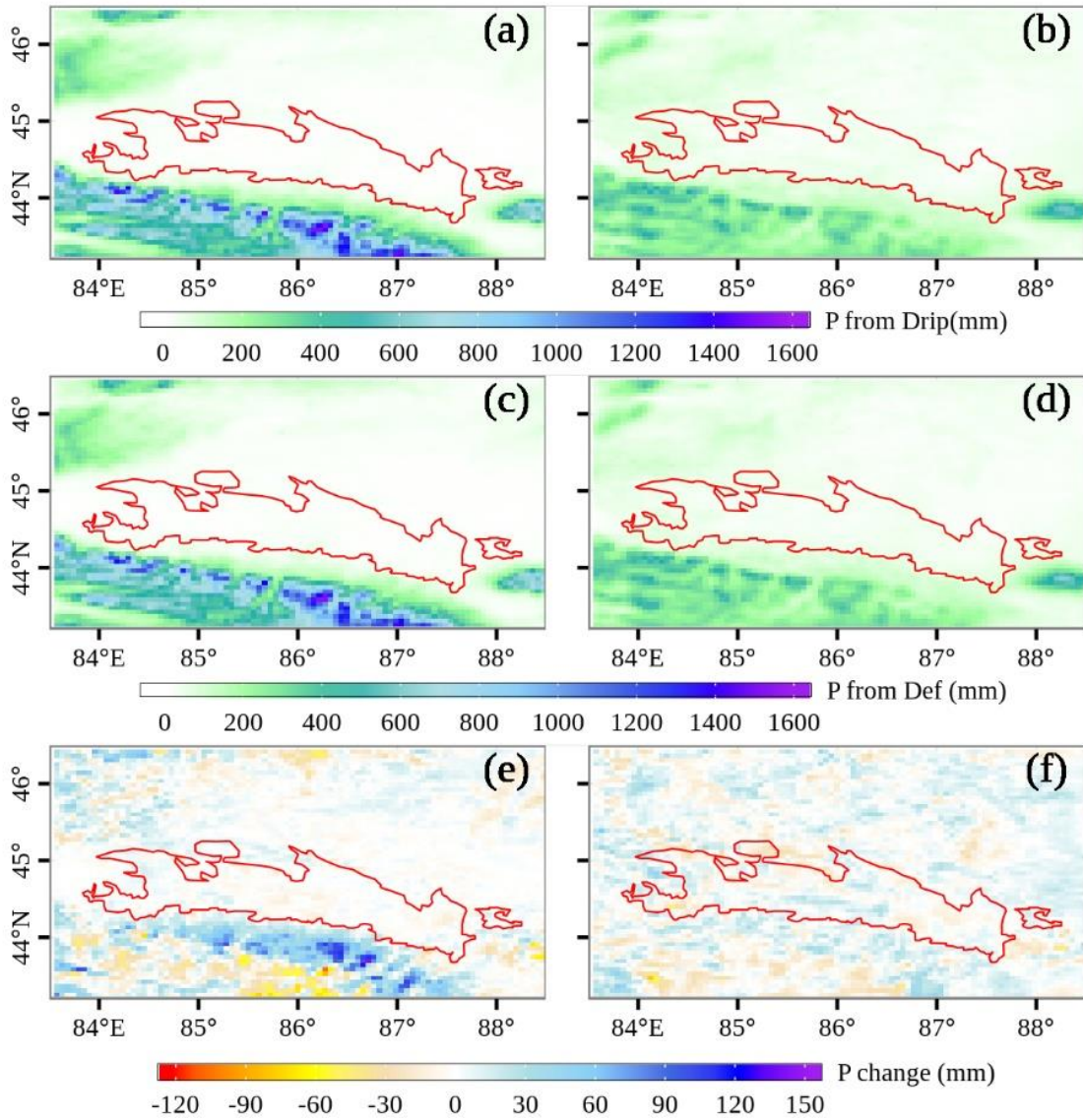


**Figure 3-9. Spatial patterns of total precipitation amount (TP) from the (a, b) IRR and (c, d) CON simulations in the irrigation season, and (e, f) TP difference between the IRR and CON simulations. The red line represents the border of the oasis.**

We examine the possible relationships of irrigation on precipitation and its change as shown the scatter plot in Figure 3-10a and c, it is difficult to determine whether the irrigation has effects on precipitation, at least over oasis (Observation sites are all located in oasis area). However, irrigation has significant impacts on ET and its change. When irrigation rate is greater than 2.5 mm/day, the ET increased 0.45 times more than the case with no irrigation, while irrigation rate is less than 2.5 mm/day, the ET increased 1.59 times more.



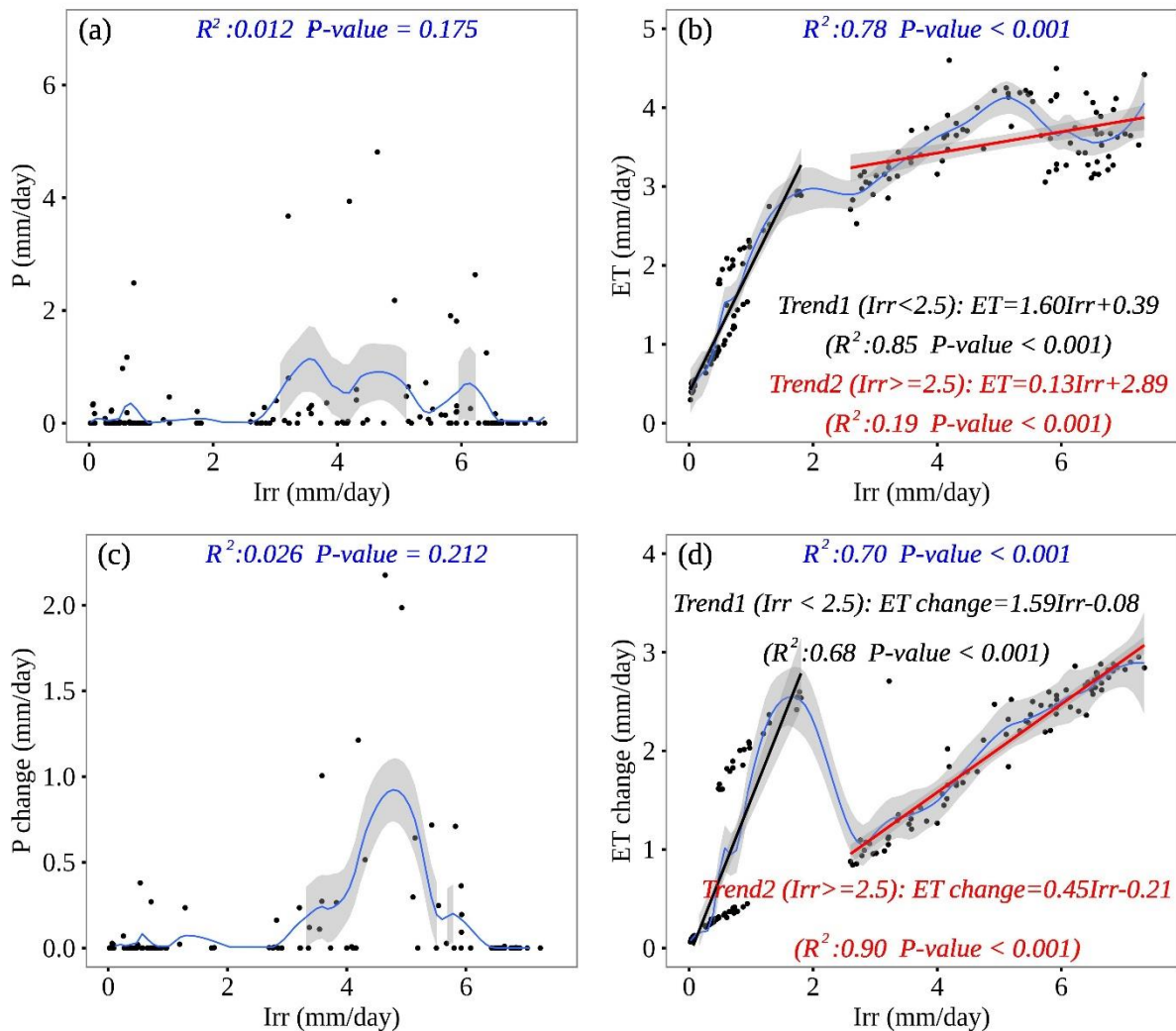


**Figure 3-10.** The scatter plot shows the correlation between the irrigation amount rate and (a) precipitation (P), (b) added Evapotranspiration (ET), (c) P change, and (d) ET change.

### 3.5 Discussion

The aim of the study was to explore impacts of drip irrigation on energy balances, temperature, precipitation and atmosphere structure in a mountain-oasis-desert system using WRF with a new irrigation scheme, since accurate representation of heat-water conditions of irrigated drop is a prerequisite to further study the climate effect of oasis evolution on climate or on water resources (Zaitchik et al., 2005). The performance of the Drip simulation yielded a reasonable representation for climate elements and irrigation water amount estimates at the site level. Irrigation increases the LE of  $80.81\text{ W/m}^2$  and decreases H  $63.03\text{ W/m}^2$  over oasis, thereby strengthening cold-wet island effects of oasis and OBC in the irrigation season. However, some important findings in the results are different from those of previous studies. Our modeling results show that the impacts of drip

irrigation on temperature, H and LE were mainly restricted over oasis, but the impact on humidity spread to across whole NTM. Moreover, irrigation increased precipitation amount in upwind mountains areas with elevation value of approximately 1000-2000 m, and decreased precipitation amount at the mountain top with elevation value greater than approximately 2000 m. Meanwhile, an increase seems to be observed in the basin at nighttime. That the impacting range of irrigation on humidity and precipitation spread to non-irrigation area might be relevant to mountain-valley winds. During daytime, since intense lower level valley wind is blowing from wet-cold oasis to mountainous area and forms precipitation at elevation of 1000-2000 m. During night, intense lower level cold-wet mountain wind is blowing from mountainous, through oasis, even extend to part of desert area, thus an increased precipitation in upwind mountainous area and increased humidity spreading whole NTM were observed. These mechanisms might accelerate the hydrological cycle in MODS .

The following uncertainties should be taken into consideration in interpretations of model estimates. All crop were threatened and irrigation field, as crops would not grow in the absence of irrigation in the CA. This treatment may enlarge the irrigation area, as there may be actually other land use/cover, such as bare land, within the cropland grids in the WRF's simulation. In addition, simulated ET and RH are overall underestimated, although we greatly improved simulation of water-heat conditions of oasis by adding drip irrigation schemes. These errors can be attributed to the fact that plastic mulching inhibits soil evaporation (Xie et al., 2005), which is not considered in the simulations of WRF (Wen et al., 2012; Meng et al., 2009). Adding plastic mulching process may help to correct these errors.

### **3.6 Conclusions**

The aim of the present study is to explore impacts of drip irrigation on water-heat conditions in a MODS using WRF with a new irrigation scheme. Model evaluations for temperature, humidity, energy and irrigation amounts further reveal that our simulation with new irrigation scheme realistically represented heat-water conditions of drip irrigated oasis. Irrigation strengthens cold-wet island effects of oasis and the OBC in the irrigation season. The impacts of drip irrigation on temperature, H and LE were mainly restricted over oasis, but the impact on humidity spread to across whole NTM. Moreover, irrigation increased

precipitation amount in upwind mountains areas with elevation of approximately 1000-2000 m, and decreased precipitation amount at the mountain top with elevation greater than approximately 2000 m. The increased precipitation in upwind mountainous and widely spread humidity implied that irrigation might accelerate the hydrological cycle in MODS.



# CHAPTER 4

## THE WATER-HEAT PATTERNS AND OASIS EFFECTS IN MODS

---

*Modified from: Zhang, Miao., Luo, Geping., Hamdi, Rafiq., Qiu, Yuan. Wang, Xinxin., De. Maeyer, Philippe., Kurban, Alishir. (2016). Numerical Simulations of the Impact of Mountain on Oasis Effects in Arid Central Asia. Atmosphere. 2017, 8, 212; doi:10.3390/atmos8110212.*

## ABSTRACT

The oases in the mountain-basin systems of Central Asia are extremely fragile. Investigating oasis effects and oasis-desert interactions is important for understanding the ecological stability of oases. However, previous studies have been performed only in oasis-desert environments and have not considered the impacts of mountains. In this study, oasis effects were explored in the context of mountain effects in the north Tianshan Mountains (NTM) using the Weather Research and Forecasting (WRF) model. Four numerical simulations are performed. The ‘def’ simulation uses the default terrestrial datasets provided by the WRF model. The ‘mod’ simulation uses actual terrestrial datasets from satellite products. The ‘non-oasis’ simulation is a scenario simulation in which oasis areas are replaced by desert conditions, while all other conditions are the same as the mod simulation. Finally, the ‘non-mountain’ simulation is a scenario simulation in which the elevation values of all grids are set to a constant value of 300 m, while all other conditions are the same as in the mod simulation. The mod simulation agrees well with near-surface measurements of temperature, relative humidity and latent heat flux. The Tianshan Mountains exert a cooling and wetting effects in the NTM region. The oasis breeze circulation (OBC) between oases and the deserts is counteracted by the stronger background circulation. Thus, the self-supporting mechanism of oases originating from the OBC plays a limited role in maintaining the ecological stability of oases in this mountain-basin system. However, the mountain wind causes the “cold-wet” island effects of the oases to extend into the oasis-desert transition zone at night, which is beneficial for plants in the transition region.

**Keywords:** oasis effects; mountain-basin system; oasis breeze circulation; mountain-valley wind; WRF; Central Asia arid area

### 4.1 Introduction

Oases are common in the deserts of arid areas (Souza et al., 2006; Smith et al., 2007; Soltan, 1999; Li et al., 2007), especially in the hinterland of arid Central Asia (CA). The formation of an oasis in this region is closely related to the geomorphic characteristics of high mountain-basin systems, because the melting of snow and glaciers and the precipitation in tall mountain ranges provide necessary water resources for oasis survival and development

in these mountain-basin systems (Luo et al., 2010). Accordingly, watersheds represent a basic unit in this mountain-oasis-desert system (MODS). The North Tianshan Mountains (NTM) is one of the typical geomorphic regions of CA and consists of a large number of complex MODSs. Although oases account for only a small proportion of the land surface (e.g., 4–5% in Xinjiang, a typical region in the hinterlands of Central Asia), more than 90% of the local population and >95% of the socioeconomic wealth are concentrated in oases (Meng et al., 2009). Thus, oases play a vital role in social and economic development. Since the 1950s, the region has experienced distinct and intense land reclamation, characterized mainly by oasis expansion. The total oasis area has expanded to 4.23 times its original value (from  $121.0 \times 10^4$  ha in 1949 to  $512.5 \times 10^4$  ha in 2010). As a result, a series of ecological problems have appeared due to the limited water and soil conditions (Hong et al., 2003; Zhang et al., 2017b; Jia et al., 2004), such as desertification and soil salinization (Sun et al., 2011; Wang et al., 2008). These problems have hindered the sustainable development of the oases.

Oasis effects are thought to play an important role in maintaining the existence of oases over time. In the recent literature, several studies based on both field observations and numerical simulations have focused on the exchanges of water and energy between oases and the surrounding deserts (Li et al., 2013; Li et al., 2016b; Ling et al., 2013; Wang et al., 2016). The differences in the geographical and ecological characteristics between oasis areas and desert areas result in significant differences in their energy budgets, create exchanges of momentum and water vapor and affect the amounts of heat and moisture released to the atmosphere within the convective boundary layer. During daytime, solar radiation heats the desert surface and rapidly increases the near-surface temperatures over desert areas. In contrast, the temperature over oases is lower due to the intense level of evaporation occurring in oases (Li et al., 2016a). At the same time, the humidity over oases is higher than that over the desert. The air density and pressure in the near-surface layer over the desert are lower than over the oasis, thereby causing cold moist air to flow from the oasis to the desert, resulting in a moisture inversion over the desert (Liu et al., 2007b). At higher elevation, the hot dry air over the desert flows toward the oasis, resulting in the oasis becoming a cold, wet island capped by warm, dry air. This phenomenon has been observed to create a temperature inversion layer and negative sensible heat fluxes over oases (Li et al., 2013; Su and Hu, 1987; Rosenberg, 1969; Wang et al., 1993) and is known

as the “oasis effects” (Li et al., 2016a). The water and heat differences between the oasis and the desert cause local atmospheric circulation patterns, called OBC. Recent numerical simulations of OBC have been performed using regional climate models coupled to sophisticated land surface schemes, such as the NCAR MM5 or the WRF model (Chu et al., 2005; Gao et al., 2004; Han et al., 2010; Liu et al., 2007b; Lv et al., 2005; Meng et al., 2015; Meng et al., 2012; Meng et al., 2009; Nnamchi, 2011; Wen et al., 2012). These studies have improved our understanding of the mechanisms and processes associated with the oasis-desert interactions. The conception of the “self-supporting mechanism of oasis” has been proposed based on OBC. Specifically, the downdrafts over an oasis decrease evaporation within the oasis, whereas the updrafts over the desert areas adjacent to the oasis act as a wall that hinders the transfer of cold, wet air to the dry surrounding desert (Wen et al., 2012; Li et al., 2016a). Thus, the OBC helps to maintain the ecological stability of oases by reducing the exchanges of heat and moisture between oases and the surrounding desert areas.

However, an oasis cannot survive without a supply of water from the nearby large mountains in a MODS. Therefore, studies should explore the oasis effects, i.e., the oasis-desert interactions, under the impacts of these surrounding mountains rather than focusing only on the oasis and desert areas (Chu et al., 2005; Gao et al., 2004; Han et al., 2010; Liu et al., 2007b; Lv et al., 2005; Meng et al., 2015; Meng et al., 2012; Meng et al., 2009; Nnamchi, 2011; Wen et al., 2012). Failing to consider the impacts of the mountains may result in an incorrect or incomplete understanding of the oasis-desert interactions within a MODS. For example, what are the spatial patterns of water and heat throughout MODS? Do intense mountain-valley winds occur within current MODSs (Zardi and Whiteman, 2013; Helgason and Pomeroy, 2012)? Finally, how does the mountain-valley wind, if present, impact the oasis effects and OBC? The answers to these questions are not clear and deserve additional and comprehensive investigation. Since, once OBC ceases to operate within a MODS, the self-supporting mechanism of oasis originated from OBC will disappear and the water vapor over the oasis may flow into the surrounding deserts. Consequently, the oasis will become drier and drier, perhaps resulting in a vicious cycle of water deficiency and desertification (Meng et al., 2009). Accordingly, answering the above questions is essential, both theoretically and practically, to the sustainable development and ecological stability of oases and will provide useful information for further investigating



the impact of oasis expansion on regional climate changes (Yan et al., 2014) under global warming.

The WRF model coupled to the sophisticated land surface scheme Noah has been used to simulate regional climates over the past 10 years (Branch et al., 2014; Cao et al., 2015). The WRF model is sensitive to land surface properties (Lenderink et al., 2007; Vidale et al., 2007), especially primary parameters such as land use/cover (LU) and secondary parameters such as the green vegetation fraction (GVF), the leaf area index (LAI) and albedo, which can be determined from the LU. However, the default values of these parameters are usually from the outdated 1992–1993 Advanced Very High Resolution Radiometer (AVHRR) dataset. Realistic representation of these land surface properties is necessary to improve WRF-based simulations over complex areas, such as MODSs (Müller et al., 2014). In this study, actual LU, albedo, LAI and GVF data from the MODerate Resolution Imaging Spectroradiometer (MODIS) products are used.

Our ultimate goals in this paper are to realistically depict the temperature, humidity and circulation patterns of a complex MODS and to describe the impacts of mountain on oasis effects within MODS in Central Asia using the WRF model. The paper is structured as follows. Section 2 presents a description of the study area, the datasets used in this work, the WRF model and the design of the experiments performed here. Section 3 presents the results of the simulations. Section 4 offers a discussion and identifies avenues for future investigation. The final section summarizes the findings of this study.

## **4.2 Study area**

The information of NTM has been introduced in the section 1.2 and the oasis expansion situation has also been introduced in the section 1.1.1. Detailed three-nested domain information can be seen in section 1.3.2.

## **4.3 Datasets**

### **4.3.1 Forcing Data and In Situ Measurements**

The detailed elements and information of ERA-Interim are seen in section 1.4.1. We select hourly observation in 2012 at meteorological stations S1, S2, S3, and S4 to validate simulation results (Table 1-4), because the four stations are distributed in irrigated oasis areas in the D03. Hourly climate elements were retrieved to validate the simulation results.

#### 4.3.2. Actual Land Surface Parameters

In this study, we converted an actual LU dataset with a hierarchical classification system (Table S1) into the USGS classification system used in the WRF model (Zhang et al., 2017a), based on the corresponding relations shown in Table S2. The default albedo, LAI and GVF provided by the WRF model have been replaced with the actual MODIS products MCD43A4, MYD15A2 and a GVF dataset computed from MOD13A2 (Yin et al., 2016; Miller et al., 2006; Seungbum et al., 2009), respectively. These products were downloaded from <https://modis.gsfc.nasa.gov/data> and correspond to 3 July 2012 and the strip numbers h23v04 and h24v04. We reprocessed these products using the same coordinate systems and resolutions as in the numerical simulations.

### 4.4 Methodology

#### 4.4.1. Model Description and Configuration

The detailed WRF configuration has been introduced in section 1.3.2. The simulation results from domain D02 are stored hourly and provide hourly lateral boundary conditions for D03.

#### 4.4.2. Experimental Design

Four simulations were conducted as follows. (i) The def simulation uses the default LU, GVF, LAI, albedo datasets provided by the WRF model and without drip irrigation process; (ii) In the mod simulation, the default LU, albedo, LAI and GVF datasets are updated using the MODIS products mentioned in Section 2.3.2 and with adding drip irrigation process. (iii) The non-oasis simulation is a sensitivity simulation in which the oasis areas are replaced with desert conditions and the other conditions are the same as in the mod simulation. (iv) Finally, the reference non-mountain simulation involves setting the elevation value of the grid cells to a constant value of 300 m, while the other conditions are the same as in the mod simulation. The differences between the ‘def’ simulation and the ‘mod’ simulation are used to examine the performance of the WRF model using actual biophysical parameters and drip irrigation process. The differences between the mod simulation and the non-oasis simulation and the differences between the mod simulation and the non-mountain simulation were used to quantitatively investigate the effects of oases

and mountains, respectively, on temperature, humidity and circulation features within the complete MODS.

All of the experimental simulations are initialized during the period of the most vigorous vegetation growth and extend from 00:00 UTC on 1 July 2012, to 18:00 UTC on 31 July 2012. In this study, the soil moisture values of the oasis and desert areas are initialized via interpolation from observed soil moistures data from similar oasis and desert regions referenced in a previous paper (Wen et al., 2012) (Table 1-3. Four layer of soil moisture values for oases and desert areas in the NOAH (Wen et al., 2012)

Land Use Type	Noah Soil Layer	Soil Moisture (cm <sup>3</sup> cm <sup>-3</sup> )
Oasis	0–10 cm	0.38 (at 5 cm)
	10–40 cm	0.47 (at 25 cm)
	40–100 cm	0.33 (at 70 cm)
	100–200 cm	0.26 (at 150 cm)
Desert	0–10 cm	0.07 (at 5 cm)
	10–40 cm	0.10 (at 25 cm)
	40–100 cm	0.05 (at 70 cm)
	100–200 cm	0.06 (at 150 cm)

The ERA-Interim reanalysis data provides the initial and lateral boundary conditions for simulations at 6-h intervals (detailed can be seen in section 1.3.1). The simulation results from domain D02 are stored and provide hourly lateral boundary conditions for D03. All domains ran with 35 unevenly spaced full eta levels with 15 levels below the height of 5 km from the ground surface. The model top was fixed at 50 hPa. The different parameterizations of the physical atmospheric schemes have been performed previously in the study region by Qiu et al. (Qiu et al., 2017). We referenced the best one of WRF configurations (of physical schemes) shown in Table 1-2. The initial soil moisture and the soil boundary temperatures are derived from the forcing data; however, the soil moisture levels of the oases and desert areas are adjusted using observations (**Error! Not a valid bookmark self-reference.**).

). In addition, also following similar previous simulations of mesoscale water, surface energy and circulation processes (Chu et al., 2005; Meng et al., 2012; Meng et al., 2009), the first 15 days of the simulations are skipped as spin-up to enable the soil moisture of the

other land use types in the MODS to reach relative equilibrium. The simulation results covering the periods from 19:00 UTC on 15 July 2012, to 18:00 UTC on 20 July 2012 (i.e. from 00:00 Beijing time on 16 July to 23:00 Beijing time on 20 July), are used for analysis. This 5-day period is characterized by anticyclonic and clear-sky conditions; thus, the effects of cloud distribution are excluded from the results (not shown). All of the spatial patterns of temperature, humidity and circulation during the daytime and nighttime represent the average of the simulation results over these 5 days.

## 4.5 Results

### 4.5.1 Simulation Evaluation

Figure 4-1 shows a comparative analysis of the observed and simulated 2-m air temperature (T2), 2-m relative humidity (RH) and latent heat flux (LE) over the oasis surface. The ‘mod’ simulation is closer to the observations than the ‘def’ simulation. The LE computed from the ‘mod’ simulation over the oasis surface provides a much better representation of the peak values and correctly reproduces the overall shape of the observed value.

The mean LE value at the daily maximum from the mod simulation is approximately 400 W/m<sup>2</sup>, which is two times greater than that of the def simulation (Figure 4-1c). The mod LE values are closer to the observations and the mean bias (modeled values minus observations) is up to 40.6 W/m<sup>2</sup> smaller than those of the def simulation over the whole period (not shown).

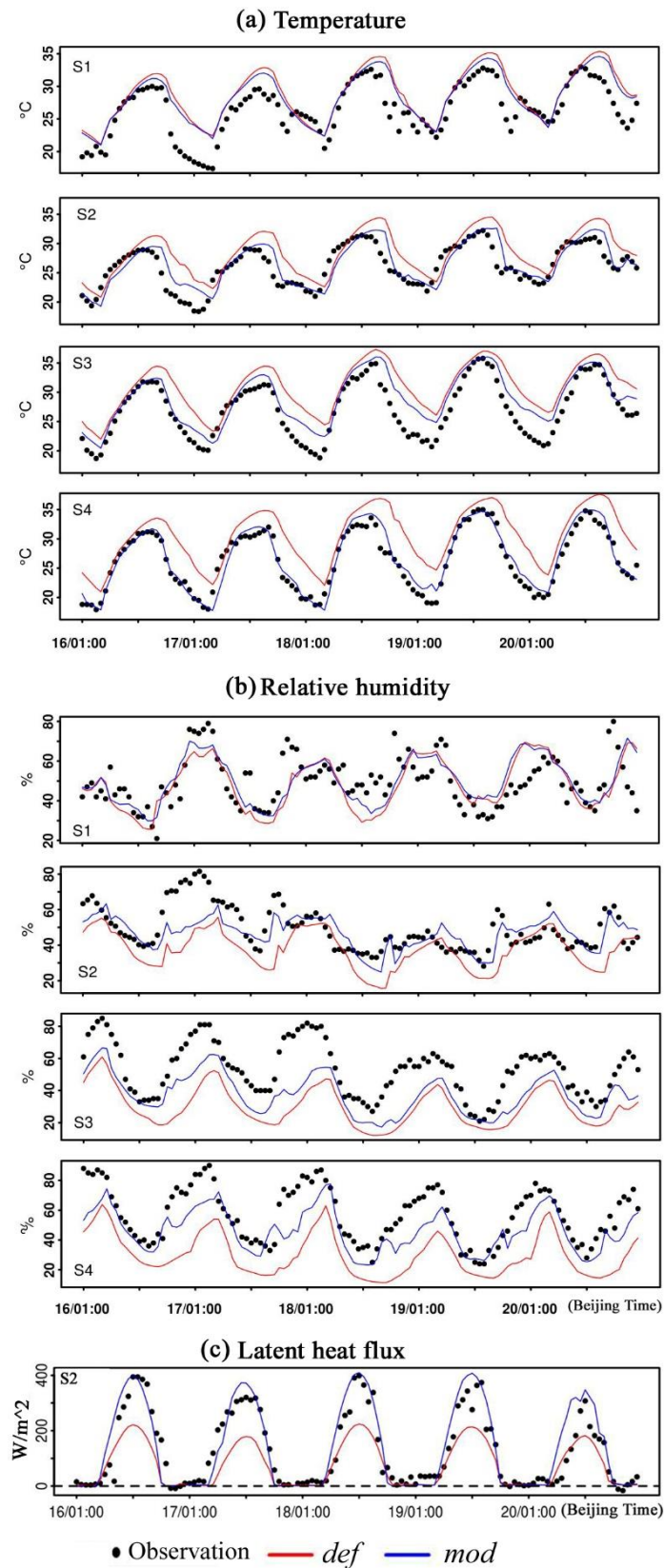


**Figure 4-1. Comparisons of the observed and simulated (a) 2-m air temperature (T<sub>2</sub>), (b) 2-m relative humidity (RH) and (c) latent heat flux (LE) at the four stations (S1, S2, S3 and S4) during 16 July to 20 July.**

Figure 4-2 compares the mean bias error (MBE), root mean square error (RMSE) and the Pearson correlation coefficient ( $r$ ) computed from the mod and def simulations for T2 and RH. For the four sites, the ‘mod’ simulation is clearly closer to the observed values and is associated with significant reductions in the MBE and the RMSE (the p-value is less than 0.01) and a significant increase in the Pearson correlation coefficient (the p-value is less than 0.01). The performance of the WRF model in the mod simulation shows considerable improvements due to the updates of the LC, albedo, LAI and GVF datasets. In fact, the bias in T2 is corrected to approximately 0.3-2.4 °C and that of RH is corrected to 1.9–12.9% in the mod simulation.

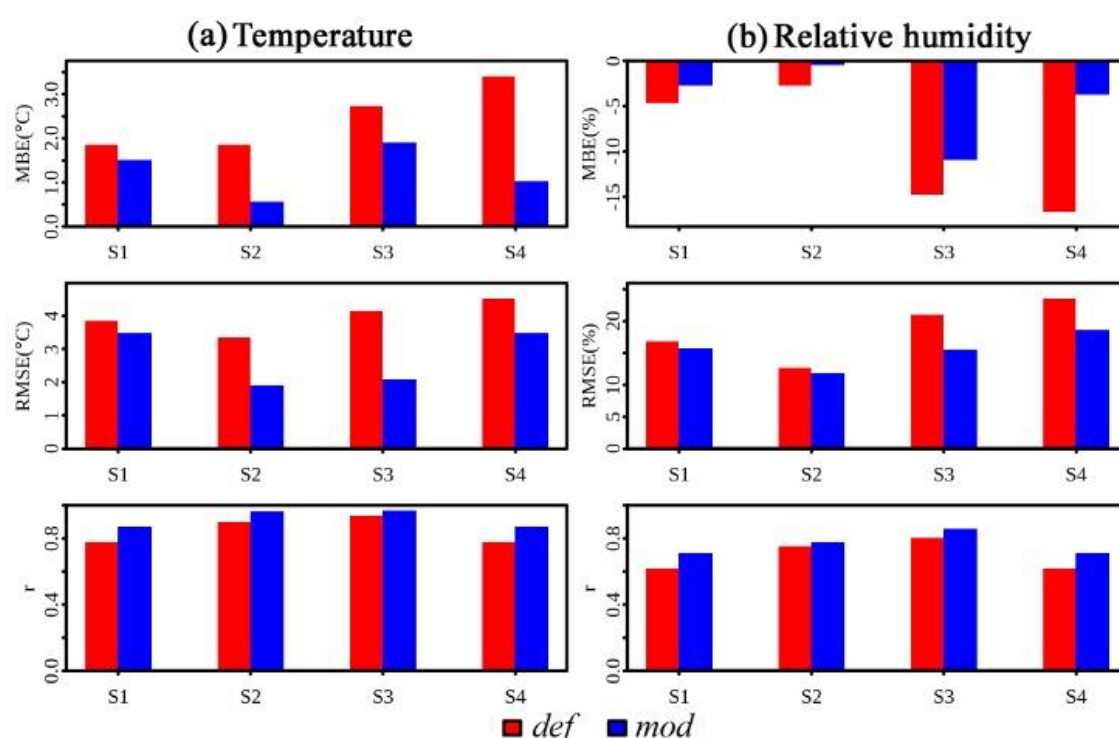


**Figure 4-2. The mean bias error (MBE), root mean squared error (RMSE) and Pearson correlation coefficient ( $r$ ) between the simulated and observed (a) air temperature and (b) relative humidity at 2 m at the four stations (S1, S2, S3 and S4).**

Note that the reductions in the biases associated with T2, RH and LE are larger at stations S2 and S4 than at the other two locations shown in Figure 4-1. This pattern occurs because the actual LAI and GVF values at S2 and S4 improved to a much greater degree than those at the other two sites. Specifically, the LAI values at S2 and S4 changed from 1.08 and 0.52 to 4.8 and 3.0, respectively and the GVF values at S2 and S4 changed from 36.6% and 13.5% to 84.7% and 82.15%, respectively (Figure 4-2g,h). The LU types at S2 and S4 are

homogenous cropland but those at S1 and S3 include cropland combined with urban areas (S1) or desert areas (S3), respectively. As a result, more consistent trends and similar magnitudes of T2, RH and LE are observed at the four stations in the mod simulation than in the def simulation, as shown in Figure 4-1. This validation indicates that the simulated temperature, humidity and latent heat flux trends obtained from the mod simulation are consistent with the observations and realistically represent the water and heat conditions of the oasis surface.

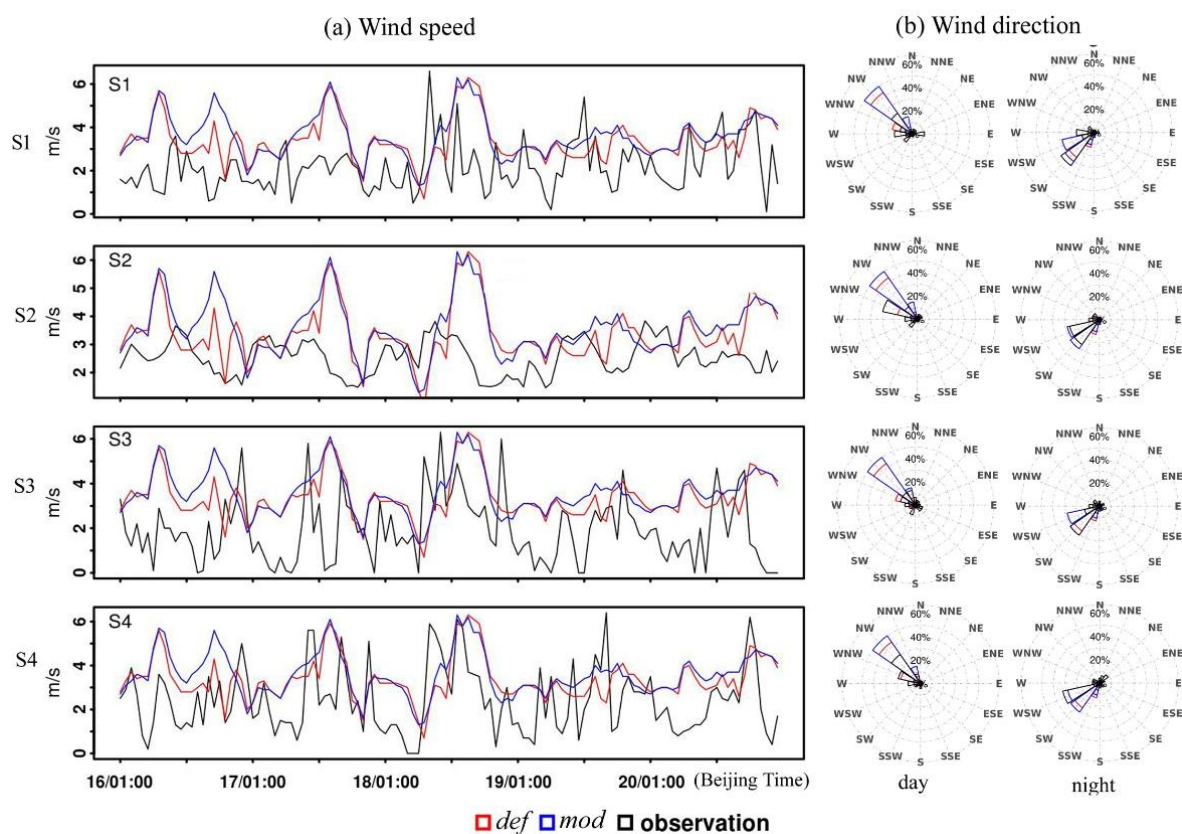


**Figure 4-3. Comparison between the observed and simulated (a) wind speed (WS) and (b) wind direction (WD) from the mod and def simulations at the four stations (S1, S2, S3 and S4) during 16 July to 20 July.**

A comparison of observed and simulated 10-m horizontal wind at the four meteorological stations, as represented by the mod and def simulations, is shown in Figure 4-3. Stations S1 and S2 are located in the upper part of oasis near its southern border and stations S3 and S4 are located in the lower part of the oasis near its northern border. Most of the simulated WS values are slightly higher than the observed values; 60 percent of the simulated WS values lie within a range of 2–5 m/s, whereas the observed values range from 2–4 m/s. The reason for this bias in WS is that the uncertainty of randomized turbulence processes

hinders the accurate simulation of wind (Hanna and Yang, 2001). However, the trend in WD agrees well with the observations. The observed dominant WD is WNW or NW during daytime and WSW or SW at night for all four stations. The simulated WD and its diurnal changes are consistent with the observations. This validation demonstrates that the simulated WD agrees well with the observation and represents the circulation characteristics of the mountain-valley wind in the study area.

#### 4.5.2 The spatial patterns of temperature of MODS

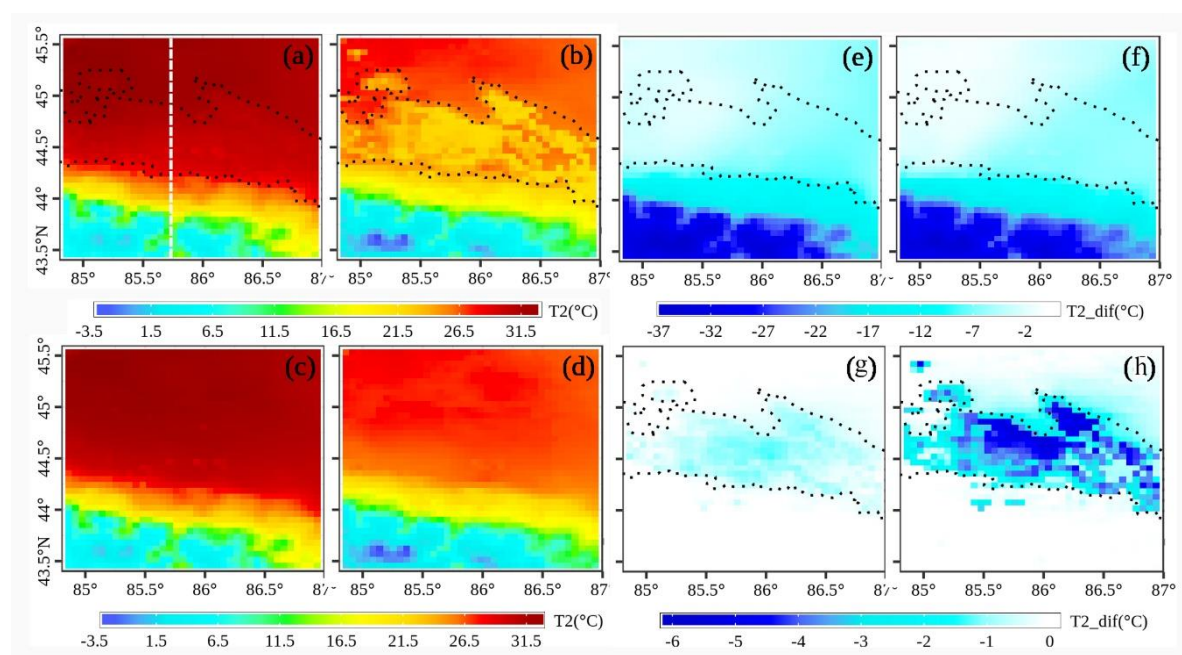


**Figure 4-4.** Mean 2-m air temperatures ( $T_2$ ) from the (a,b) mod simulation and (c,d) the non-oasis simulation; (e,f) and the differences between the mod simulation and non-mountain simulation; and (g,h) the differences between the mod simulation and the non-oasis simulation during daytime and nighttime, respectively. The black dotted line represents the border of the oasis and the white dotted line (a) represents the location of the vertical section (longitude 85.7° E) represented in Figure 4-6.

The 2-m air temperatures from both the mod and non-oasis simulations generally exhibit continuous stripe-like increases from the mountainous areas to the oasis areas and to the desert areas (Figure 4-4a–d). This pattern indicates that the spatial temperature pattern seen in the MODS reflects the TLR due to the elevation gradient difference within the MODS. An obvious temperature gradient line is observed along the northern boundary of the oasis in the mod simulation (Figure 4-4a,b) but not in the non-oasis simulation (Figure 4-4c,d),



indicating that the water and heat differences between the oasis and desert areas obviously disturb the stripe-like increases in temperature in the MODS.

The mean near-surface air temperatures over the oasis area are 30.44 °C and 23.36 °C during the daytime and nighttime, respectively (Table 4-1). In contrast, the near-surface air temperatures over the desert are approximately 32.5 °C and 28.0 °C, respectively (Figure 4-4a,b). The differences in the near-surface air temperatures between the oasis and desert areas indeed indicate that the oasis areas represent a “cold island” compared to the surrounding desert during daytime and nighttime. The intensity of this “cold island” resulting from the oasis cooling effect is as large as  $-0.61$  °C in daytime and as large as  $-3.37$  °C at night, as computed using the mean oasis temperature difference between the mod simulation and non-oasis simulation (these differences are statistically significant at  $p < 0.01$ , Table 3). During the daytime, because the soil moisture and thermal capacity values are higher in the oasis areas than the desert areas, more energy is required to increase the temperatures over the oasis areas and evapotranspiration takes place in the oasis, causing cooling (Wen et al., 2012) (as can be seen in Figure S5a,c). The possible reasons for the more intense cooling effect of the oasis at night include evaporation from the surface soil (Figure S4f) and the TLR; the slightly higher elevation of the oasis areas (Figure 4-4e,f) enhances the intensity of this “cold island” effect. Note that the near-surface temperature patterns from the non-mountain simulation (Figure S1a,b) and the difference patterns between the mod simulation and the non-mountain simulation (Figure 4-4e,f) are also consistent with circulation patterns, illustrating that the water and heat patterns in the study area are controlled by larger-scale circulation in the absence of high-relief terrain.

The continuous stripe-like temperature patterns and the oasis cooling effect are further illustrated by the vertical section of temperature patterns from the mod and non-oasis simulations and the temperature differences between the mod and the non-oasis simulations and between the mod and non-mountain simulations (Figure 4-5). In the daytime, the air temperatures in the oasis area in the mod simulation are clearly lower than those over the northern desert area and the southern mountainous area at the same altitude of approximately 1500 m and this temperature pattern forms a concave-shaped vertical temperature pattern in the MODS (Figure 4-5a). At night, a clearly defined temperature inversion layer (TIL) is observed near the surface over the oasis area. Its thickness varies from 200 m in the southern part of the oasis with an elevation of 450 m to 600 m in the

northern part with an elevation of 300 m (Figure 4-5b). However, the concave-shaped vertical temperature pattern observed during the daytime and the TIL that developed during the nighttime are not observed in the non-oasis simulation (Figure 4-5c,d), indicating the concave low-temperature center and the TIL over the oasis areas result from the oasis cooling effect. Based on the differences between the mod and non-oasis simulations, the “cold island” effect of the oasis extends to a height of approximately 1.5 km above the oasis surface, as shown by the n-shaped cooling center (Figure 4-5d,g). Moreover, the cooling effect of the oasis extends horizontally into the desert-oasis transition areas to a distance of approximately 25 km (Figure 4-5h and Figure 4-6h) at night due to the mountain-wind. In addition, the existence of high-relief terrain (mountains) decreases the whole temperature over the basin during the daytime and the nighttime, based on the differences between the non-oasis and non-mountain simulations (Figure 4-4 and Figure 4-5e,f).

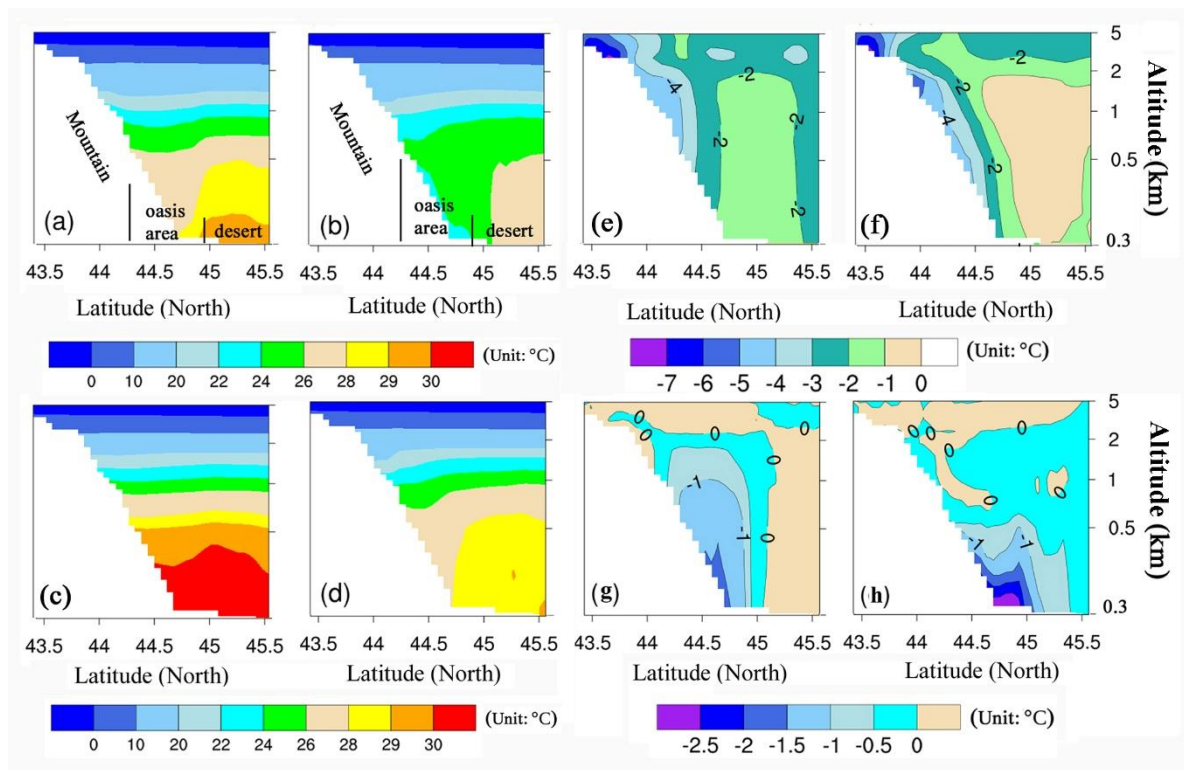


**Figure 4-5.** The same as Figure 4-5 but showing for a vertical cross section of air temperature along the white line shown in Figure 4-5a.

#### 4.5.3 The spatial patterns of humidity of MODS

The mean near-surface specific humidity ( $Q_2$ ) values over the oasis in the mod simulation are  $9.99 \text{ g kg}^{-1}$  and  $10.05 \text{ g kg}^{-1}$  during the daytime and nighttime, respectively (Table 3). In contrast, values of approximately  $8.4 \text{ g kg}^{-1}$  (Figure 4-6a) and  $9.9 \text{ g kg}^{-1}$  (Figure 4-6b)

occur at almost the same elevation in the surrounding desert areas, respectively. The oasis indeed represents a “wet island” compared with the surrounding desert at almost the same elevation but the mechanism underlying the “wet island” effect differs between daytime and nighttime.

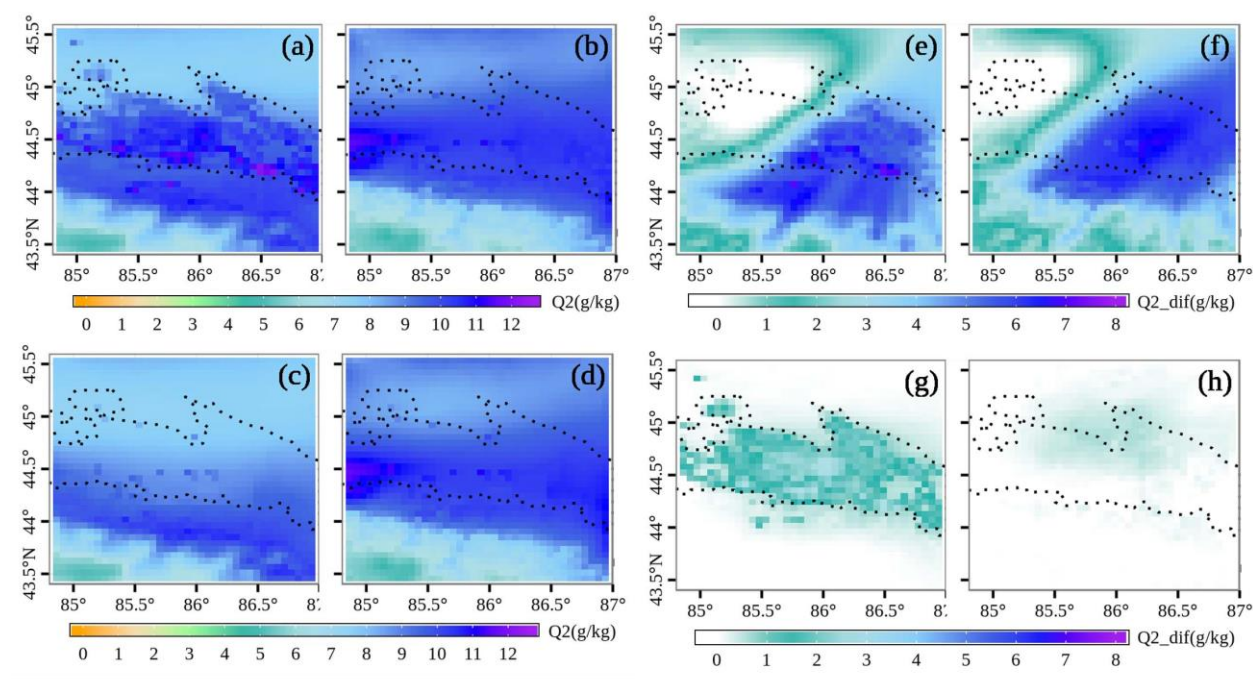


**Figure 4-6.** The same as Figure 6 but for surface specific humidity  $Q_2$  ( $\text{g kg}^{-1}$ ).

A clearly defined humidity gradient line along the northern boundary of the oasis during the daytime is observed in the mod simulation (Figure 4-6a) but the gradient line is not observed at night in the mod simulation (Figure 4-6b) or in the non-oasis simulation (Figure 4-6c,d). The patterns of differences between the mod and the non-oasis simulations show that there is indeed a remarkable difference in specific humidity over the oasis areas during the daytime, whereas a slight difference occurs along the northern oasis boundary and in the desert area at night (Figure 4-6g,h). Based on Student’s t-test, the mean humidity difference over the oasis between the mod simulation and the non-oasis simulation is extremely statistically significant (the p-value is far less than 0.01) during the daytime but statistically insignificant (the p-value is 0.075) at night (Table 4-1). This result indicates that the “wet island” results from the wetting effect of the oasis during the daytime but the cause during the nighttime is uncertain. The mean intensity of this “wet island” resulting from the oasis wetting effect is  $1.56 \text{ g kg}^{-1}$  during the daytime (Table 4-1). In addition, nighttime moisture differences between the mod and the non-oasis simulations are mainly

located along the northern boundary of the oasis area, rather than over the oasis itself (Figure 4-6). This result appears to be consistent with the circulation patterns, suggesting that the wetting effect of the oasis might be present at night but that the spatial extent of the wetting effect changes due to the mountain wind. Moreover, the surface specific humidity patterns from the non-mountain simulation and the differences between the mod and the non-mountain simulations (Figure 4-6e,f) are also consistent with the circulation patterns. Thus, the water and heat patterns in the study area would be controlled by larger-scale circulation patterns and the climate background in the absence of high-relief terrain.

**Table 4-1. Statistical significance of the differences in temperature and humidity between the mod and non-oasis simulations, as assessed using the Student's t-test**

Time Periods	Statistics	Temperature (°C)		Specific Humidity (g kg <sup>-1</sup> )	
		<i>mod</i>	<i>non-oasis</i>	<i>mod</i>	<i>non-oasis</i>
Day	Mean	30.44	31.05	9.99	8.43
	Variance	1.67	1.69	0.78	0.38
	<i>p</i> -value	3.16*10 <sup>-10</sup> << 0.01 *		1.64*10 <sup>-113</sup> << 0.01 *	
Night	Mean	23.36	26.73	10.05	9.97
	Variance	1.77	1.50	0.38	0.47
	<i>p</i> -value	8.47*10 <sup>-165</sup> << 0.01 *		0.075 > 0.05	

\* Indicates that the difference between the mod and the non-oasis simulations is extremely significant.

Figure 4-7 shows the vertical section of humidity patterns from the mod and non-oasis simulations, as well as the differences between the mod and non-oasis simulations and between the mod and non-mountain simulations. The specific humidity in the mountainous area at an equivalent altitude of 1 km during the daytime and nighttime is higher than that over the basin area at the same elevation of 1 km in the non-oasis simulation (Figure 4-7c,d). This higher specific humidity in the mountainous areas may be due to the wetting effect of daytime evaporation from forest and grassland and the radiative cooling of mountainous areas decreases the saturated vapor pressure, leading to a higher specific humidity (Whiteman, 2000) during nighttime. The differences between the mod and non-oasis simulations (Figure 4-8g,h) and between the mod and non-mountain simulations (Figure 4-7e,f) provide further confirmation of the wetting effects of oases and mountains based on the decrease in the cooling gradient from the oasis surface over a distance of approximately 1 km (Figure 4-7g,h) and from the mountainous areas to their surroundings (Figure 4-7e,f). Moreover, the wetting effect of the oasis areas at night extends horizontally into the desert areas to a distance of approximately 25 km (Figure 4-7h and Figure 4-8h). This horizontal

extension results primarily from the ground-hugging nighttime mountain wind, since the extension is consistent with the direction of the mountain wind (Figure 4-8b,d).

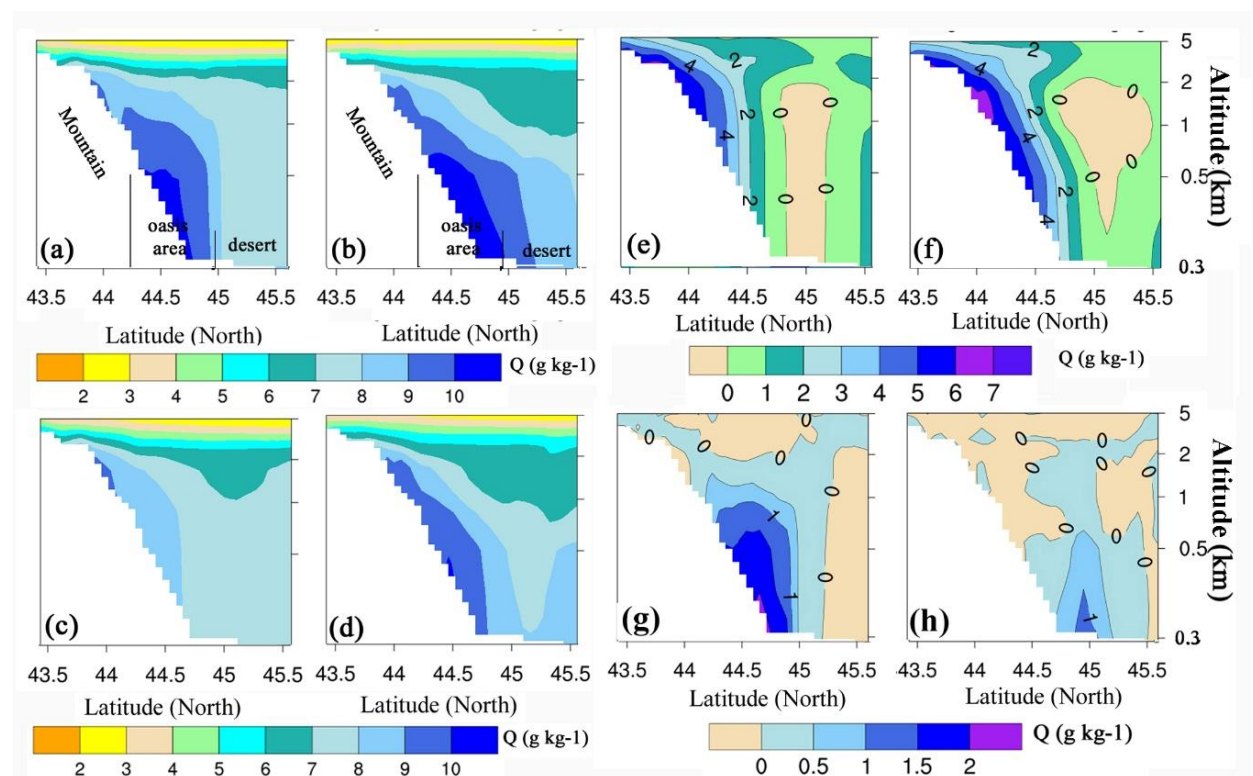


**Figure 4-7.** Same as Figure 6 but for the vertical section of specific humidity  $Q$  ( $\text{g kg}^{-1}$ ) along the white line (longitude  $85.7^\circ \text{E}$ ) shown in Figure 6a.

#### 4.5.4 The spatial patterns of the 10-m horizontal circulation of MODS

Figure 4-8 shows the diurnal mean WS and WD patterns from the mod, non-oasis and non-mountain simulations, as well as the differences between the mod and non-oasis simulations. In the context of the prevailing westerly wind, mountain-valley wind are clearly observed (Figure 4-8a,c and b,d) in both the mod and non-oasis simulations covering the MODS. An intense southwesterly wind with a wind speed exceeding 7 m/s is observed during both daytime and nighttime in the non-mountain simulation (Figure 4-8e,f) and the intense southwesterly wind represents a combination of the prevailing westerly wind and the summer subtropical jet stream resulting from the Southwest Asian low-pressure system over northeastern India (Bothe et al., 2012; Zhiping, 2015). However, the intense southwesterly wind is blocked in the mod and non-oasis simulations. Therefore, the diurnal change in the wind direction from WNW to SW in the mod and non-oasis

simulations is produced by the high-relief terrain, further demonstrating the existence of mountain-valley winds in the MODS.

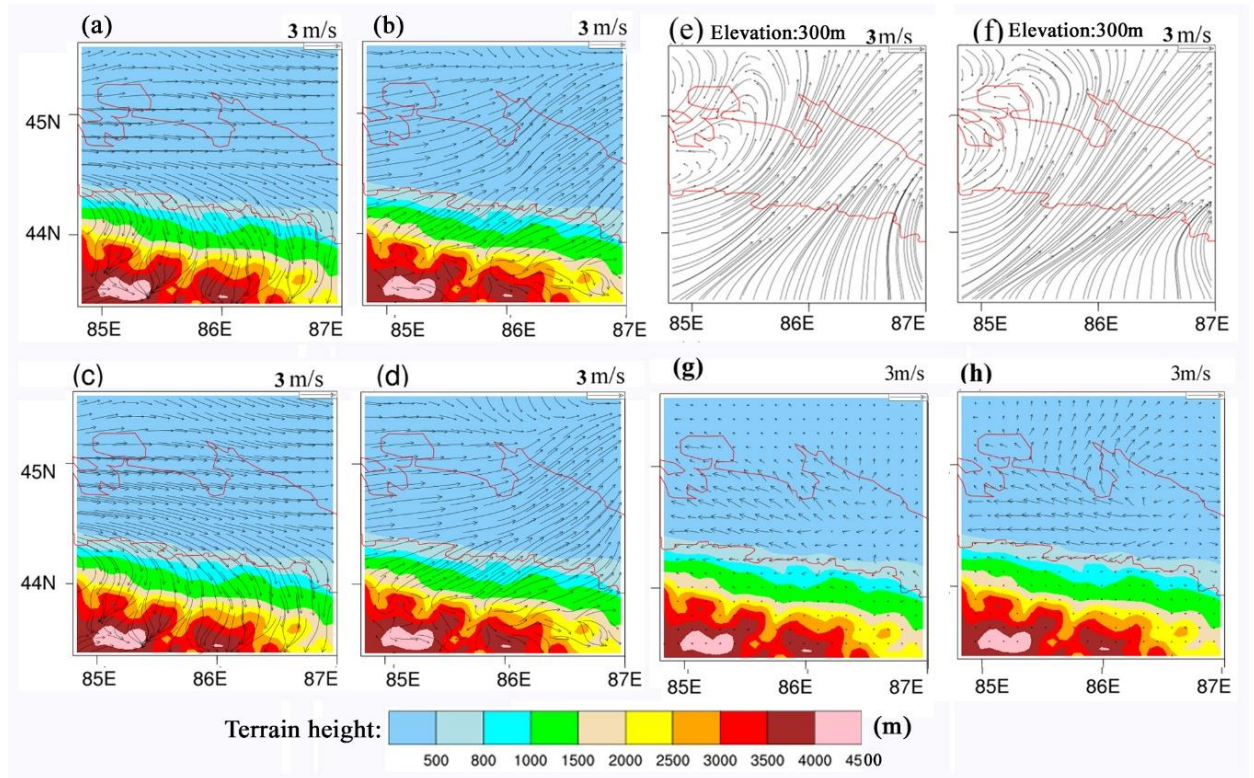


**Figure 4-8. The mean diurnal WS and WD patterns (mean wind speed and direction at a height of 10 m during the daytime and nighttime) in the mod, non-oasis and non-mountain simulations and the differences between the mod and non-oasis simulations. (a) Daytime WS and WD from the mod simulation; (b) nighttime WS and WD from the mod simulation; (c) daytime WS and WD from the non-oasis simulation; (d) nighttime WS and WD from the non-oasis simulation; (e) daytime WS and WD from the non-mountain simulation; (f) nighttime WS and WD from the non-mountain simulation; (g) daytime WS and WD difference between the mod and non-oasis simulations; (h) nighttime WS and WD difference between the mod and non-oasis simulations.**

**The red line represents the border of the oasis.**

The difference between the mod simulation and the non-oasis simulation is characterized by an obvious divergent wind blowing from the center of the oasis area to the surrounding desert with a speed of less than approximately 1.5 m/s at a height of 10 m height (Figure 4-8g,h). This divergent wind is oriented in the opposite direction of the combination of the mountain-valley wind and the prevailing westerly wind. However, no obvious downdrafts or updrafts occur over the oasis or deserts based on the vertical component difference between the mod and non-oasis simulations (Figure 4-9). This divergence indicates that

OBC may indeed exist between the oasis and desert areas and the possible OBC is counteracted by the stronger background circulation produced by the combination of the mountain-valley wind and the prevailing westerly wind.

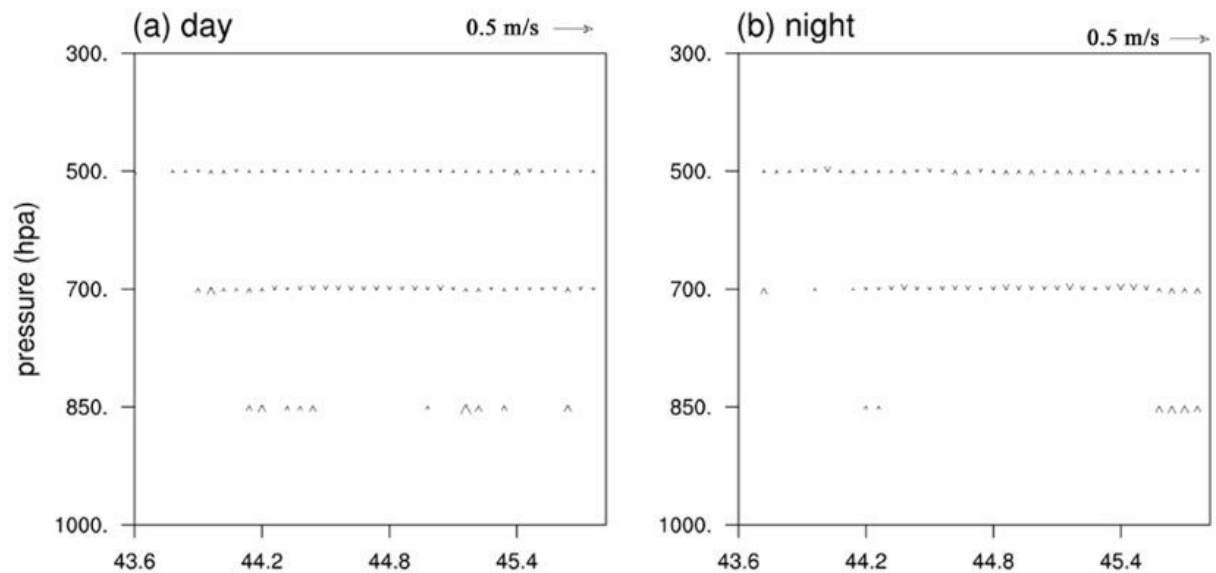


**Figure 4-9. The W component difference between the mod simulation and non-oasis simulation during daytime and nighttime.**

#### 4.6 Comparison with previous studies and an assessment of model uncertainties

In this study, the effects of oases on temperature, humidity and regional circulation patterns within an typical MODS in the NTM were investigated using the WRF model with actual terrestrial datasets. The mod simulation provides a significantly better representation of diurnal temperature and humidity due to use of updated terrestrial datasets and better reflects the exchanges of water and heat in the MODS.

The differences between the mod and non-oasis simulations confirm the typical “cold island” effect and “wet island” effect of an oasis during the day. Thus, a TIL develops over the oasis areas at night from the mod simulation. The oasis cooling-wetting effect reaches a vertical height of approximately 1.5 km above the oasis surface and this result is similar to findings reported in previous investigations (Chu et al., 2005; Liu et al., 2007b; Liu et al., 2007a; Lv et al., 2005; Meng et al., 2012; Meng et al., 2009; Nnamchi, 2011; Wen et al., 2012). However, our study also contributes certain new findings. The Tianshan Mountains act as the background of the oasis-desert interaction and exert a cooling and wetting effect on the entire MODS in the NTM region. Moreover, the horizontal range of

the oasis wetting effect appears to extend into the desert areas, rather than being restricted over the oasis areas, due to the presence of the mountain wind at night. This horizontal extension may produce favorable conditions for desert plants in the oasis-desert transition zone.

In previous studies, researchers proposed the concept that oases have a self-supporting mechanism originating from OBC. They argued that the OBC between an oasis and the surrounding desert helps maintain the ecological stability of the oasis by reducing heat and moisture exchange (Chu et al., 2005; Lv et al., 2005; Meng et al., 2012; Wen et al., 2012). The results from the mod simulation and the differences between the mod and non-oasis simulations show that the water and heat differences between the oasis and surrounding desert do produce OBC. However, the OBC is not observed in the actual weather or climate conditions (the mod simulation in this study), because it is counteracted by the stronger background circulation that results from a combination of mountain-valley wind and the prevailing westerly wind in the MODS. Therefore, the effects of OBC on the ecological stability of oasis systems within an MODS may have been overestimated by previous studies. Consequently, studies related to oasis effects should consider the regional context of the MODS, if the oasis is located in a large mountain-basin system. Such investigations will help provide a better understanding of the ecological and climatic effects of oasis systems, but also may result in the identification of new features of such systems. In addition, this study represents necessary preliminary work for further investigating the contributions of oasis expansion to historical and future climate changes at local or regional scales. Whether and how the typical wetting and cooling effects of oases impact local or regional climate change will be further investigated in the next stage of this work, which will include long-period simulations.

#### **4.7 Conclusions**

In this study, the effects of oasis areas were investigated within a complete MODS located in the NTM using the WRF model. Studies of oasis effects should consider the entire MODS, which will help to fully understand the ecological and climatic effects of oasis systems. The typical “cold-wet” island effects of the oasis, nighttime TIL over oasis areas and OBC are fully described within the context of the MODS in this study through the use of the WRF model with actual terrestrial datasets. The Tianshan Mountains exert a cooling



and wetting effects on the whole MODS in the NTM region. The mountain wind causes the “cold-wet” island effects of the oasis to extend into the surrounding desert area at night, which may produce conditions favorable for desert plants in the oasis-desert transition zone. However, the OBC was counteracted by stronger background winds resulting from a combination of the prevailing westerly winds and the mountain-valley wind in the MODS. The proposed “self-supporting mechanism of the oasis” associated with the OBC cannot play a significant role in maintaining the stability of the oasis in this MODS.



# CHAPTER 5

## GENERAL DISCUSSION

---

*This chapter presents an overview of the research objectives and reviews the main answers to the research questions (Section 5.1). Then, critical reflections on the methodologies are summarized, including how to answer the research questions in a more effective way (Section 5.2). Eventually, recommendations for future work are proposed (Section 5.3).*

## 5.1 Summary and discussion of research questions

Exploring the local climate of a complex MODS and the impact of mountain on oasis effects and interaction between each subsystem of the MODS in NTM can provide the scientific support to oasis water resources management, and is essential to the sustainable development and ecological stability of oases from a comprehensive perspective. Because each subsystem in complex MODS is highly differentiated in space, but are functionally coupled due to sharing of limited water resources. Moreover, it provides useful information for further investigation of the impact of LUCC on regional climate changes under global warming in the CA. From the general goal, this study firstly makes WRF localized in NTM. During this process, four research questions were distilled.

***RQ1: What are the responses of the WRF performance to various actual terrestrial parameters derived from satellite products ?***

***RQ2: How does the WRF coupled with a newly developed drip irrigation process perform in simulating the water-heat conditions of irrigated oasis?***

***RQ3: What are the effects of drip irrigation on atmosphere structure of MODS?***

***RQ4: What are the impacts of large mountains on irrigated oasis-desert interaction in a typical mountain-oasis-desert ecosystem?***

The four research questions were rephrased and answered in Chapters 2-4. An overview of the research objectives, methods used and findings are given in Table 5-1. This table aids in understanding the links between the research objectives and the research questions, and how they are presented in each chapter.

Table 5-1 Overview of the contents of this dissertation

Chapter	RQ	Objectives	Main findings
<b>Chapter 2:</b> The response of WRF to various actual terrestrial datasets.	RQ1	<ul style="list-style-type: none"> <li>Investigate the performances of the WRF in simulating water-heat patterns of MODS;</li> <li>Examine the impact of using actual LU, albedo, LAI, and GVF data on the model performance</li> </ul>	<ul style="list-style-type: none"> <li>In general, WRF with actual LU, albedo, LAI, and GVF data derived from satellite products to improve the simulation of weather and climate conditions of MODS;</li> <li>Using actual VF data results in error correction values of 62%, 87% and 92%, respectively, for simulated 2-m temperature, relative humidity and latent heat flux;</li> <li>Using actual LU data is crucial for near-surface water and heat simulation, since it determines the values of additional secondary parameters.</li> </ul>
<b>Chapter 3:</b> The impacts of drip irrigation on atmospheric structure and local climate.	RQ2 and RQ3	<ul style="list-style-type: none"> <li>To develop a drip irrigation scheme suitable for NTM land management.</li> <li>Exploring irrigation's effects on water-heat patterns of complex MODS;</li> </ul>	<ul style="list-style-type: none"> <li>Our simulation with new irrigation scheme realistically represented heat-water conditions of drip irrigated oasis based on validation of temperature, humidity, energy and irrigation amounts ;</li> <li>Irrigation strengthens cold-wet island effects of oasis and the OBC in the irrigation season;</li> <li>The impacts of drip irrigation on temperature, sensible heat and latent heat flux were mainly restricted over oasis, but the impact on humidity and precipitation spread to across whole NTM;</li> <li>The irrigation might accelerate the hydrological cycle in MODS.</li> </ul>
<b>Chapter 4:</b> The water-heat patterns and oasis effects in typical mountain-oasis-desert system	RQ4	<ul style="list-style-type: none"> <li>To simulate the water-heat patterns and local climate of MODS;</li> <li>To simulate the impact of mountain on oasis effects in a MODS;</li> <li>To analyze the interaction of each subsystem of MODS.</li> </ul>	<ul style="list-style-type: none"> <li>The typical “cold-wet” island effects of the oasis, nighttime temperature inversion layer over oasis areas and oasis breeze circulation (OBC) are confirmed;</li> <li>The Tianshan Mountains exert a cooling and wetting effects on the whole MODS;</li> <li>The mountain wind causes the “cold-wet” island effects of the oasis to extend into the surrounding desert area at night, favorable for desert plants in the oasis-desert transition zone;</li> <li>The OBC was counteracted by stronger background winds, and the self-supporting mechanism of the oasis associated with the OBC cannot play a significant role in maintaining the stability of the oasis in this MODS.</li> </ul>

**RQ1: What are the responses of the WRF performance to various actual terrestrial parameters derived from satellite products ?**

In chapter 2, we used the WRF model with observed estimates of LU, albedo, LAI, and GVF datasets from satellite products to examine which terrestrial datasets have a great impact on simulating water and heat conditions over heterogeneous oasis-desert systems in the NTM.

We firstly compared the differences between the actual LU, albedo, LAI, and GVF data and the corresponding default datasets one by one in the NTM. Both the defaults and the actual satellite images showed significant differences, especially in oasis and desert areas, that were strongly impacted by human activities. Large areas of cropland and barren desert in oases and north-eastern desert areas are apparent in the actual LU data, while the default data show grassland and shrubland in these oases and desert areas; the default LU data shows a large area of forest in the Ili River basin, and did not indicate ice type, which are misclassified. The actual albedo level is overall higher than the default data, ranging from 0.05–0.25; The albedo over crops in the actual image is higher than over the surrounding northern desert area, but this is not the case for the default data, the reason is that oasis salinization and larger areas with plastic mulching could increase the actual albedo levels. The differences between actual LAI and GVF data and the corresponding default data range from 0 to 3 and from 0 to 85%, respectively. Major differences are evident across the basin, especially near the Ili River basin and the northern oasis border. The differences between the actual and default terrestrial datasets confirm that the default datasets are outdated and less representative of current land surface situations of MODIS in the NTM

We then examined the impact of using actual LU, albedo, LAI, and GVF data from satellite products in WRF on the model performance. Results show that WRF simulations of temperature, humidity, energy, and wind are improved step-by-step by the incorporation of actual LU, albedo, LAI, and GVF into the model, as evidenced by the decrease in RMSE values and increase in  $R^2$  in both years of 2010 and 2012. The bias of T2 was corrected by up to 2.25 °C, that of RH was corrected by up to 8.85%, and that of LE was corrected by up to 34.12 W/m<sup>2</sup> at the site level in total. Using actual GVF data greatly affects the

simulation of T2, RH, and LE in the oasis-desert system, contributing to error correction values of 62%, 87% and 92%, respectively. LU data is a primary parameter and it determines the values of many secondary parameters. Although all of the simulations conducted in this study produce the characteristic of the “wet-cold” island effect over the oasis area, WRF can more accurately reflect the intensity of the oasis cold–wet effects when using all actual LU, albedo, LAI, and GVF data. The results of this study contribute to a greater knowledge of the impacts of land surface parameters on the performance of WRF (Wen et al., 2012), which is beneficial for various applications, especially for land surface and climate modelling.

**RQ2: How does the WRF coupled with a newly developed drip irrigation process perform in simulating the water-heat conditions of irrigated oasis?**

The premise of studying historic contribution of irrigation and oasis evolution on regional climate change is to realistically simulate heat and water conditions of such drip-irrigated oases. However, there were no irrigation schemes implemented in the accompanying NOAA in official releases of WRF (Chen and Dudhia, 2001b; Chen and Dudhia, 2001a), also in most of other RCMs. Because an oasis cannot survive without irrigation in NTM, and drip irrigation under plastic film since 1995 have been an effective method to conserve limited water resources in this region (Fan et al., 2013), using which crop in NTM was irrigated by dripping water into root and most of crops were under plastic film. Irrigation in this region usually occurs when the soil moisture drops to a low level that threatens crop growth, especially as irrigation is largely constrained by the shortage of water resources in NTM oases area.

In chapter 3, we developed an new drip irrigation scheme with assumption that irrigated crops always have enough moisture to transpire without being stressed but no excess water is added, and that very little moisture reached 25 cm away from the drip radially on the basis of detailed field experiment (Fernández et al., 2006). That means there is always enough water available for the vegetation to transpire without water limited, even though the mean grid cell soil moisture may continue to decrease.

Then we coupled the scheme into WRF, and compare simulated near-surface temperature, humidity, ET, energy and irrigation amount with the observations. Results show the bias

of simulated temperature was corrected by up to 0.35 °C in each hour, that of relative humidity was corrected by up to 2.84% in each hour, and that of evapotranspiration was corrected by up to 0.61 mm/day when using WRF with new developed scheme. Moreover, our modified WRF shows that the annual irrigation amount is 475.67 mm, which is comparable to the climatological irrigation consumption of 477 mm estimated from ground measurements (Ma et al., 2015) and the irrigation quota of approximately 397.5-487.14 mm (Zhou et al., 2013). Our modified model performance evaluation yielded a reasonable representation for climate elements and irrigation water amount estimates at the site level. Added drip irrigation scheme improves performance of the WRF in simulating water and heat patterns in the MODS in the irrigation season.

### **RQ3: What are the effects of drip irrigation on atmosphere structure of MODS?**

We conducted two simulations with drip irrigation (IRR) and without irrigation(CON) and the differences between the two simulations show the effects of the drip irrigation on the water-heat conditions in relatively close mountain-basin structures.

Results show that drip irrigation in NTM increases the LE of 80.81 W/m<sup>2</sup> and decreases H 63.03 W/m<sup>2</sup> over oasis; Drip irrigation has a cooling and wetting effects on the atmospheric temperature and humidity in MODS, with values up to 0- -2 °C and 0-2 g/kg from near surface to approximately 1.5 km over the irrigated oasis region, thereby strengthening cold-wet island effects of oasis and OBC in the irrigation season; the impacts of drip irrigation on temperature, sensible heat flux and latent heat flux were mainly restricted over oasis, but the impact on humidity spread to across whole NTM; Moreover, drip irrigation produced a weak divergent wind blowing from the center of the oasis area to the surrounding desert with a speed of less than approximately 0.5 m/s at a height of 10 m in daytime, indicating drip irrigation increased the intensity of OBC; From the difference between IRR and CON simulations, the TP seems obviously increased in upwind mountains areas with elevation value of approximately 1000-2000 m, decreased at the mountain top with elevation value greater than approximately 2000 m in daytime, and all grids averaged P in the domain are increased 3.75 mm and 2.48 mm in daytime and nighttime, respectively; The impacting range of irrigation on humidity and precipitation spread to non-irrigated area might be relevant to mountain-valley winds. During daytime,



since intense lower level valley wind is blowing from wet-cold oasis to mountainous areas and forms precipitation at elevation of 1000-2000 m. During night, intense lower level cold-wet mountain wind is blowing from mountainous, through oasis, even extend to part of desert area, thus an increased precipitation in upwind mountainous area and increased humidity spreading whole NTM were observed. These mechanisms might accelerate the hydrological cycle in MODS. But, irrigation makes local convective processes closer to oasis surface based on lower PBLH over oasis, which implied that the air mass over the oasis tends to be more stable when irrigation happened in the MODS, and the precipitation over oasis might decrease; When irrigation rate is greater than 2.5 mm/day, the ET increased 0.45 times more than that without irrigating, while irrigation rate is less than 2.5 mm/day, the ET increased 1.59 times more.

**RQ4: What are the impacts of large mountains on irrigated oasis-desert interaction in a typical mountain-oasis-desert ecosystem?**

Because the previous studies have been performed only in oasis-desert environments and have not considered the impacts of mountain, and interaction between each subsystem in MODS, which may result in an incorrect or incomplete understanding of the oasis-desert interactions within a MODS. In chapter 4, the effects of oasis areas were investigated within a complete MODS located in the NTM using the WRF model. The mod simulation uses actual terrestrial datasets from satellite products and irrigation scheme developed in chapter 3. The non-oasis simulation is a scenario simulation in which oasis areas are replaced by desert conditions, while all other conditions are the same as the mod simulation. The non-mountain simulation is a scenario simulation in which the elevation values of all grids are set to a constant value of 300 m.

Result show the overall spatial patterns of H, LE, T2 and Q2 in daytime and nighttime generally exhibit continuous stripe-like increases from the mountainous areas to the oasis areas and to the desert areas, except for H and LE patterns in nighttime. An obvious gradient line is observed along the northern boundary of the oasis and desert, indicating irrigated oasis region obviously disturb the stripe-like change of the water-heat patterns. The near surface water-heat patterns of MODS are not only impacted by various underlying LU

differences of mountain, oasis and desert, but are controlled by TLR caused by elevation difference.

The differences between the mod and non-oasis simulations show the typical “cold island” effect and “wet island” effect of an oasis during the day. At 2 m, the intensity of this “cold island” resulting from the oasis cooling effect is as large as  $-0.61\text{ }^{\circ}\text{C}$ , while the mean intensity of this “wet island” resulting from the oasis wetting effect is  $1.56\text{ g kg}^{-1}$ . Thus, a temperature inverse layer develops over the oasis areas at night from the mod simulation.

The oasis cooling-wetting effect reaches a vertical height of approximately 1.5 km above the oasis surface; The horizontal range of the oasis cooling-wetting effect appears to extend into the desert areas to a distance of approximately 25 km, rather than being restricted over the oasis areas favorable conditions for desert plants in the oasis-desert transition zone. The Tianshan Mountains act as the background of the oasis-desert interaction and exert a cooling and wetting effect on the whole MODS in the NTM.

In the context of the prevailing westerly wind, the typical mountain-valley winds are confirmed in MODS from the mod and non-oasis simulations. An intense southwesterly wind with a wind speed exceeding 7 m/s is observed during both daytime and nighttime in the non-mountain simulation, which is the representation of larger-scale circulation. An obvious divergent wind blowing from the center of the oasis area to the surrounding desert with a speed of less than approximately 1.5 m/s at a height of 10 m height, but no obvious downdrafts or updrafts were observed over the oasis or deserts based on the vertical component difference between the mod and non-oasis simulations. These results indicate the OBC may indeed exist between the oasis and desert areas and the OBC is counteracted by the stronger background circulation. Therefore, the proposed self-supporting mechanism of the oasis associated with the OBC cannot play a significant role in maintaining the stability of the oasis in this MODS.

## **5.2 Critical reflections**

This dissertation studied the effects of irrigated oasis on the water-heat patterns and local climate in the NTM, and the interaction between each subsystem in a MODS in the NTM. In this section, some critical aspects are being presented concerning the current methodology and results in this dissertation.

In chapter 2, the impact of using actual LU, albedo, LAI, and GVF data from satellite products in WRF on the model performance were examined. Several uncertainties existed in data processing process and updating outdated default terrestrial datasets in WRF. For example, the actual LU data used hierarchical classification system while the default LU in WRF used the USGS classification system. These two classification system have conflicting classification definition, because some categories from the hierarchical classification system could not completely be attributed into any category in USGS classification system. We converted LU of the hierarchical classification system into LU based on USGS classification system, which caused uncertainties (Zhang et al., 2017c). Moreover, the actual terrestrial datasets, including LU, albedo, LAI and GVF have inconsistent spatial resolution with the defaults, therefore, were reprocessed using the same coordinate system and resolution in WRF, which also caused some uncertainties. In addition, we examined the impacts of only from LU, albedo, LAI, and GVF data on WRF performance. Others parameters, such as emissivity, rough length of land surface might have a great impacts in WRF performance and were not applied in this study.

In chapter 3, on the basis of adding irrigation process and updating outdated default terrestrial datasets with actual datasets from satellite products, the performance of WRF improved much more than before, but simulated ET and RH are overall underestimated relative to the observations. These errors can be attributed to the fact that plastic mulching inhibits soil evaporation (Xie et al., 2005), which is not considered in the simulations of WRF (Wen et al., 2012; Meng et al., 2009). Adding plastic mulching process may help to correct these errors. In addition, all crops were treated as irrigation field, this treatment may enlarge the irrigation area, as there may be actually other land use/cover, such as bare land, within the cropland grids in the WRF's simulation.

In chapter 4, on the basis of WRF localized, we investigated oasis effects, mountain effects and oasis-desert interactions in complex MODS using scenario simulations. Our objectives in this thesis is to explore the relationship between irrigated oasis and regional or local climate change in complex MODS in CA. However, we only finished short-term simulations. The long-period simulation can quantitatively answer the climate effects of historical oases expansion on the regional climate.

### **5.3 Recommendations for future work**

Every dissertation is subject to some limitations, there are no exceptions for this one. In this section, we try to shed some light on the potential direction and improvement of the current study. Several actions are being proposed, concentrating on the following topics.

#### 5.3.1. Future work on datasets

Remote sensing data have constituted the major data resource for climate modelling. As section 5.2 showed, we examined the impacts of only from LU, albedo, LAI, and GVF data on WRF performance, the impacts from other parameters, such as emissivity, rough length of land surface on WRF performance will be further examined in the future work. In addition, we will collect more field data, even do some observation, such as the fluxes, actual evaporation, soil water infiltration, etc. , although it may be time consuming and require a lot of money.

#### 5.3.2. Future work on model development

Concerning our work of climate localization, we made large efforts in describing drip irrigation process in this dissertation. In fact, drip irrigation under plastic film is an effective farm management after 1995, and large-area flooding irrigation was used before 1995. Thus, we will try to develop a flooding irrigation scheme and drip irrigation under plastic film scheme suitable to current crop management in arid area, and coupled them into climate model in the future.

#### 5.3.3. Future work on research topics

This dissertation provides important information on the water-heat interaction mechanisms among subsystem in complex MODS in a period, which represents necessary preliminary work for further investigation in the contribution of historical oasis expansion at local and regional scales. The contribution s of oases expansion impact on local/regional climate change, distinguishing from the global climate change, will be further investigated in the next stage of this work.

In addition, we found each subsystem in mountain-oasis-desert system highly differentiated in space, but are functionally coupled due to sharing of limited water resources. The oasis

expansion will certainly affect the other system changes, such as desert vegetation degradation. These interaction and feedback mechanisms between each subsystem in MODS are complex and interesting, and will play a key role in analyzing the dynamics of ecosystem services under limited water-soil resources. We need to figure out urgently the relationship of mutual interactions between each subsystem in MODS in a dynamic stage of historical development, which will provide basic knowledge and information on how complex systems respond to future climate changes.



# CHAPTER 6

## GENERAL CONCLUSIONS

---

*The general findings of this dissertation are concluded in this chapter. According to the research objective, they are given in a logical way to deepen understanding.*

The historic climate of the NTM changed obviously from a warm-dry to a warm-wet trend with the year of 1987 as turning point, while the change range of other arid regions in CA was less intense and developed warm-dry trend. We assumed that the abnormal regional climate change in the NTM may be likely to respond to the rapid oases expansion and intensive irrigation in the complex MODS. This dissertation studies the local climate of a complex MODS in short-period and the contribution of irrigated oasis and mountain on the local climate conditions in the NTM using WRF model. This is a preliminary work, further investigations will study the impacts of historic oasis expansion on regional climate change.

**Firstly**, because the regional climate model WRF has outdated default terrestrial datasets, limiting its abilities to accurately simulate weather and climate conditions over heterogeneous underlying surface of MODS. Integrating actual terrestrial datasets from satellite products or observation in the model simulations is a novel way to overcome these limitations. However, actual terrestrial datasets from satellite products are scarce and field measurements are temporally and spatially limited, especially in complex terrain. In addition, simulations using real-time, even monthly, actual various satellite terrestrial datasets in RCMs are very time- and labor-consuming processes. In order to overcome the restriction of WRF model and check whether only updating several key observed datasets can meet expected results in land surface modelling or climate modelling in NTM, we conducted two different year simulations with gradually updating default terrestrial datasets by actual datasets from satellite products, including LU, Albedo, LAI and GVF in chapter 2, and examined the contribution of each dataset on error correction of WRF simulating land surface energy partition, T2, RH and WS and WD in MODS. Our main conclusions in chapter 2 are that using actual GVF data greatly affects the simulation of T2, RH, and LE in the oasis–desert system, contributing to error correction values of 62%, 87% and 92%, respectively. The LU data is a primary parameter and it determines the values of many secondary parameters. The default LU and GVF, at least, should be updated by actual datasets in simulating both weather and climate processes using the WRF.

**Secondly**, the regional climate model WRF does not include any detailed irrigation process suitable for the drip irrigation management in the NTM, and the oasis cannot survive without irrigation in the NTM. Moreover, water is a particularly scarce and valuable good for both human livelihoods and ecosystems in this region, because water resource is from important hydrologic processes of limited snow and glacial melt, and precipitation from



mountain ranges. Exploring irrigation's effects on water and heat patterns of complex MODS is very significant for regional sustainable development under the limited water and soil conditions. We developed a drip irrigation scheme and coupled it into the WRF in order to make WRF localized. Our main conclusions in the chapter 3 are that irrigation impacts the patterns of temperature, H and LE, and the influencing range were mainly restricted over oasis; while that the impacting range of irrigation on humidity and precipitation spread to non-irrigation area might be relevant to mountain-valley winds; During daytime, since intense lower level valley wind is blowing from the wet-cold oasis to mountainous area and forms precipitation at elevation of 1000-2000 m. During night, intense lower level cold-wet mountain wind is blowing from mountainous, through oasis, even extending to part of desert area, thus an increased precipitation in upwind mountainous area and increased humidity spreading whole NTM were observed. These mechanisms might accelerate the hydrological cycle in MODS.

**Thirdly**, the localized WRF model is applied for simulating water-heat patterns of the whole MODS and exploring water-heat interaction among mountain, oasis, and desert. All of work aims to explore the relationship between irrigated oasis and regional climate change in complex MODS. The answer can provide the scientific support to oasis water resources management and is essential to the sustainable development and ecological stability of oases. In chapter 4, we mainly conducted three scenario simulations, which represents real local climate situation (mod), the unreal local climate situation due to without irrigated oasis (non-oasis), and the unreal local climate situation due to without terrain (non-mountain), respectively. Our objective is to understand the water-heat movements and interaction of complex MODS. Our main conclusions in chapter 4 are that the typical "cold-wet" island effects of the oasis, nighttime TIL over oasis areas and OBC are fully confirmed, but the OBC was counteracted by stronger background winds, thereby the self-supporting mechanism of the oasis associated with the OBC cannot play a significant role in maintaining the stability of the oasis in this MODS.



# CHAPTER 7

## APPENDIX

---

*This chapter main lists the paremeters and codes in the modelling and experiment.*

## 7.1 namelist.wps

&share

wrf\_core = 'ARW',

max\_dom = 2,

start\_date = '2011-10-01\_00:00:00', '2011-10-01\_00:00:00', '2011-10-01\_00:00:00',

end\_date = '2012-09-31\_18:00:00', '2012-09-31\_18:00:00', '2012-09-31\_18:00:00',

interval\_seconds = 21600,

io\_form\_geogrid = 2,

opt\_output\_from\_geogrid\_path = '/media/annabelle/Miao/WRF/ERA-Intermin/TB\_Short/geo/paper3\_new3',

debug\_level = 0,

/

&geogrid

parent\_id = 1,1,2,

parent\_grid\_ratio = 1,3,3,

i\_parent\_start = 1,19,28,

j\_parent\_start = 1,16,21,

e\_we = 74,115,109,

e\_sn = 56,76,76,

geog\_data\_res = '2m','30s', '30s',

dx = 0.166916,

dy = 0.166405,

map\_proj = 'lat-lon',

ref\_lat = 44.893,

ref\_lon = 86.107,

truelat1 = 44.893,

truelat2 = 44.893,

stand\_lon = 86.107,

geog\_data\_path = '/home/annabelle/WRF/WPS\_GEOG',

```

opt_geogrid_tbl_path = '/home/annabelle/WRF/WPS/geogrid',
ref_x = 37.0,
ref_y = 28.0,
/
&ungrib
  out_format = 'WPS',
  prefix = '/home/annabelle/WRF/WPS/ungrib/Paper3/3D',
/
&metgrid
fg_name =
'/home/annabelle/WRF/WPS/ungrib/Paper3/3D','/home/annabelle/WRF/WPS/ungrib/P
aper3/SFC',
io_form_metgrid = 2,
opt_output_from_metgrid_path = '/media/annabelle/Miao/WRF/ERA-
Intermin/TB_Short/met/paper3_new3/2012',
opt_metgrid_tbl_path = '/home/annabelle/WRF/WPS/metgrid/',
/

```

## 7.2 namelist.input

```

&time_control
run_days = 365,
run_hours = 18,
run_minutes = 0,
run_seconds = 0,
start_year = 2011, 2011, , 2011,
start_month = 09, 09, 09,
start_day = 01, 01, 01,
start_hour = 00, 00, 00,
start_minute = 00, 00, 00,
start_second = 00, 00, 00,
end_year = 2012, 2012, 2012,

```

```
end_month           = 09,      09,      09,
end_day             = 31,      31,      31,
end_hour            = 18,      18,      18,
end_minute          = 00,      00,      00,
end_second          = 00,      00,      00,
interval_seconds    = 21600,
input_from_file     = .true., .true., .true.,
history_interval    = 60,      60,      60,
frames_per_outfile  = 1,      1,      1,
restart             = .false.,
restart_interval    = 5000,
io_form_history     = 2,
io_form_restart     = 2,
io_form_input       = 2,
io_form_boundary    = 2,
debug_level         = 0,
io_form_auxinput4   = 2,
auxinput4_inname    = "wrflowinp_d<domain>"
auxinput4_interval  = 360,      360,
/
&domains
time_step           = 60,
time_step_fract_num = 0,
time_step_fract_den = 1,
max_dom             = 2,
e_we                = 74,      115,      109,
e_sn                = 56,      76,      76,
e_vert              = 35,      35,      35,
p_top_requested     = 5000,
num_metgrid_levels  = 31,
```

```

num_metgrid_soil_levels = 4,
dx                       = 18557.299, 6185.766, , 2061.922,
dy                       = 18500.487, 6166.829, , 2055.61,
grid_id                  = 1,          2,          3,
parent_id                = 1,          1,          2,
i_parent_start           = 1,          19,         28,
j_parent_start           = 1,          16,         21,
parent_grid_ratio        = 1,          3,          3,
parent_time_step_ratio   = 1,          3,          3,
feedback                 = 1,
smooth_option            = 0,
/
&physics
mp_physics               = 3,          3,          3,
ra_lw_physics            = 3,          3,          3,
ra_sw_physics            = 3,          3,          3,
radt                     = 10,         10,         10,
sf_sfclay_physics       = 1,          1,          1,
sf_surface_physics      = 2,          2,          2,
bl_pbl_physics           = 1,          1,          1,
bldt                     = 0,          0,          0,
cu_physics               = 1,          1,          1,
cudt                     = 5,          5,          5,
isflx                    = 1,
ifsnow                   = 0,
icloud                   = 1,
surface_input_source     = 1,
num_soil_layers          = 4,
sf_urban_physics        = 1,          1,
usemonalb                = .true.,

```

```
rdlai2d                = .true.,
sst_update              = 1,
/
&fdda
grid_fdda               = 1,          0,
gfdda_inname            = "wrffdda_d<domain>"
gfdda_interval_m       = 360
gfdda_end_h             = 5154
io_form_gfdda           = 2
fgdt                   = 0
if_no_pbl_nudging_uv   = 1
if_no_pbl_nudging_t    = 1
if_no_pbl_nudging_q    = 1
if_zfac_uv              = 0
k_zfac_uv               = 10
if_zfac_t               = 0
k_zfac_t                = 10
if_zfac_q               = 0
k_zfac_q                = 10
guv                     = 0.0003
gt                      = 0.0003
gq                      = 0.0003
if_ramping              = 1
dtramp_min              = 60.
/
&dynamics
w_damping               = 0,
diff_opt                = 1,
km_opt                  = 4,
diff_6th_opt            = 0,          0,          0,
```



```

diff_6th_factor      = 0.12,    0.12,    0.12,
base_temp            = 290.,
damp_opt             = 0,
zdamp                = 5000.,   5000.,   5000.,
dampcoef             = 0.2,     0.2,     0.2,
khdif                = 0,       0,       0,
kvdif                = 0,       0,       0,
non_hydrostatic     = .true.,   .true.,   .true.,
moist_adv_opt        = 1,       1,       1,
scalar_adv_opt       = 1,       1,       1,
/
&bdy_control
spec_bdy_width       = 5,
spec_zone             = 1,
relax_zone           = 4,
specified             = .true.,   .false., .false.,
nested                = .false.,  .true.,  .true.,
/
&grib2
/
&namelist_quilt
nio_tasks_per_group  = 0,
nio_groups            = 1,
/
&namelist_quilt
nio_tasks_per_group  = 0,
nio_groups            = 1,
/

```

### 7.3 programme Wgeogrid

```
integer :: i,j
integer :: isigned, endian, wordsize
integer :: nx, ny, nz
real :: scalefactor
real*8 :: xllcorner, yllcorner, cellsize, missvalue
character :: head12
real, allocatable :: rarray(:,:), iarray(:,:)
isigned = 1
endian = 0
wordsize = 2
scalefactor = 1.0
nz = 1
open (10, file = '2013.txt')
read(10,*) head12, nx
read(10,*) head12, ny
read(10,*) head12, xllcorner
read(10,*) head12, yllcorner
read(10,*) head12, cellsize
read(10,*) head12, missvalue
allocate(rarray(nx,ny))
allocate(iarray(nx,ny))
do j = 1,ny
read(10,*) iarray(:,j)
end do
! reverse the data so that it begins at the lower-left corner
do j = 1,ny
rarray(:,j) = iarray(:,ny-(j-1))
end do
call write_geogrid(rarray, nx, ny, nz, isigned, endian, scalefactor, wordsize)
end program Wgeogrid
```

## 7.4 NCL code for updating the LU and monthly GVF in wrfinput and wrflowinp

```
begin
original_file1=addfile("/home/annabelle/soil_moisture/paper3_new/year/2011_12/wrflowinp_d02","w")

edited_file_1=addfile("/home/annabelle/soil_moisture/paper3_new/year/2011_12/1_GVF_02.nc","r")
SMOIS_edited_1=edited_file_1->VG(74:0,0:113)

edited_file_2=addfile("/home/annabelle/soil_moisture/paper3_new/year/2011_12/2_GVF_02.nc","r")
SMOIS_edited_2=edited_file_2->VG(74:0,0:113)

edited_file_3=addfile("/home/annabelle/soil_moisture/paper3_new/year/2011_12/3_GVF_02.nc","r")
SMOIS_edited_3=edited_file_3->VG(74:0,0:113)

edited_file_4=addfile("/home/annabelle/soil_moisture/paper3_new/year/2011_12/4_GVF_02.nc","r")
SMOIS_edited_4=edited_file_4->VG(74:0,0:113)

edited_file_5=addfile("/home/annabelle/soil_moisture/paper3_new/year/2011_12/5_GVF_02.nc","r")
SMOIS_edited_5=edited_file_5->VG(74:0,0:113)

edited_file_6=addfile("/home/annabelle/soil_moisture/paper3_new/year/2011_12/6_GVF_02.nc","r")
SMOIS_edited_6=edited_file_6->VG(74:0,0:113)

edited_file_7=addfile("/home/annabelle/soil_moisture/paper3_new/year/2011_12/7_GVF_02.nc","r")
SMOIS_edited_7=edited_file_7->VG(74:0,0:113)

edited_file_8=addfile("/home/annabelle/soil_moisture/paper3_new/year/2011_12/8_GVF_02.nc","r")
SMOIS_edited_8=edited_file_8->VG(74:0,0:113)

edited_file_9=addfile("/home/annabelle/soil_moisture/paper3_new/year/2011_12/9_GVF_02.nc","r")
SMOIS_edited_9=edited_file_9->VG(74:0,0:113)

edited_file_10=addfile("/home/annabelle/soil_moisture/paper3_new/year/2011_12/10_GVF_02.nc","r")
SMOIS_edited_10=edited_file_10->VG(74:0,0:113)
```

```
edited_file_11=addfile("/home/annabelle/soil_moisture/paper3_new/year/2011_12/11_
GVF_02.nc","r")
```

```
SMOIS_edited_11=edited_file_11->VG(74:0,0:113)
```

```
edited_file_12=addfile("/home/annabelle/soil_moisture/paper3_new/year/2011_12/12_
GVF_02.nc","r")
```

```
SMOIS_edited_12=edited_file_12->VG(74:0,0:113)
```

```
do i = 0, 119, 1
```

```
original_file->VEGFRA(i,,:)=(/SMOIS_edited_9/)
```

```
end do
```

```
do i = 120, 243, 1
```

```
original_file->VEGFRA(i,,:)=(/SMOIS_edited_10/)
```

```
end do
```

```
do i = 244, 363, 1
```

```
original_file->VEGFRA(i,,:)=(/SMOIS_edited_11/)
```

```
end do
```

```
do i = 364, 487, 1
```

```
original_file->VEGFRA(i,,:)=(/SMOIS_edited_12/)
```

```
end do
```

```
do i = 488, 611, 1
```

```
original_file->VEGFRA(i,,:)=(/SMOIS_edited_1/)
```

```
end do
```

```
do i = 612, 727, 1
```

```
original_file->VEGFRA(i,,:)=(/SMOIS_edited_2/)
```

```
end do
```

```
do i = 728, 851, 1
```

```
original_file->VEGFRA(i,,:)=(/SMOIS_edited_3/)
```

```
end do
```

```
do i = 852, 971, 1
```

```
original_file->VEGFRA(i,,:)=(/SMOIS_edited_4/)
```

```
end do
```

```
do i = 972, 1095, 1
```

```
original_file->VEGFRA(i,,:)=(/SMOIS_edited_5/)
```

```
end do
```

```
do i = 1096, 1215, 1
original_file->VEGFRA(i,,:)=(/SMOIS_edited_6/)
end do

do i = 1216, 1339, 1
original_file->VEGFRA(i,,:)=(/SMOIS_edited_7/)
end do

do i = 1340, 1463, 1
original_file->VEGFRA(i,,:)=(/SMOIS_edited_8/)
end do

do i = 1464, 1583, 1
original_file->VEGFRA(i,,:)=(/SMOIS_edited_9/)
end do

do i = 1584, 1707, 1
original_file->VEGFRA(i,,:)=(/SMOIS_edited_10/)
end do

do i = 1708, 1827, 1
original_file->VEGFRA(i,,:)=(/SMOIS_edited_11/)
end do

do i = 1828, 1951, 1
original_file->VEGFRA(i,,:)=(/SMOIS_edited_11/)
end do

original_file_lu=addfile("/home/annabelle/soil_moisture/paper3_new/year/2011_12/wrfi
nput_d02","w")

edited_file_13=addfile("/home/annabelle/soil_moisture/paper3_new/year/2011_12/lu_0
2_ok.nc","r")
SMOIS_edited_13=edited_file_13->LU_INDEX(74:0,0:113)

original_file_lu->LU_INDEX(0,,:)=(/SMOIS_edited_13/)

end
```



---

## References

- Bonan GB, Lawrence PJ, Oleson KW, Levis S, Jung M, Reichstein M, Lawrence DM, Swenson SC. 2011. Improving canopy processes in the Community Land Model version 4 (CLM4) using global flux fields empirically inferred from FLUXNET data. *Journal of Geophysical Research: Biogeosciences* (2005–2012). **116**.
- Bonan GB. 1996. A land surface model (LSM version 1.0) for ecological, hydrological, and atmospheric studies: technical Description and User's guide. *NCAR Tech. Note NCAR/TN-417 + STR, Boulder, CO*.
- Bothe O, Fraedrich K, Zhu XH. 2012. Precipitation climate of Central Asia and the large-scale atmospheric circulation. *Theoretical and Applied Climatology*. **108**:345-354. doi:10.1007/s00704-011-0537-2.
- Branch O, Warrach-Sagi K, Wulfmeyer V, Cohen S. 2014. Simulation of semi-arid biomass plantations and irrigation using the WRF-NOAH model—a comparison with observations from Israel. *Hydrology and Earth System Sciences*. **18**:1761-1783. doi:10.5194/hess-18-1761-2014.
- Bretherton CS, McCaa JR, Grenier H. 2004. A new parameterization for shallow cumulus convection and its application to marine subtropical cloud-topped boundary layers. Part I: Description and 1D results. *Monthly Weather Review*. **132**:864-882. doi:http://dx.doi.org/10.1175/1520-0493(2004)132<0864:ANPFSC>2.0.CO;2.
- Cao F, Dan L, Zhuguo M. 2014. A Regional Climate Coupled Model and Its influences on Climate Simulation over East Asia. *Chinese Journal of Atmospheric Sciences*. **38**:322-336. doi:10.3878/j.issn.1006-9895.2013.13112.
- Cao Q, Yu DY, Georgescu M, Han Z, Wu JG. 2015. Impacts of land use and land cover change on regional climate: a case study in the agro-pastoral transitional zone of China. *Environmental Research Letters*. **10**:124025. doi:https://doi.org/10.1088/1748-9326/10/12/124025.
- Cescatti A, Marcolla B, Vannan SKS, Pan JY, Román MO, Yang X, Ciais P, Cook RB, Law BE, Matteucci G. 2012. Intercomparison of MODIS albedo retrievals and in situ measurements across the global FLUXNET network. *Remote Sensing of Environment*. **121**:323-334. doi:http://doi.org/10.1016/j.rse.2012.02.019.
- Chen F, Dudhia J. 2001a. Coupling an advanced land surface–hydrology model with the Penn State–NCAR MM5 modeling system. Part I: Model implementation and sensitivity. *Monthly Weather Review*. **129**:569-585.
- Chen F, Dudhia J. 2001b. Coupling an advanced land surface–hydrology model with the Penn State–NCAR MM5 modeling system. Part II: Preliminary model validation. *Monthly Weather Review*. **129**:587-604.
- Chen F, Mitchell K, Schaake J, Xue YK, Pan HL, Koren V, Duan QY, Ek M, Betts A. 1996. Modeling of land surface evaporation by four schemes and comparison with FIFE observations. *Journal of Geophysical Research: Atmospheres*. **101**:7251-7268. doi:10.1029/95JD02165.
- Chen G, Iwasaki T, Qin H, Sha W. 2014. Evaluation of the Warm-Season Diurnal Variability over East Asia in Recent Reanalyses JRA-55, ERA-Interim, NCEP CFSR, and NASA MERRA. *Journal of Climate*. **27**:5517-5537. doi:10.1175/JCLI-D-14-00005.1.

- 
- Chen X. 2008. Land use/cover change in arid area in China.
- Chu P, Liv SH, Chen YC. 2005. A numerical modeling study on desert oasis self-supporting mechanisms. *Journal of Hydrology*. **312**:256-276. doi:10.1016/j.jhydrol.2005.02.043.
- Collins W, Rasch P, Boville BA, Hack JJ, McCaa JR, Williamson DL, Kiehl JT, Briegleb B, Bitz C, Lin SJ. 2004. Description of the NCAR community atmosphere model (CAM 3.0). *NCAR Tech. Note NCAR/TN-464 STR*. **226**.
- Davin EL, Stöckli R, Jaeger EB, Levis S, Seneviratne SI. 2011. COSMO-CLM2: A new version of the COSMO-CLM model coupled to the Community Land Model. *Climate Dynamics*. **37**:1889-1907.
- De Troch R, Hamdi R, Van de Vyver H, Geleyn J-F, Termonia P. 2013. Multiscale performance of the ALARO-0 model for simulating extreme summer precipitation climatology in Belgium. *Journal of Climate*. **26**:8895-8915.
- Dee DP, Uppala SM, Simmons AJ, Berrisford P, Poli P, Kobayashi S, Andrae U, Balmaseda MA, Balsamo G, Bauer P. 2011. The ERA - Interim reanalysis: Configuration and performance of the data assimilation system. *Quarterly Journal of the Royal Meteorological Society*. **137**:553-597. doi:10.1002/qj.828.
- Deng XZ, Shi QL, Zhang Q, Shi CC, Yin F. 2015. Impacts of land use and land cover changes on surface energy and water balance in the Heihe River Basin of China, 2000–2010. *Physics and Chemistry of the Earth, Parts A/B/C*. **79-82**:2-10. doi:10.1016/j.pce.2015.01.002.
- Dickinson RE, Kennedy P, Henderson-Sellers A. 1993. *Biosphere-atmosphere transfer scheme (BATS) version 1e as coupled to the NCAR community climate model*. National Center for Atmospheric Research, Climate and Global Dynamics Division.
- Didan K. 2015. MOD13A2 MODIS/Terra Vegetation Indices 16-Day L3 Global 1km SIN Grid V006. *NASA EOSDIS Land Processes DAAC*. doi: 10.5067/MODIS/MOD13A2.006.
- Evans J, Zaitchik B. 2008. ZY-Modeling the large - scale water balance impact of different irrigation systems. *Water Resources Research*. **44**.
- Fan Z, Wu S, Wu Y, Zhang P, Zhao X, Zhang J. 2013. The land reclamation in Xinjiang since the founding of new China. *Journal Natural Resources*. **28**:713-720.
- Fensholt R, Sandholt I, Rasmussen MS. 2004. Evaluation of MODIS LAI, fAPAR and the relation between fAPAR and NDVI in a semi-arid environment using in situ measurements. *Remote Sensing of Environment*. **91**:490-507. doi:http://doi.org/10.1016/j.rse.2004.04.009.
- Fernández - Gálvez J, Simmonds L, Barahona E. 2006. Estimating detailed soil water profile records from point measurements. *European Journal of Soil Science*. **57**:708-718.
- Feser F, Rockel B, von Storch H, Winterfeldt J, Zahn M. 2011. Regional Climate Models Add Value to Global Model Data: A Review and Selected Examples. *Bulletin of the American Meteorological Society*. **92**:1181-1192. doi:10.1175/2011BAMS3061.1.
- Gao Y, Chen F, Barlage M, Liu W, Cheng G, Li X, Yu Y, Ran Y, Li H, Peng H. 2008. Enhancement of land surface information and its impact on atmospheric modeling in the Heihe River Basin, northwest China. *Journal of Geophysical Research: Atmospheres*. **113**.
- Gao YH, Chen YC, Lü SH. 2004. Numerical simulation of the critical scale of oasis maintenance and development in the arid regions of northwest China. *Advances in Atmospheric Sciences*. **21**:113-124.



- 
- Gessner U, Naeimi V, Klein I, Kuenzer C, Klein D, Dech S. 2013. The relationship between precipitation anomalies and satellite-derived vegetation activity in Central Asia. *Global and Planetary Change*. **110**:74-87.
- Gsella A, de Meij A, Kerschbaumer A, Reimer E, Thunis P, Cuvelier C. 2014. Evaluation of MM5, WRF and TRAMPER meteorology over the complex terrain of the Po Valley, Italy. *Atmospheric Environment*. **89**:797-806.
- Gu LH, Meyers T, Pallardy SG, Hanson PJ, Yang B, Heuer M, Hosman KP, Riggs JS, Sluss D, Wullschleger SD. 2006. Direct and indirect effects of atmospheric conditions and soil moisture on surface energy partitioning revealed by a prolonged drought at a temperate forest site. *Journal of Geophysical Research: Atmospheres*. **111**. doi:10.1029/2006JD007161.
- Gutman G, Ignatov A. 1998. The derivation of the green vegetation fraction from NOAA/AVHRR data for use in numerical weather prediction models. *International Journal of Remote Sensing*. **19**:1533-1543.
- Hamdi R, Degrauwe D, Duerinckx A, Cedilnik J, Costa V, Dalkilic T, Essaouini K, Jerczynki M, Kocaman F, Kullmann L. 2014. Evaluating the performance of SURFEXv5 as a new land surface scheme for the ALADINcy36 and ALARO-0 models. *Geoscientific Model Development*. **7**:23.
- Hamdi R, Degrauwe D, Duerinckx A, Cedilnik J, Costa V, Dalkilic T, Essaouini K, Jerczynki M, Kocaman F, Kullmann L. 2013. Evaluating the performance of SURFEXv5 as a new land surface scheme for the ALADINcy36 and ALARO-0 models. *Geoscientific Model Development Discussions*. **6**:4053-4104.
- Han B, Lü S, Ao Y. 2010. Analysis on the interaction between turbulence and secondary circulation of the surface layer at Jinta oasis in summer. *Advances in Atmospheric Sciences*. **27**:605.
- Hanna SR, Yang RX. 2001. Evaluations of mesoscale models' simulations of near-surface winds, temperature gradients, and mixing depths. *Journal of Applied Meteorology*. **40**:1095-1104. doi:http://dx.doi.org/10.1175/1520-0450(2001)040<1095:EOMMSO>2.0.CO;2.
- He Q, Yang Q, LI H-j. 2003. Variations of Air Temperature, Precipitation and Sand-Dust Weather in Xinjiang in Past 40 Years [J]. *Journal of Glaciology and Geocryology*. **4**:009.
- Helgason W, Pomeroy JW. 2012. Characteristics of the near-surface boundary layer within a mountain valley during winter. *Journal of Applied Meteorology and Climatology*. **51**:583-597. doi:http://dx.doi.org/10.1175/JAMC-D-11-058.1.
- Hong Z, Jian-Wei W, Qiu-Hong Z, Yun-Jiang Y. 2003. A preliminary study of oasis evolution in the Tarim Basin, Xinjiang, China. *Journal of Arid Environments*. **55**:545-553.
- Horton DE, Johnson NC, Singh D, Swain DL, Rajaratnam B, Diffenbaugh NS. 2015. Contribution of changes in atmospheric circulation patterns to extreme temperature trends. *Nature*. **522**:465-469.
- Hu Z, Zhang C, Hu Q, Tian H. 2014. Temperature changes in Central Asia from 1979 to 2011 based on multiple datasets. *Journal of Climate*. **27**:1143-1167.
- Immerzeel WW, Van Beek LP, Bierkens MF. 2010. Climate change will affect the Asian water towers. *Science*. **328**:1382-1385.
- IPCC. 2012. Intergovernmental Panel on Climate Change.

- Jia B, Zhang Z, Ci L, Ren Y, Pan B, Zhang Z. 2004. Oasis land-use dynamics and its influence on the oasis environment in Xinjiang, China. *Journal of Arid Environments*. **56**:11-26.
- Jiang L, Kogan FN, Guo W, Tarpley JD, Mitchell KE, Ek MB, Tian Y, Zheng W, Zou CZ, Ramsay BH. 2010. Real - time weekly global green vegetation fraction derived from advanced very high resolution radiometer - based NOAA operational global vegetation index (GVI) system. *Journal of Geophysical Research: Atmospheres*. **115**. doi:10.1029/2009JD013204.
- Jiang L, Ma E, Deng X. 2014. ZY-Impacts of irrigation on the heat fluxes and near-surface temperature in an inland irrigation area of Northern China. *Energies*. **7**:1300-1317.
- Kalnay E, Kanamitsu M, Kistler R, Collins W, Deaven D, Gandin L, Iredell M, Saha S, White G, Woollen J, Zhu Y, Leetmaa A, Reynolds R, Chelliah M, Ebisuzaki W, Higgins W, Janowiak J, Mo KC, Ropelewski C, Wang J, Jenne R, Joseph D. 1996. The NCEP/NCAR 40-Year Reanalysis Project. *Bulletin of the American Meteorological Society*. **77**:437-471. doi:10.1175/1520-0477(1996)077<0437:TNYRP>2.0.CO;2.
- Kanamitsu M, Ebisuzaki W, Woollen J, Yang S-K, Hnilo JJ, Fiorino M, Potter GL. 2002. NCEP-DOE AMIP-II Reanalysis (R-2). *Bulletin of the American Meteorological Society*. **83**:1631-1643. doi:10.1175/BAMS-83-11-1631.
- Kueppers LM, Snyder MA. 2012. ZY-Influence of irrigated agriculture on diurnal surface energy and water fluxes, surface climate, and atmospheric circulation in California. *Climate Dynamics*. **38**:1017-1029. doi:10.1007/s00382-011-1123-0.
- Kumar A, Chen F, Barlage M, Ek MB, Niyogi D. 2014. Assessing impacts of integrating MODIS vegetation data in the weather research and forecasting (WRF) model coupled to two different canopy-resistance approaches. *Journal of Applied Meteorology and Climatology*. **53**:1362-1380. doi:http://dx.doi.org/10.1175/JAMC-D-13-0247.1.
- Kyselý J, Rulfová Z, Farda A, Hanel M. 2016. Convective and stratiform precipitation characteristics in an ensemble of regional climate model simulations. *Climate Dynamics*. **46**:227-243. doi: 10.1007/s00382-015-2580-7.
- Lamptey B, Barron E, Pollard D. 2005. Impacts of agriculture and urbanization on the climate of the Northeastern United States. *Global and Planetary Change*. **49**:18. doi:10.1016/j.gloplacha.2005.10.001.
- Le Moigne P, Boone A, Calvet J, Decharme B, Faroux S, Gibelin A. 2009. SURFEX scientific documentation. *Note de centre (CNRM/GMME), Météo-France, Toulouse, France*.
- Lenderink G, Van Ulden A, Van den Hurk B, Van Meijgaard E. 2007. Summertime inter-annual temperature variability in an ensemble of regional model simulations: analysis of the surface energy budget. *Climatic Change*. **81**:233-247. doi:10.1007/s10584-006-9229-9.
- Li CF, Zhang C, Luo GP, Chen X, Maisupova B, Madaminov AA, Han QF, Djenbaev BM. 2015. Carbon stock and its responses to climate change in Central Asia. *Global Change Biology*. **21**:1951-1967. doi:10.1111/gcb.12846.
- Li FM, Wang P, Wang J, Xu J-Z. 2004. Effects of irrigation before sowing and plastic film mulching on yield and water uptake of spring wheat in semiarid Loess Plateau of China. *Agricultural Water Management*. **67**:77-88.
- Li Fuxian YJ, Zhang Ling , Chen Duofang. 2002. The Experiment Report on Cotton Requiring Water Rules and the Maximums Water Consumption Periods and Capacity in Mulch Drip Irrigation. *Journal of Xinjiang Agricultural University*. **25**:43-47.

- 
- Li J, Zhao C, Zhu H, Li Y, Wang F. 2007. Effect of plant species on shrub fertile island at an oasis–desert ecotone in the South Junggar Basin, China. *Journal of Arid Environments*. **71**:350-361. doi:http://doi.org/10.1016/j.jaridenv.2007.03.015.
- Li L. 2014. An overview of BCC climate system model development and application for climate change studies. *Journal of Meteorological Research*. **28**:34-56.
- Li M. 2011. Simulation of Drought Change Trend in Shaanxi Province in the Future Based on PRECIS. *Journal of Anhui Agriculture*. **39**:9073-9076.
- Li X, Cheng GD, Liu SM, Xiao Q, Ma MG, Jin R, Che T, Liu QH, Wang WZ, Qi Y. 2013. Heihe watershed allied telemetry experimental research (HiWATER): Scientific objectives and experimental design. *Bulletin of the American Meteorological Society*. **94**:1145-1160. doi:http://dx.doi.org/10.1175/BAMS-D-12-00154.1.
- Li X, Yang K, Zhou Y. 2016a. Progress in the study of oasis-desert interactions. *Agricultural and Forest Meteorology*. **230**:1-7.
- Li XS, Zhang J. 2016. Derivation of the green vegetation fraction of the whole China from 2000 to 2010 from MODIS data. *Earth Interactions*. **20**:1-16. doi:10.1175/EI-D-15-0010.1.
- Li XW, Jin MG, Zhou NQ, Huang J, Jiang S, Telesphore H. 2016b. Evaluation of evapotranspiration and deep percolation under mulched drip irrigation in an oasis of Tarim basin, China. *Journal of Hydrology*. **538**:677-688.
- Li XW, Jin MG, Zhou NQ, Huang J, Jiang S, Telesphore H. 2016b. Evaluation of evapotranspiration and deep percolation under mulched drip irrigation in an oasis of Tarim basin, China. *Journal of Hydrology*. **538**:677-688.
- Lianmei Y. 2003. Climate Change of Extreme Precipitation in Xinjiang [J]. *Acta Geographica Sinica*. **4**:012.
- Lim Y-J, Hong J, Lee T-Y. 2012. Spin-up behavior of soil moisture content over East Asia in a land surface model. *Meteorology and Atmospheric Physics*. **118**:151-161.
- Ling HB, Xu HL, Fu JY, Fan ZL, Xu XW. 2013. Suitable oasis scale in a typical continental river basin in an arid region of China: A case study of the Manas River Basin. *Quaternary International*. **286**:116-125. doi:10.1016/j.quaint.2012.07.027.
- Lioubimtseva E, Henebry GM. 2009. Climate and environmental change in arid Central Asia: Impacts, vulnerability, and adaptations. *Journal of Arid Environments*. **73**:963-977.
- Litan S, Shalamu A, Yu-dong S. 2011. Effects of Drip Irrigation Volume on Soil Water-salt Transfer and Its Redistribution. *Arid Zone Research*. **1**:013.
- Liu S, Liu H, Hu Y, Zhang CY, Liang FM, Wang JH. 2007a. Numerical simulations of land surface physical processes and land-atmosphere interactions over oasis-desert/Gobi region. *Science in China Series D: Earth Sciences*. **50**:290-295. doi:10.1007/s11430-007-2009-1.
- Liu X, Tian C. 2005. Study on dynamic and balance of salt for cotton under plastic mulch in south Xinjiang. *Journal of Soil Water Conservation*. **6**:020.
- Lu Q, Pan X, Zhong K, Li Y. 2003. Research Progress of Regional Climate Model. *Journal of Nanjing Institute of Meteorology*. 557-565.
- Luo GP, Feng YX, Zhang BP, Cheng WM. 2010. Sustainable land-use patterns for arid lands: A case study in the northern slope areas of the Tianshan Mountains. *Journal of Geographical Sciences*. **20**:510-524. doi:10.1007/s11442-010-0510-5.

- 
- Luo P, Peng Pa, Gleixner G, Zheng Z, Pang Z, Ding Z. 2011. Empirical relationship between leaf wax n-alkane  $\delta D$  and altitude in the Wuyi, Shennongjia and Tianshan Mountains, China: Implications for paleoaltimetry. *Earth and Planetary Science Letters*. **301**:285-296.
- Lv SH, Shang LY, Liang L, Luo SQ. 2005. Numerical Simulation of Microclimate Effect in Jinta Oasis. *Plateau Meteorology*. **24**:649-655.
- MA Jinlong, Liu Lijuan, LI Xiaoyu, WANG Jin, Huijin Y. 2015. Evapotranspiration process of cotton field under mulched drip irrigation of oasis in arid region. *Chinese Journal of Ecology*. **34**:7. doi:10.13292/j.1000-4890.20150311.027.
- Manabe S. 1969. CLIMATE AND THE OCEAN CIRCULATION 1: I. THE ATMOSPHERIC CIRCULATION AND THE HYDROLOGY OF THE EARTH'S SURFACE. *Monthly Weather Review*. **97**:739-774.
- Meng X, Lu S, Gao Y, Guo J. 2015. Simulated effects of soil moisture on oasis self - maintenance in a surrounding desert environment in Northwest China. *International Journal of Climatology*. **35**:4116-4125.
- Meng XH, Lu S, Zhang T, Ao Y, Li S, Bao Y, Wen L, Luo S. 2012. Impacts of inhomogeneous landscapes in oasis interior on the oasis self-maintenance mechanism by integrating numerical model with satellite data. *Hydrology and Earth System Sciences*. **16**:3729-3738. doi:10.5194/hess-16-3729-2012.
- Meng XH, Lü SH, Zhang TT, Guo JX, Gao YH, Bao Y, Wen LJ, Luo SQ, Liu YP. 2009. Numerical simulations of the atmospheric and land conditions over the Jinta oasis in northwestern China with satellite - derived land surface parameters. *Journal of Geophysical Research: Atmospheres*. **114**. doi:10.1029/2008JD010360.
- Miller J, Barlage M, Zeng X, Wei H, Mitchell K, Tarpley D. 2006. Sensitivity of the NCEP/Noah land surface model to the MODIS green vegetation fraction data set. *Geophysical Research Letters*. **33**. doi:10.1029/2006GL026636.
- Miller N, Jin J, Schlegel N, Snyder M, O'Brien T, Sloan L, Duffy P, Hidalgo H, Kanamaru MK, Yoshimura K. 2009. An analysis of simulated California climate using multiple dynamical and statistical techniques. *California Energy Commission report CEC-500-2009-017-F*.
- Mingjiang D. 2009. Current situation and its potential analysis of exploration and utilization of groundwater resources of Xinjiang. *Arid Land Geography*. **5**:003.
- Müller OV, Berbery EH, Alcaraz-Segura D, Ek MB. 2014. Regional model simulations of the 2008 drought in southern South America using a consistent set of land surface properties. *Journal of Climate*. **27**:6754-6778. doi:http://dx.doi.org/10.1175/JCLI-D-13-00463.1.
- Niu GY, Yang ZL, Mitchell KE, Chen F, Ek MB, Barlage M, Kumar A, Manning K, Niyogi D, Rosero E. 2011. The community Noah land surface model with multiparameterization options (Noah - MP): 1. Model description and evaluation with local - scale measurements. *Journal of Geophysical Research: Atmospheres*. **116**.
- Nnamchi HC. 2011. Numerical simulation of fluxes generated by inhomogeneities of the underlying surface over the Jinta Oasis in Northwestern China. *Advances in Atmospheric Sciences*. **28**:887-906. doi:10.1007/s00376-010-0041-0.
- Noilhan J, Mahfouf J-F. 1996. The ISBA land surface parameterisation scheme. *Global and Planetary Change*. **13**:145-159.

- 
- Ozdogan M, Rodell M, Kato H. 2007. The role of irrigation in North American hydroclimates. In *AGU Spring Meeting Abstracts*.
- Pachauri RK, Allen M, Barros V, Broome J, Cramer W, Christ R, Church J, Clarke L, Dahe Q, Dasgupta P. 2014. Climate Change 2014: Synthesis Report. Contribution of Working Groups I, II and III to the Fifth Assessment Report of the Intergovernmental Panel on Climate Change.
- Pei L, Moore N, Zhong S, Kendall AD, Gao Z, Hyndman DW. 2016. ZY-Effects of irrigation on summer precipitation over the United States. *Journal of Climate*. **29**:3541-3558.
- Pitman AJ. The evolution of, and revolution in, land surface schemes designed for climate models[J]. *International Journal of Climatology*. 2003. 23:479-510.
- Qiu Y, Hu Q, Zhang C. 2017. WRF simulation and downscaling of local climate in Central Asia. *International Journal of Climatology*.
- Qu R, Cui X, Yan H, Ma E, Zhan J. 2013. ZY-Impacts of land cover change on the near-surface temperature in the North China Plain. *Advances in Meteorology*. **2013**.
- Román MO, Gatebe CK, Shuai Y, Wang Z, Gao F, Masek JG, He T, Liang S, Schaaf CB. 2013. Use of in situ and airborne multiangle data to assess MODIS-and Landsat-based estimates of directional reflectance and albedo. *IEEE Transactions on Geoscience and Remote Sensing*. **51**:1393-1404. doi:10.1109/TGRS.2013.2243457.
- Rosenberg NJ. 1969. Seasonal patterns in evapotranspiration by irrigated alfalfa in the central Great Plains. *Agronomy Journal*. **61**:879-886.
- Rydsaa J, Stordal F, Tallaksen L. 2015. Sensitivity of the regional European boreal climate to changes in surface properties resulting from structural vegetation perturbations. *Biogeosciences*. **12**:3071-3087. doi:10.5194/bg-12-3071-2015.
- Sacks WJ, Cook BI, Buening N, Levis S, Helkowski JH. 2009. Effects of global irrigation on the near-surface climate. *Climate Dynamics*. **33**:159-175.
- Samuelsson P, Jones CG, Willén U, Ullerstig A, Gollvik S, Hansson U, Jansson C, Kjellström E, Nikulin G, Wyser K. 2011. The Rossby Centre Regional Climate model RCA3: model description and performance. *Tellus A*. **63**:4-23.
- Sellers P, Mintz Y, Sud Yea, Dalcher A. 1986. A simple biosphere model (SiB) for use within general circulation models. *Journal of the Atmospheric Sciences*. **43**:505-531.
- Seneviratne SI, Lüthi D, Litschi M, Schär C. 2006. Land-atmosphere coupling and climate change in Europe. *Nature*. **443**:205-209. doi:10.1038/nature05095.
- Seneviratne SI, Lüthi D, Litschi M, Schär C. 2006. Land-atmosphere coupling and climate change in Europe. *Nature*. **443**:205-209. doi:10.1038/nature05095.
- Sesnie SE, Dickson BG, Rosenstock SS, Rundall JM. 2012. A comparison of Landsat TM and MODIS vegetation indices for estimating forage phenology in desert bighorn sheep (*Ovis canadensis nelsoni*) habitat in the Sonoran Desert, USA. *International Journal of Remote Sensing*. **33**:276-286. doi:http://dx.doi.org/10.1080/01431161.2011.592865.
- Seungbum H, Lakshmi V, Small EE, Chen F, Tewari M, Manning KW. 2009. Effects of vegetation and soil moisture on the simulated land surface processes from the coupled WRF/Noah model. *Journal of Geophysical Research: Atmospheres*. **114**. doi:10.1029/2008JD011249.

- 
- Sims DA, Rahman AF, Vermote EF, Jiang Z. 2011. Seasonal and inter-annual variation in view angle effects on MODIS vegetation indices at three forest sites. *Remote Sensing of Environment*. **115**:3112-3120. doi:http://dx.doi.org/10.1016/j.rse.2011.06.018.
- Skamarock WC, Klemp JB, Dudhia J, Gill DO, Barker DM, Wang W, Powers JG. 2005. A description of the advanced research WRF version 2: DTIC Document.
- Smith JR, Hawkins AL, Asmerom Y, Polyak V, Giegengack R. 2007. New age constraints on the Middle Stone Age occupations of Kharga Oasis, Western Desert, Egypt. *Journal of Human Evolution*. **52**:690-701. doi:New age constraints on the Middle Stone Age occupations of Kharga Oasis, Western Desert, Egypt.
- Soltan M. 1999. Evaluation of ground water quality in Dakhla Oasis (Egyptian Western Desert). *Environmental Monitoring and Assessment*. **57**:157-168. doi:10.1023/A:1005948930316.
- Song YH, Dudhia J, Chen SH. 2004. A revised approach to ice microphysical processes for the bulk parameterization of clouds and precipitation. *Monthly Weather Review*. **132**:103-120. doi:http://dx.doi.org/10.1175/1520-0493(2004)132<0103:ARATIM>2.0.CO;2.
- Sorg A, Bolch T, Stoffel M, Solomina O, Beniston M. 2012. Climate change impacts on glaciers and runoff in Tien Shan (Central Asia). *Nature Climate Change*. **2**:725-731. doi:10.1038/nclimate1592.
- Souza V, Espinosa-Asuar L, Escalante AE, Eguiarte LE, Farmer J, Forney L, Lloret L, Rodríguez-Martínez JM, Soberón X, Dirzo R. 2006. An endangered oasis of aquatic microbial biodiversity in the Chihuahuan desert. *Proceedings of the National Academy of Sciences*. **103**:6565-6570.
- Stroeve J, Box JE, Wang Z, Schaaf C, Barrett A. 2013. Re-evaluation of MODIS MCD43 Greenland albedo accuracy and trends. *Remote Sensing of Environment*. **138**:199-214. doi:http://dx.doi.org/10.1016/j.rse.2013.07.023.
- Su CX, Hu YQ. 1987. The structure of the oasis cold island in the planetary boundary layer. *Acta Meteorologica Sinica*. **45**:322-328.
- Sun D, Zhao C, Wei H, Peng D. 2011. Simulation of the relationship between land use and groundwater level in Tailan River basin, Xinjiang, China. *Quaternary International*. **244**:254-263.
- Sun S. 2002. Advance in Land surface processes *Xinjiang weather*.1-6.
- Tewari M, Chen F, Wang W, Dudhia J, LeMone MA, Mitchell K, Ek M, Gayno G, Wegiel J, Cuenca RH. 2004. Implementation and verification of the unified NOAA land surface model in the WRF model. In *20th conference on weather analysis and forecasting/16th conference on numerical weather prediction*, 11-15.
- Vidale PL, Lüthi D, Wegmann R, Schär C. 2007. European summer climate variability in a heterogeneous multi-model ensemble. *Climatic Change*. **81**:209-232. doi:10.1007/s10584-006-9218-z.
- Wang J, Li F, Song Q, Li S. 2003. Effects of plastic film mulching on soil temperature and moisture and on yield formation of spring wheat. *Ying yong sheng tai xue bao= The journal of applied ecology/Zhongguo sheng tai xue xue hui, Zhongguo ke xue yuan Shenyang ying yong sheng tai yan jiu suo zhu ban*. **14**:205-210.
- Wang P, Li XY, Huang YM, Liu SM, Xu ZW, Wu XC, Ma YJ. 2016. Numerical modeling the isotopic composition of evapotranspiration in an arid artificial oasis cropland ecosystem

- 
- with high-frequency water vapor isotope measurement. *Agricultural and Forest Meteorology*. **230**:79-88.
- Wang W, Beezley C, Duda M. 2012. WRF ARW V3: User's Guide. Wang, C. Beezley, M. Duda, et al. URL: <http://www.mmm.ucar.edu/wrf/users> (accessed: 11.01. 2013).
- Wang Y, Xiao D, Li Y, Li X. 2008. Soil salinity evolution and its relationship with dynamics of groundwater in the oasis of inland river basins: case study from the Fubei region of Xinjiang Province, China. *Environmental Monitoring and Assessment*. **140**:291-302.
- Wang ZH, Bouzeid E. 2012. A novel approach for the estimation of soil ground heat flux. *Agricultural and Forest Meteorology*. **154**:214-221. doi:10.1016/j.agrformet.2011.12.001.
- Wen J, Dou B, You D, Tang Y, Xiao Q, Liu Q, Qinhuo L. 2017. Forward a Small-Timescale BRDF/Albedo by Multisensor Combined BRDF Inversion Model. *IEEE Transactions on Geoscience and Remote Sensing*. **55**:683-697.
- Wen J, Zhao X, Liu Q, Tang Y, Dou B. 2014. An improved land-surface albedo algorithm with DEM in rugged terrain. *IEEE Geoscience and Remote Sensing Letters*. **11**:883-887.
- Wen XH, Lu SH, Jin JM. 2012. Integrating remote sensing data with WRF for improved simulations of oasis effects on local weather processes over an arid region in northwestern China. *Journal of Hydrometeorology*. **13**:573-587. doi:<http://dx.doi.org/10.1175/JHM-D-10-05001.1>.
- Whiteman CD. 2000. *Mountain meteorology: fundamentals and applications*. Oxford University Press.
- Xie Z-k, Wang Y-j, Li F-m. 2005. Effect of plastic mulching on soil water use and spring wheat yield in arid region of northwest China. *Agricultural Water Management*. **75**:71-83.
- Xu ZF, Mahmood R, Yang ZL, Fu C, Su H. 2015. Investigating diurnal and seasonal climatic response to land use and land cover change over monsoon Asia with the Community Earth System Model. *Journal of Geophysical Research: Atmospheres*. **120**:1137-1152. doi:10.1002/2014JD022479.
- Yan JW, Liu JY, Chen BZ, Feng M, Fang SF, Xu G, Zhang HF, Che ML, Liang W, Hu YF. 2014. Changes in the land surface energy budget in eastern China over the past three decades: contributions of land-cover change and climate change. *Journal of Climate*. **27**:9233-9252. doi:<http://dx.doi.org/10.1175/JCLI-D-13-00492.1>.
- Yan K, Park T, Yan G, Chen C, Yang B, Liu Z, Nemani RR, Knyazikhin Y, Myneni RB. 2016a. Evaluation of MODIS LAI/FPAR product collection 6. Part 1: Consistency and improvements. *Remote Sensing*. **8**:359. doi:10.3390/rs8050359.
- Yang Z, Niu G, Mitchell KE, Chen F, Ek MB, Barlage M, Longuevergne L, Manning K, Niyogi D, Tewari M. 2011. The community Noah land surface model with multiparameterization options (Noah - MP): 2. Evaluation over global river basins. *Journal of Geophysical Research: Atmospheres*. **116**.
- Yao YH, Zhang BP. 2013. A preliminary study of the heating effect of the Tibetan Plateau. *PLOS ONE*. **8**:e68750.
- Yin JF, Zhan XW, Zheng YF, Hain CR, Ek M, Wen J, Fang L, Liu JC. 2016. Improving Noah land surface model performance using near real time surface albedo and green vegetation fraction. *Agricultural and Forest Meteorology*. **218**:171-183. doi:10.1016/j.agrformet.2015.12.001.

- 
- Yu GR, Wen XF, Sun XM, Tanner BD, Lee XH, Chen JY. 2006. Overview of ChinaFLUX and evaluation of its eddy covariance measurement. *Agricultural and Forest Meteorology*. **137**:125-137.
- Zaitchik BF, Evans J, Smith RB. 2005. ZY-MODIS-derived boundary conditions for a mesoscale climate model: Application to irrigated agriculture in the Euphrates basin. *Monthly Weather Review*. **133**:1727-1743.
- Zardi D, Whiteman CD. 2013. Diurnal mountain wind systems. In *Mountain Weather Research and Forecasting*, 35-119: Springer.
- Zeng XB, Dickinson RE, Walker A, Shaikh M, DeFries RS, Qi J. 2000. Derivation and evaluation of global 1-km fractional vegetation cover data for land modeling. *Journal of Applied Meteorology*. **39**:826-839. doi: [http://dx.doi.org/10.1175/1520-0450\(2000\)039<0826:DAEOGK>2.0.CO;2](http://dx.doi.org/10.1175/1520-0450(2000)039<0826:DAEOGK>2.0.CO;2).
- Zeng Y, Xie Z, Liu S. 2017. ZY-Seasonal effects of irrigation on land-atmosphere latent heat, sensible heat, and carbon fluxes in semiarid basin. *Earth System Dynamics*. **8**:113.
- Zhang Bp, Tan Y, Mo KG. 2004. Digital Spectrum and Analysis of Altitudinal Belts in the Tianshan Mountains. *Mountain Research*. **22**:8.
- Zhang C, Fan G, Ma Z, Cheng B, Zhao B, Feng J, Wang H. 2015. Characteristics of Albedo over Different Underlying Surface in the Semi-Arid Area. *Plateau Meteorology*. **34**:11.
- Zhang L, Jiang P, Wu H, Li M. 2013. Research on Spectral Characteristics of Typical Soil in North Xinjiang. *Journal of Soil and Water Conservation*. **4**.
- Zhang M, Luo G, De Maeyer P, Cai P, Kurban A. 2017a. Improved Atmospheric Modelling of the Oasis-Desert System in Central Asia Using WRF with Actual Satellite Products. *Remote Sensing*. **9**:1273.
- Zhang M, Luo G, De Maeyer P, Cai P, Kurban A. 2017a. Improved Atmospheric Modelling of the Oasis-Desert System in Central Asia Using WRF with Actual Satellite Products. *Remote Sensing*. **9**:1273.
- Zhang M, Luo G, Hamdi R, Qiu Y, Wang X, Maeyer PD, Kurban A. 2017b. Numerical Simulations of the Impacts of Mountain on Oasis Effects in Arid Central Asia. *Atmosphere*. **8**:212.
- Zhang M, Ma M, De Maeyer P, Kurban A. 2017a. Uncertainties in Classification System Conversion and an Analysis of Inconsistencies in Global Land Cover Products. *ISPRS International Journal of Geo-Information*. **6**:112.
- Zhang Q, Hu Y. 2001. Oasis effects in arid areas. *Zi Ran Za Zhi*. **23**:234-236.
- Zhang Q, Luo G, Li L, Zhang M, Lv N, Wang X. 2017b. An analysis of oasis evolution based on land use and land cover change: A case study in the Sangong River Basin on the northern slope of the Tianshan Mountains. *Journal of Geographical Sciences*. **27**:223-239.
- Zhang Q, Luo G, Li L, Zhang M, Lv N, Wang X. 2017b. An analysis of oasis evolution based on land use and land cover change: A case study in the Sangong River Basin on the northern slope of the Tianshan Mountains. *Journal of Geographical Sciences*. **27**:223-239.
- Zhiping L. 2015. Analysis of Dry and Wet Change in Northwest China in Recent 700 Years: Lanzhou University.
- ZHOU H, WANG Y, Sun Z, CHEN J. 2013. Irrigation Quota and Its Changes of Different Irrigation Modes in Arid Xinjiang Region. *water saving irrigation*. **12**. doi:1007-4929(2013)12-0005-07.



---

Zhou Y, Zhang L, Fensholt R, Wang K, Vitkovskaya I, Tian F. 2015. Climate contributions to vegetation variations in central Asian drylands: Pre-and post-USSR collapse. *Remote Sensing*. **7**:2449-2470.

Zhu L, Luo GP, Chen X, Xu W, Feng Y, Zhen Q, Wang J, Zhou D, Yin C. 2010. Detection of Land Use/Land Cover Change in the Middle and Lower Reaches of the Ili River, 1970-2007. *Progress in Geography*. **29**:9.



---

## SUMMARY

Central Asia is one of the most representative mid-latitudes arid regions, accounting for 29% of the total area of the world's arid and semi-arid regions. The North Tianshan Mountains (NTM), which is located in the hinterland of Central Asia, is a microcosm of the terrain and climate of the CA and consists of a great number of complex mountains and basins in the world. The NTM has been experiencing distinct intense human activities in the recent 30 years. Based on limited runoff from snow- and glacial-melt in mountainous region and unrestrained extraction of groundwater for irrigation, oases have developed between mountains and basins, thus the NTM can be consisting of mountains, oasis, and desert areas, named as Mountain-Oasis-Desert ecoSystem (MODS). The total oases area has expanded to 4 times more than its original size. Meanwhile, recent studies indicate that annual mean air temperature in the NTM has been increasing at an average rate of  $0.8\text{ }^{\circ}\text{C decade}^{-1}$ , which is far larger than the average rate of other arid area in the Central Asia (i.e.,  $0.40\text{ }^{\circ}\text{C decade}^{-1}$  from 1975 to 2015). Precipitation has an obvious increasing tendency at an increase rate of 11.3% in NTM while average precipitation in the other arid area in the Central Asia has a decreasing tendency. How does the abnormal regional temperature and precipitation change in NTM respond to the rapidly expanding irrigation oases located in the complex MODS? The answer is not yet clear. Answering the above questions are essential, both theoretically and practically, to the sustainable development and ecological stability of oases and will provide useful information for further investigating the impact of oasis expansion on regional climate changes under global climate change.

In this study, the available energy partition, temperature, humidity, atmospheric structure and circulation patterns of a typical MODS were explored using the Weather Research and Forecasting (WRF) model, and the focus is to explore the effects of irrigated oasis on the water-heat patterns of the entire MODS. The main contents of this dissertation included the following:

Because of outdated terrestrial datasets, including Land Use (LU), Albedo, Leaf Area Index (LAI) and Green Vegetation Fraction (GVF), the climate model WRF has a limited ability to accurately simulate weather and climate conditions over heterogeneous MODS at such scale. Using actual terrestrial datasets from satellite products in climate models is

---

the only possible solution to the limitation; however, it is impractical for long-period simulations due to the extremely time- and labor-consuming processes involved. We used the WRF model with observed estimates of LU, albedo, LAI, and GVF datasets from satellite products to examine which terrestrial datasets have a great impact on simulating water and heat conditions over heterogeneous oasis-desert systems. We found using actual GVF data has a much greater effect on the simulation of 2-m air temperature, 2-m relative humidity, and latent heat flux than the other parameters, resulting in mean error correction values of 62%, 87% and 92%, respectively. In addition, the LU data is the primary parameter because it strongly influences other secondary land surface parameters in the WRF.

The ability of WRF to accurately simulate water and heat conditions of irrigated oasis is limited due to lack of irrigation processes. A drip irrigation scheme was incorporated into the WRF to realistically represent water-heat patterns of oasis and to explore irrigation's effects on local climate of the complex MODS. Model evaluation further reveals that WRF with this new irrigation approach can generate irrigation water amounts that are in close agreement with the observation. Irrigation strengthened cold-wet island effects of oasis and oasis breeze circulation (OBC) in the irrigation season, and increased precipitation amount in upwind mountains areas with elevation approximately 1000-2000 m in daytime.

Due to the barrier effect of the terrain, the air temperatures of MODS generally exhibit continuous stripe-like increases from the mountainous areas to the oasis areas and to the desert areas, the specific humidity in the mountainous area is higher than that over the basin area at the same elevation; in the context of the prevailing westerly wind, a northwest west with a wind speed of approximately 3 m/s occurs during the daytime, whereas a southwest wind with a wind speed of approximately 4 m/s occurs at night covering the entire MODS, these are the typical valley wind characteristics in the MODS. The typical "cold-wet" island effects of the oasis and the OBC are fully described within the context of the MODS. There is an obvious temperature-humidity gradient line along the northern boundary of the oasis at the horizontal scale, and the air temperature (specific humidity) over the oasis during the day was significantly lower (higher) than the other areas at the same vertical height. The intensity of such cold (wetting) island of the oasis is approximately  $-0.61\text{ }^{\circ}\text{C}$  ( $1.56\text{ g kg}^{-1}$ ) at 2-m, and extends to a height of approximately 1.5 km above the oasis surface. The OBC

---

between oases and the deserts is counteracted by the stronger background circulation, thus the self-supporting mechanism of oases originating from the OBC plays a limited role in maintaining the ecological stability of oases in MODS. The airflow with increased moisture over irrigated oasis is brought to mountains areas with elevation approximately 1000-2000 m by intense valley wind in daytime, and forms precipitation due to adiabatic cooling and condensation in this region. Meanwhile intense mountain wind bring increased moisture over irrigated oasis to extend into the surrounding desert area at night, which may produce wet conditions favorable for desert plants in the oasis-desert transition zone. These effects accelerated hydrological process in the MODS.

---

## SAMENVATTING (DUTCH SUMMARY)

De aride regio van Centraal-Azië (CA) is één van de meest representatieve midden-breedtegraads droge gebieden en omvat 29 % van het totale wereldgebied qua aride en semi-aride regio's. Het noordelijke Tianshan gebergteketen (*northern Tianshan Mountains*, NTM), welke gelegen is in het hinterland van CA, vormen een microkosmos van het terrein en het klimaat van CA en bestaan uit een groot aantal complexe bergen en bekkens. De NTM waren de laatste 30 jaar onderhevig aan bijzonder intense menselijke activiteiten. Omwille van een beperkte afwatering (afkomstig van sneeuw en gesmolten ijs uit het bergachtig gebied) en een ongelimiteerde extractie van grondwater voor irrigatie, ontwikkelden zich oases tussen bergen en bekkens, aldus omvatten de NTM bergen, oases en woestijnregio's, genaamd het Berg-Oasis-Woestijn Systeem (MODS). De totale oasisregio breidde uit tot 4 maal de originele omvang. Ondertussen tonen recente studies aan dat de jaarlijkse gemiddelde luchttemperatuur in de NTM verhoogde aan een gemiddelde van 0.8 °C per decennium, wat veel groter is dan de gemiddelde ratio voor andere droge streken in CA (0.40 °C decennium<sup>-1</sup> van 1975 tot 2015). De neerslag vertoont een duidelijke stijgende trend in NTM en nam toe met 11.3 % terwijl de gemiddelde neerslag in andere aride CA gebieden een dalende trend heeft. Hoe reageert de abnormale regionale temperatuur en de wijziging in NTM neerslag op de snel uitbreidende geïrrigeerde oases (die in de complexe MODS gelegen zijn) ? Het antwoord is nog niet duidelijk. Een antwoord op de bovengenoemde vragen is essentieel, zowel theoretisch als praktisch, voor de duurzame ontwikkeling en de ecologische stabiliteit van oases en zal nuttige informatie opleveren die kan dienen voor verder onderzoek naar de impact van de oase-uitbreiding op de regionale klimaatveranderingen onder globale klimaatwijziging.

In deze studie onderzochten we de beschikbare energieverdeling, temperatuur, vochtigheid, atmosferische structuur en circulatiepatronen van typische MODS gebruik makend van het *Weather Research and Forecasting model* (WRF) en de focus ligt op het ontdekken van de gevolgen van een geïrrigeerde oase op de water-

---

hitte patronen van de volledige MODS. De belangrijkste inhoud van deze PhD behelst het volgende :

Door het gebruik van gedateerde terrestrische datasets, met inbegrip van *Land Use* (LU), *Albedo*, *Leaf Area Index* (LAI) en *Green Vegetation Fraction* (GVF), heeft het WRF klimaatmodel een beperkt vermogen om de weers- en klimaatomstandigheden accuraat te simuleren in heterogene MODS (op zo een schaal). Het gebruik van de huidige terrestrische datasets op basis van satellietproducten in klimaatmodellen is de enige mogelijke oplossing voor deze beperking; het is desalniettemin onpraktisch voor lange termijn simulaties en dit is te wijten aan de betrokken extreme tijds- en arbeidsintensieve processen. We benutten het WRF model met geobserveerde schattingen van LU, albedo, LAI en GVF datasets van satellieten om te onderzoeken welke terrestrische datasets een grote impact hebben op de simulatie van de water en hittecondities in heterogene oase-woestijn modellen. Door het gebruik van de huidige GVF gegevens is er een grotere invloed op de simulatie van 2-m luchttemperatuur, 2-m relatieve vochtigheid en latente hittestroming dan andere parameters, resulterend in gemiddelde foutcorrectiewaarden van respectievelijk 62 %, 87 % en 92 %. Bovendien vormen de LU gegevens de belangrijkste parameter omdat deze de andere secundaire landoppervlakteparameters in het WRF sterk beïnvloeden.

De mogelijkheid van WRF om de water en hitte toestand van een geïrrigeerde oase accuraat te simuleren is beperkt en dit is te wijten aan het gebrek aan irrigatieprocessen. Een drupirrigatieschema werd ingevoerd in de WRF om de water-hitte patronen van de oase realistisch weer te geven en om de effecten van irrigatie op het lokaal klimaat van complexe MODS na te gaan. Verder brengt een modevaluatie aan het licht dat de WRF (met deze nieuwe irrigatie-aanpak) waterhoeveelheden kan genereren die nauw aansluiten bij de waarneming. Irrigatie versterkte de koud-natte eilandinvloeden van de oase en de oasebries- circulatie (*oasis breeze circulation* OBC) in het irrigatie seizoen en verhoogde de neerslaghoeveelheid in loefzijdse berggebieden met ongeveer 1,000-2,000 m overdag.

---

Door het barrière-effect van het terrein, vertoont de luchttemperatuur van de MODS over het algemeen een aanhoudende strookachtige toename van de bergstreken tot de oase- en de woestijngebieden, de specifieke vochtigheid in het bergachtig gebied is hoger dan deze in het bekken op dezelfde hoogte; in de context van de overheersende westenwind, een windrichting van NWW met een windsnelheid van ongeveer 3 m/s gedurende de dag terwijl een windrichting SW met een snelheid van circa 4 m/s genoteerd werd 's nachts (die de volledige MODS beslaat, dit zijn de typische valleiwindkenmerken in de MODS). De typische “koud-natte” eilandinvloeden van de oase en OBC worden volledig beschreven in de context van de MODS, als bewijs voor een duidelijke temperatuurvochtigheidsgradiëntlijn langs de noordelijke grens van de oase op de horizontale schaal. De luchttemperatuur (specifieke vochtigheid) in de oase tijdens de dag was beduidend lager (hoger) dan in andere gebieden op dezelfde verticale hoogte. De intensiteit van zo een koud (nat) eiland in de oase is ongeveer  $-0.61\text{ }^{\circ}\text{C}$  ( $1.56\text{ g kg}^{-1}$ ) op 2-m en strekt zich uit tot een hoogte van circa 1.5 km boven het oase-oppervlak. De oasebries-circulatie (OBC) tussen oases en woestijnen wordt tegengewerkt door de sterkere achtergrondcirculatie. Dus, het zelfvoorzienende mechanisme van de oases die afstammen van het OBC speelt een beperkte rol in het behoud van de ecologische stabiliteit van de MODS oases. De luchtstroom met toegenomen vocht in de geïrrigeerde oase wordt naar de bergzones gevoerd met hoogtes van ongeveer 1,000-2,000 m door een hevige valleiwind overdag en vormt neerslag door adiabatische koeling en condensatie in deze streek. Intussen brengt een intense bergwind 's nachts een verhoogde hoeveelheid vocht over de geïrrigeerde oase die zich uitstrekt over de omliggende woestijnstreek, wat natte condities teweeg kan brengen die gunstig zijn voor woestijnplanten in de oase-woestijn overgangszone. Deze gevolgen versnelden het hydrologisch proces in de MODS.



---

## 摘要 (CHINESE SUMMARY)

---

亚洲中部干旱区是中纬度最具代表性的干旱区之一，主要包括中亚五国地区（以哈萨克斯坦、乌兹别克斯坦、吉尔吉斯斯坦、土库曼斯坦以及塔吉克斯坦为主）以及我国新疆等地区，占世界干旱与半干旱地区总面积的 29%。我国新疆的天山北坡是亚洲中部干旱区气候与地形的缩影。该区域地形复杂，包含世界上最多的山盆结构，气候变化异常敏感，近 30 年气候与降水呈现显著增加的趋势，而其它亚洲干旱区域气温变化幅度较小且降水总体呈现减少的趋势。具体来说，天北降雨明显增加，增加幅度为 22%-33%，呈现 11.3% 的增长趋势；天山北坡变暖速率均高于全球和其它干旱区域，天山南北坡变暖以 0.8 °C /10 年，而亚洲干旱区和全球陆地的变暖速率分别以 0.39° C/10 年和 0.27-0.31° C/10 年；同时在这个区域又经历了剧烈的人类活动，主要表现为绿洲在山盆有限水土资源下通过大规模的灌溉的急剧扩张。这种发展于复杂的山盆之间的灌溉绿洲对区域气候的效应是还不是很清楚，需要进一步深入的研究。因为绿洲是这个区域的精华，决定着这个区域人类生存与发展的命脉，绿洲的稳定是绿洲学和干旱区地理学研究的核心内容之一。深入探讨天北灌溉绿洲对局地气候的效应、以及这种效应与山盆之间的交互对于认识干旱区人类活动与气候变化的相互作用机理具有重要的科学意义，也对发展于有限水土资源的绿洲稳定，与可持续发展有着现实的意义。

本研究作者在 Land Use/Cover Change(LUCC) 与气候变化之间关系的大科学问题背景下，旨在使用高分辨率的区域气候模式 Weather Research and Forecasting (WRF)，从可利用能量分配、温度、湿度、降雨、大气结构与环流等多方面模拟、综合分析了复杂的天山北坡整个山地-绿洲-荒漠复合生态系统 (Mountain-Oasis-Desert System, MODS)的水热格局与局地气候，重点是探讨灌溉绿洲对整个 MODS 的水热格局的影响、以及与山盆地形气候背景的交互。本文研究主要包括以下几个方面：

**WRF 对陆面地理参数的敏感性：**由于 WRF 内嵌的基础地理数据集陈旧过时，且在这种复杂缺资料区域利用真实遥感陆面参数替换所有内嵌地理数据耗时、耗力、不具操作性的问题，我们探讨了 WRF 对于 Land Use (LU)、Albedo、Leaf Area Index (LAI) 和 Green Vegetation Fraction (GVF) 的敏感性，旨在寻找决定 WRF 模拟这种小尺度的局地气候研究的关键参数。结果表明，WRF 对于真实的 VF 陆面地理数据

---

最为敏感，对模拟温度、湿度和潜热模拟误差校正贡献比率为 62%, 87%, 和 92%。LU 数据作为模式一级参数决定了二级参数的量，在模拟过程中也不可忽视。

耦合灌溉过程。针对 WRF 也没有刻画适用于天山北坡绿洲管理的滴灌物理过程，限制了模式对灌溉绿洲水热状态的真实反映，本文新开发一滴灌框架并将其与 WRF 耦合。结果表明：WRF 与新发展的滴灌框架耦合现实地模拟了灌溉绿洲的水热状态，模拟结果在站点水平上与观测的灌溉量与气候、气象要素一致；灌溉加强了灌溉季绿洲的冷湿岛效应和绿洲-荒漠局地环流，也增加了上游山区地形大约为 1000-2000m 的降水量，对 WRF 的本地化过程至关重要。

灌溉绿洲效应、及与山地气候背景交互。由于地形的屏障作用，MODS 的气温呈现从山地到绿洲到荒漠条带性增长格局，而比湿在 1 km - 2 km 高程左右区域显著的高于同高度盆地地区，10-m 环流在盛行西风控制下，展示了明显的白天大约 3 m/s 的 WNW (West Northwest Wind) 风和晚上大约 4 m/s 的 SW (Southwest wind) 风的昼夜山谷风格局。在这种水热格局下，我们观测到北部绿洲-荒漠边界一条明显温湿梯度及白天绿洲上空气温（比湿）显著低于（高于）同高度其它区域，这是典型的绿洲冷湿岛效应，这种效应强度可以达到 $-0.61\text{ }^{\circ}\text{C}$  ( $1.56\text{ g kg}^{-1}$ )，影响范围可以达到绿洲上空大约 1500 m 的高度。由于强劲山谷风的存在隐匿了由绿洲荒漠水热差异产生的绿洲-荒漠局地微环流机制，使得前人研究提出的绿洲自我维持机制对绿洲的自我稳定在山盆中不能发挥有效作用。而且，白天谷风使得绿洲的冷湿气团水平移动到山区大约 1000 - 2000 m 区域成云致雨，山风将绿洲上空的冷湿气团携带进入部分荒漠区域而消耗，尽管有益于绿洲-荒漠过渡带的植被生长，但是破坏了绿洲的自我维持机制，加速了天山北坡水文循环过程。假设天山地形消失，该区域水热受控于强劲的盛行西风与印度东北部的西南亚低压系统产生的夏季副热带急流组合控制。

---

## CURRICULUM VITAE (BIOGRAPHY)

---

Miao Zhang was born in Qingyang (China) on the January 17<sup>th</sup>, 1988. In 2010, she graduated from Northwest Normal University and obtained her bachelor diploma of Geographic Information Systems. In 2013, she graduated from the Gansu Agricultural University and obtained her master diploma of Engineering in Soil and Water Conservation and Desertification Control. In the same year, she began her doctoral education at the Xinjiang Institute of Ecology and Geography, University of Chinese Academy of Sciences, and pursued her doctorate at Ghent University.



From September 2013 until June 2018, Miao worked at the Xinjiang Institute of Ecology and Geography and Ghent University, fund by the key projects from the Bureau of International Co-operation of the Chinese Academy of Science. PhD dissertation : “A study on water-heat patterns and regional climate of mountain-oasis-desert system in north Tianshan Mountains based on the WRF model” (2013-2018).

Miao has already contributed to several international conferences and is author of several papers that have been published in leading international journals in the field of physical geography and climate.

Below are listed the publications in the framework of my PhD.

1. Miao Zhang, Geping Luo, Philippe De Maeyer, Peng Cai, 2017. Improved atmospheric modeling of oasis-desert system in Central Asia using WRF with real-time satellite products. *Remote Sensing*, 2017. 9(12): 1273; doi:10.3390/rs9121273. (*IF*=3.244)
2. Miao Zhang, Mingguo Ma, Philippe De Maeyer, Alishir Kurban, 2017. Uncertainties in Classification System Conversion and an Analysis of Inconsistencies in Global Land Cover Products. *ISPRS International Journal of Geo-Information*, 6(4): 112 ; doi:10.3390/ijgi6040112. (*IF*: 1.502)

- 
3. Miao Zhang, Geping Luo, Rafiq Hamdi, et al, 2017. , et al. Numerical Simulations of the Impacts of Mountain on Oasis Effects in Arid Central Asia. *Atmosphere*, 2017, 8(11): 212; doi:10.3390/atmos8110212. (*IF*=1.487)
  4. Zhang Qi, Luo Geping, Li Longhui, Miao Zhang, et al. An analysis of oasis evolution based on land use and land cover change: A case study in the Sangong River Basin on the northern slope of the Tianshan Mountains[J]. *Journal of Geographical Sciences*, 2017, 27(2): 223-239. (*IF*=2.364)
  5. Miao Zhang, Geping Luo, Philippe De Maeyer , et al. 2017. The effects of drip irrigation on water-heat patterns in a mountain-oasis-desert system in the northern Tianshan Mountains. *JGR-Atmosphere*. *submitted*.